Master Thesis

WSL institute for Snow and avalanche research, SLF

Swiss Federal Institute of Technology in Lausanne, EPFL

Fall 2020

The effect of sublimation on snow isotopic composition

Supervisors: Prof. Michael Lehning

Dr. Pirmin Philipp Ebner

Dr. Jürg Christian Trachsel

Student: Yoann Sadowski

Sciper: 257 629

Email: yoann.sadowski@epfl.ch

Abstract

Stable water isotopes (SWIs) are natural tracers allowing to reconstruct the history of a water parcel. SWIs are used in hydrology, notably because they reflect the water residence time in underground storages. SWIs are also used as climate proxies since snow isotopic composition is strongly linked to the temperature at the time of deposition. This isotopic signal can be retrieved in ice cores and enables reconstruction of the past temperatures. The snow isotopic composition can be altered after deposition by heat and mass exchanges. Those processes are usually ignored in paleoclimate studies, and their respective significance is highly discussed in the literature.

This thesis aims to bring a better understanding on SWIs fractionation occurring during snow surface sublimation. This work is based on three datasets including isotopic composition of snow and vapour from the Swiss Alps. Each dataset was produced during a distinct period and with different samples collection frequency. Two methods to track specific snow layers were developed and helped interpret the data when precipitation occurred between the sampling dates. The analysis of the first two datasets showed that fractionation is probably occurring during vapour deposition. However, the influence of sublimation on snow isotopic composition remains unclear. The most recent measurement campaign was designed and realised during this master thesis. It aims to fill gaps, which were identified in the two former datasets. The laboratory results of this campaign were not available during the time allowed for this thesis but will be analysed in a forthcoming study.

Table of Contents

1. Introduction

Stable water isotopes (SWIs) are natural tracers reflecting the history of a water parcel. SWIs present a significant potential for a better understanding of the hydrological cycle. In addition, SWIs can be used in paleoclimate reconstruction because their varying concentrations in ice cores are linked to the past temperatures.

The isotopic composition of a given water parcel is altered by fractionation processes occurring during phase changes. The analysis of the isotopic signal of that parcel allows to retrieve its source and pathway, which are of great interest in hydrology. By using SWIs, it is possible to differentiate storm events and estimate the residence time of water in rivers, soils or underground storages [Genereux and Hooper, 1998]. In regions with a snow influenced hydrology, the use of SWIs from the snowpack could help better comprehend the melting rate and spatial distribution of water stored in the snow [Gat and Gonfiantini, 1981], [Ala-Aho et al., 2017].

The current isotope based hydrological models would gain in precision by capturing to what extent the snow isotopic composition is modified after deposition. Any process inducing a phase change within or at the surface of the snowpack can have an influence. The respective significance of these post-depositional processes is a current debate in the literature e.g. [Sokratov and Golubev, 2009]. Nonetheless, it is already possible to track frontal passages in an alpine snowpack based on SWIs because the hydrological history of a vapour parcel before deposition has more influence than post-depositional processes [Trachsel, 2019].

During phase transitions, the significance of the isotopic fractionation is temperature dependent [Gat, 1996]. This property allows to use SWIs in ice cores as climate proxies e.g. [Epstein et al., 1963], [Merlivat and Jouzel, 1979], [Masson-Delmotte et al., 2008], [Steen-Larsen et al., 2011]. Historically, studies on paleoclimate from ice cores considered the ice isotopic composition to be the same as the precipitation that formed it. In other words, any post-depositional processes were neglected.

Nonetheless, multiple publications have shown that the snow isotopic composition can be altered after deposition e.g. [Moser and Stichler, 1974], [Madsen et al., 2019], [Christner et al., 2017], [Ebner et al., 2017]. Due to the variability and complexity of the post-depositional processes, it is relatively difficult to separate one from the others. This thesis attempts to provide more information on the influence of surface sublimation on snow isotopic composition. The work is based on the analysis of snow samples collected in the Swiss Alps during three measurements campaigns. Results could have potential impact in hydrological studies of snow-influenced regions as well as in ice-core paleoclimatology.

This thesis starts by presenting the theory and some relevant literature results about SWIs in snow (chapter 2). It is followed by a description of the available datasets and the methods used for their analysis (chapter 3). Results are discussed in chapter 4 and their potential implications for future studies are presented in chapter 5.

2. Theoretical background

This chapter presents the notations used in this work as well as part of the current knowledge on SWIs. Some results from the literature are discussed and compared.

2.1. Isotopes notations and definitions

To differentiate atoms holding the same place in the periodic table, it is possible to compare their number of neutrons, which is directly linked to their masses. Two atoms with a given number of protons, but a different number of neutrons are isotopes (i.e. ^{1}H and ^{2}H are hydrogen isotopes). The combinations of isotopes constituting non-radioactive water molecules are referred to as stable water isotopes (SWIs).

Table 1 summarizes the properties of those isotopes. The superscripts before the element symbols correspond to the atomic mass of the element.

Table 1: Elements constituting stable water isotopes data from [West et al., 2006]

Element	Isotope	Notation in this text	Abundance [%]	Number of Protons	Number of Neutrons
Hydrogen	^{1}H	H	99.985	1	0
Hydrogen	^{2}H	D (Deuterium)	0.015	1	1
Oxygen	^{16}O	O	99.759	8	8
Oxygen	^{17}O	^{17}O	0.037	8	9
Oxygen	^{18}O	^{18}O	0.204	8	10

The term isotopologue refers to the various possible isotopic constitution of one molecule. For example, H_2O, $H_2{}^{18}O$, $H_2{}^{17}O$ and HDO are water isotopologues. In this thesis, as in many published papers in hydrologic, atmospheric and climate science e.g. [Gat, 1996], the focus is on $H_2{}^{18}O$ and HDO. SWIs are usually expressed as ratios to the most abundant isotopologue (H_2O) defined as:

$$R_{HDO} = \frac{[HDO]}{[H_2O]} \qquad \mathrm{R}_{H_2^{18}O} = \frac{[H_2^{18}O]}{[H_2O]} \tag{1}$$

Because $\mathrm{R_{HDO}}$ and $\mathrm{R}_{H_2^{18}O}$ are usually small, the widely used delta (δ) notation is used in this work. It represents a relative ratio of the sample to a common standard [Sodemann, 2006]. For SWIs, the standard is the Vienna Standard Mean Ocean Water (VSMOW) [IAEA, 2006]. The deltas are defined as:

$$\delta D = \frac{R_{HDO}}{(R_{HDO})_{\mathrm{VSMOW}}} - 1) \ * 1000\ [‰] \qquad \delta^{18}O = \left(\frac{R_{H_2^{18}O}}{\left(R_{H_2^{18}O}\right)_{\mathrm{VSMOW}}} - 1\right) \ * 1000\ [‰] \tag{2}$$

Where $(\mathrm{R_O})_{\mathrm{VSMOW}}$ and $(\mathrm{R_H})_{\mathrm{VSMOW}}$ are defined as: (values from [IAEA, 2006])

$$(R_{HDO})_{\mathrm{VSMOW}} = \frac{[HDO_{\mathrm{VSMOW}}]}{[H_2O_{\mathrm{VSMOW}}]} = 155.76 * 10^{-6} \qquad (R_{H_2^{18}O})_{\mathrm{VSMOW}} = \frac{[H_2^{18}O_{\mathrm{VSMOW}}]}{[H_2O_{\mathrm{VSMOW}}]} = 2005.20 * 10^{-6} \tag{3}$$

The different water isotopologues are present in each water phase. Yet, due to their different masses, a change in concentration occurs during phase changes. This process called isotopic fractionation can be due to stronger bonds between heavier molecules when both phases are at equilibrium [Gat and Gonfiantini, 1981]. In case of a non-equilibrium situation, the slower diffusive velocities of the heavy isotopologues also play a role and the concentration in each phase will be different to equilibrium

fractionation [Dansgaard, 1964]. This is also referred to as kinetic fractionation. More details on kinetic fractionation are given in 2.4.

During equilibrium fractionation, δD and $\delta^{18}O$ values are linearly related. Their mean relationship in precipitation is known as the Global Meteoric Water Line (GMWL) [Craig, 1961], [Gat, 1996] defined as:

$$\delta D = 8 * \delta^{18}O + 10 \text{ [‰]} \quad (4)$$

Locally, the linear relationship can be different from equation (4) and would be referred to as the Local Meteoric Water Line (LMWL) [Hürkamp et al., 2019].

As stated before, fractionation will result in a difference in isotopic composition between the two phases involved. Their equilibrium constant is called the fractionation factor α [Craig and Gordon, 1965]. The fractionation factor has been estimated in different studies for each of the 3 phase-transitions (liquid-vapour, liquid-solid, solid-vapour). It is presented for the solid-vapour equilibrium below.

$$\alpha_{i,s-v} = \frac{R_{i,s}}{R_{i,v}} \quad and \quad \alpha_{i,v-s} = \frac{1}{\alpha_{i,s-v}} \qquad i = HDO, H_2^{18}O \quad (5)$$

With $R_{i,s}$ and $R_{i,v}$ the ratios for i in the solid and in the vapour phases, respectively. In order to model the isotopic signal evolution of a single reservoir with only one sink, it is possible to use a Rayleigh distillation model [Gat, 1996], [Sodemann, 2006]. For a snow surface layer, which is assumed to only interact with the atmosphere, its isotopic composition can be estimated as:

$$R_{i,s} = R_{i,s,0} * \left(\frac{N_i}{N_{i,0}}\right)^{(\alpha_{i,v-s}-1)} \qquad i = HDO, H_2^{18}O \quad (6)$$

With N_i the number of molecules i remaining in the snow layer, $R_{i,s,0}$ and $N_{i,0}$ the initial ratio and number of molecules i in the snow layer. For simplicity, the subscript (i) is omitted (if not useful) in the equations presented further in this manuscript, but the ratios (R) and equilibrium factor (α) are specific to each isotopologue.

2.2. Post depositional processes

Multiple processes can influence the snow isotopic composition after deposition. Due to the limited understanding of their effects, it is difficult to separate one from the others [Gat and Gonfiantini, 1981]. This is probably one of the main reasons why post-depositional processes have been neglected in many paleoclimate studies using SWIs from ice-cores. [Epstein et al., 1963] suggested that after deposition, the main factor influencing isotopic profiles came from wind redistribution of snow. The effect of sublimation is also put aside in [Epstein et al., 1963] by considering a "layer-by-layer" sublimation. This idea is supported by the fact that ice has a molecular self-diffusion about 1000 times smaller than the one in vapour and cannot be considered as well-mixed [Friedman et al., 1991]. However, multiple studies challenge this layer by layer theory e.g. [Moser and Stichler, 1974], [Madsen et al., 2019], [Sokratov and Golubev, 2009], [Christner et al., 2017], [Ebner et al., 2017].

[Moser and Stichler, 1974] conducted an experiment very similar to the one presented later in this thesis. They collected snow surface samples (1-2 cm thick) twice a day during 8 consecutive days of fair weather on the Weissfluhjoch (WFJ) (2540 m. a. s. l., Temperature between -5 and 0 °C). The analysis of the isotopic composition showed an enrichment during the day, which was attributed to fractionating

sublimation. During the night a depletion of the surface isotopic composition was observed and could be explained by deposition of depleted vapour from the atmosphere. As the isotopic composition of the air vapour was not available, this supposition could not be confirmed. In any case, their results show clear post-depositional processes that should be accounted for. As deposition depends on the vapour isotopic composition, it could influence the snow surface even without fractionation.

Snow ventilation can further affect the water vapour isotopic composition of part of the snowpack. The thickness of the layer influenced by exchanges with the atmosphere depends on the pore size. For typical pore diameters, shear-driven ventilation seems to only affect the uppermost (~5 mm) layer [Clifton et al., 2008]. In some cases, topographic effects can influence a thicker layer [Bartlett and Lehning, 2011]. Those topographic effects (or "wind-pumping" effect) affect the isotopic composition of the snowpack [Ebner et al., 2017]. The air quickly reaches saturation when entering the interstitial space of the snow and enhances the vapor exchange between the atmosphere and multiple layers of the snowpack. The time a layer is at the surface (or sufficiently shallow to be influenced by the atmospheric exchanges) also plays an important role. After burial, there is still an indirect (weaker) influence of the atmosphere because of vapour transfer in the snowpack. [Johnsen et al., 2000] presented a model for the diffusion in firn depending on the tortuosity and porosity of the snow as well as on the isotopologue considered. The magnitude of the effective vapour diffusion in the snow is a current debate [Fourteau et al., 2021], and forthcoming results might have implications on the modelling of the snow isotopic composition.

Water vapour originating from other layers of the snowpack or from the atmosphere generally has a different isotopic composition. When deposited, this vapour induces changes in the snow isotopic profile [Friedman et al., 1991]. For example a temperature gradient within the snowpack creates a vapour flux [Sturm and Benson, 1997], [Jafari et al., 2020], resulting in mass exchange between snow layers with different isotopic composition. Snow metamorphism and differences in snow microstructure between layers also have an effect on the isotopic composition because of vapour transport [Schindler, 2020]. It must be noted that deposition due to intra-snowpack vapour exchange has a different influence depending on whether sublimation is a fractionating process or not.

2.3. Vapour-solid fractionation factor

This sub-chapter discusses four studies that estimated the fractionation occurring between the solid and gaseous water phases at isotopic equilibrium.

The equilibrium fractionation factor is dependent on the temperature and is typically described as [Gat, 1996]:

$$ln(\alpha) = \frac{C_1}{T^2} + \frac{C_2}{T} + C_3 \quad (7)$$

Where T (K) is the temperature and $C_{1,2,3}$ are coefficients that should be determined empirically. Table 2 presents the estimations of the equilibrium fractionation factor on solid-vapour equilibrium from the following studies: [Merlivat and Nief, 1967], [Majoube, 1970], [Ellehoj et al., 2013], [Lamb et al., 2017].

Table 2: Solid-vapour isotopic equilibrium from 4 studies

Isotope	Equation for $\alpha = \alpha_{s-v}$ (Here, T is in K)	α at -10°C	Temperature range used for regression [°C]	Reference
D	$ln(\alpha) = \frac{16289}{T^2} - 9.45 * 10^{-2}$	1.151	-40 to 0	[Merlivat and Nief, 1967]
D	$ln(\alpha) = \frac{48888}{T^2} - \frac{203.10}{T} + 21.33 * 10^{-2}$	1.159	-40 to -5	[Ellehoj et al., 2013]
D	$ln(\alpha) = \frac{13525}{T^2} - 5.59 * 10^{-2}$	1.150	-83 to -40	[Lamb et al., 2017]
^{18}O	$ln(\alpha) = \frac{11.839}{T} - 2.8224 * 10^{-2}$	1.017	-33.4 to 0	[Majoube, 1970]
^{18}O	$ln(\alpha) = \frac{8312.5}{T^2} - \frac{49.192}{T} + 8.31 * 10^{-2}$	1.016	-40 to 5	[Ellehoj et al., 2013]

The four studies found relationships fitting best their measurements that were obtained with different methodologies. In each case, the authors tried to reproduce an equilibrium situation, which according to the "layer-by-layer" theory would not occur for a snowpack in a natural environment [Epstein et al., 1963], [Friedman et al., 1991]. The results can have significant differences at low temperature, as it can be seen in Figure 1. However, for temperature between -20°C and 0°C, corresponding to most of the observations on the WFJ in winter, each of the α presented here are relatively similar (the values at -10°C are shown in the Table 1). The choice of the relationship for fractionating sublimation is thus of lower importance for our site (The WFJ). The relationships given by [Ellehoj et al., 2013] will be used in this thesis as it is based on recent measurements in the corresponding temperature range.

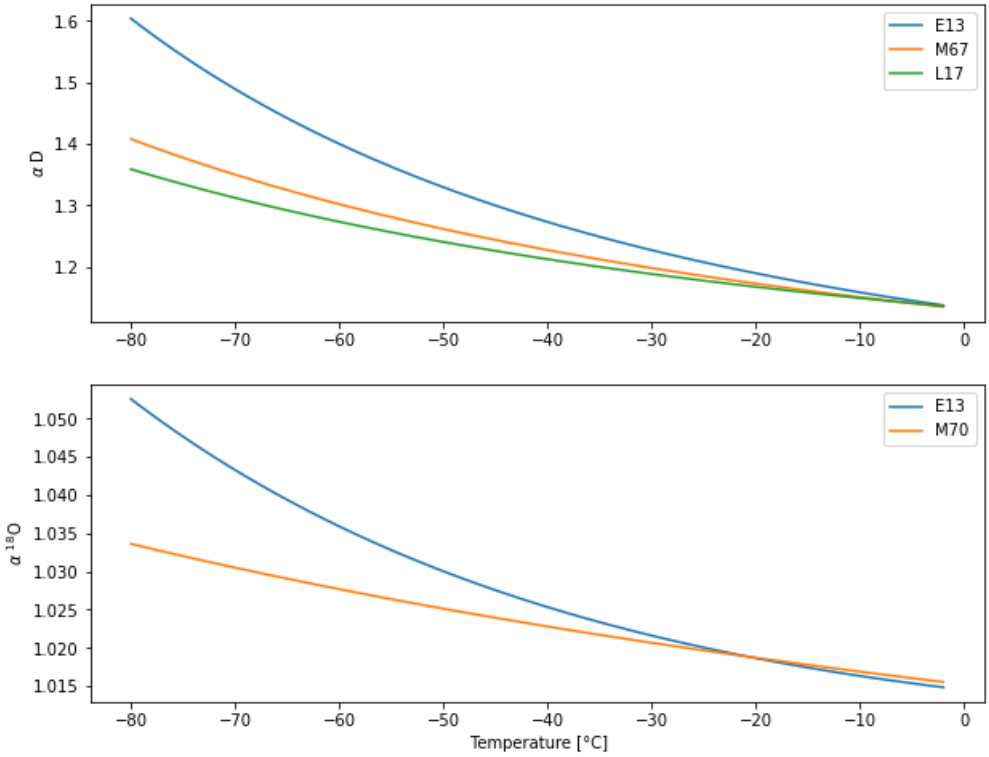

Figure 1: Comparison of the fractionation factor (α) from different studies: [Merlivat and Nief, 1967] (M67), [Majoube, 1970] (M70), [Ellehoj et al., 2013] (E13), [Lamb et al., 2017] (L17).

For studies in cooler environments, the choice of the empirical equation would have a stronger effect. This is for example the case when analysing samples from Antarctica, for which a comparison of the equations presented in Table 2 would be interesting.

2.4. Kinetic Fractionation

Kinetic fractionation occurs when the two phases cannot reach equilibrium. This is typically the case if the vapour above snow (or water) is transported away by turbulent fluxes [Sodemann, 2006]. The vapour at the very surface of the snow is at saturation and forms a transition zone where diffusive velocities are important. As diffusive velocity decreases with the weight of the molecule, each isotopologue will be subject to different fractionation effects. The importance of kinetic fractionation can be assessed using the second order parameter d-excess [Dansgaard, 1964] defined as:

$$d_{excess} = \delta D - 8 * \delta^{18}O \text{ [‰]} \quad (8)$$

The factor 8 directly comes from the GMWL defined in (4) and where d-excess is equal to 10 ‰. During a period with only sublimation or deposition (net flux in one direction), kinetic fractionation takes place [Dansgaard, 1964]. A precise estimate of the kinetic fractionation factor is relatively difficult and requires multiple parameters such as relative humidity gradients [Merlivat and Jouzel, 1979]. [Cappa et al., 2003] give a simplified estimation of the kinetic fractionation factor for water evaporation, which could be considered as an approximation for sublimation. However, [Chaar, 2020] showed that this approximation gives a kinetic fractionation factor very close to 1 (0.996 for δD). A value of 1 would equal equilibrium fractionation. For simplicity, sublimation and deposition are assumed to be equilibrium fractionation processes for the simplified model presented later (in 3.6). The validity of this assumption can partly be assessed by comparing the evolution of δD, $\delta^{18}O$ and d-excess of the snow samples.

3. Methodology

This work is based on three different datasets that were produced at different points in time: the 2017-, January 2020- and December 2020- datasets. This chapter presents the study site, the data, and the methods used in this work.

3.1. Study site

All the snow samples analysed and discussed in this thesis have been collected on the Weissfluhjoch test site (WFJ). The test site is situated on a flat area at 2536 m. a. s. l. (46°49′47″N 9°48′33″E) [SLF, 2020]. Mountain ridges approximatively 100 m higher are situated on three sides of the WFJ (a map is presented in Figure 2). The remaining South-East aspect is part of the slope of the Weissfluhjoch peak (hereafter, Weissfluhjoch or WFJ refers to the test site and not the peak). A small hill situated on the South-East makes the site relatively wind sheltered from all directions.

Long-term measurements have been conducted there [Marty and Meister, 2012] and meteorological data can be provided by [SLF, 2020] and [Weber, 2017]. Among them, air temperature (TA), snow surface temperature (TSS), snow height (HS) or relative humidity (RH) are measured continuously by automatic stations. In addition, new snow (HN), a second HS measurement and SnowMicroPen (SMP) probing are taken manually every morning.

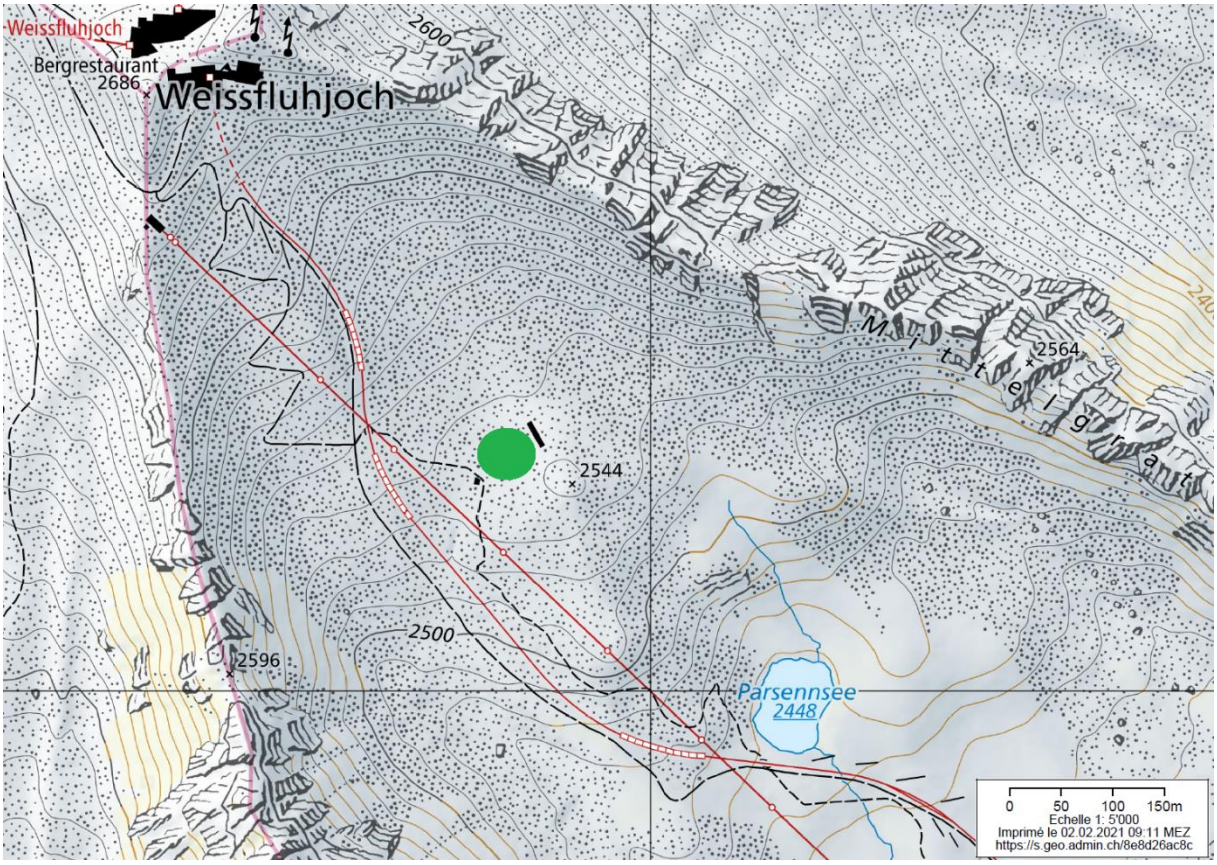

Figure 2: Map of the Weissfluhjoch. The green filled circle shows the location of the test site. map from: https://map.geo.admin.ch

3.2. SNOWPACK model

SNOWPACK [Lehning et al., 2002a], [Lehning et al., 2002b] was used during this thesis, in particular to compute latent heat fluxes and snow density. SNOWPACK is a physical, one-dimensional snow cover model. It computes the energy balance at the surface and bottom of the snowpack, as well as snow metamorphism and compaction. The snowpack is modelled as multiples small layers of various thicknesses. The snow characteristics (e.g. grain shape, grain size, density, liquid content, sphericity or dendricity) are modelled until complete melt for each layer. The figure below summarizes the main physical processes included in SNOWPACK.

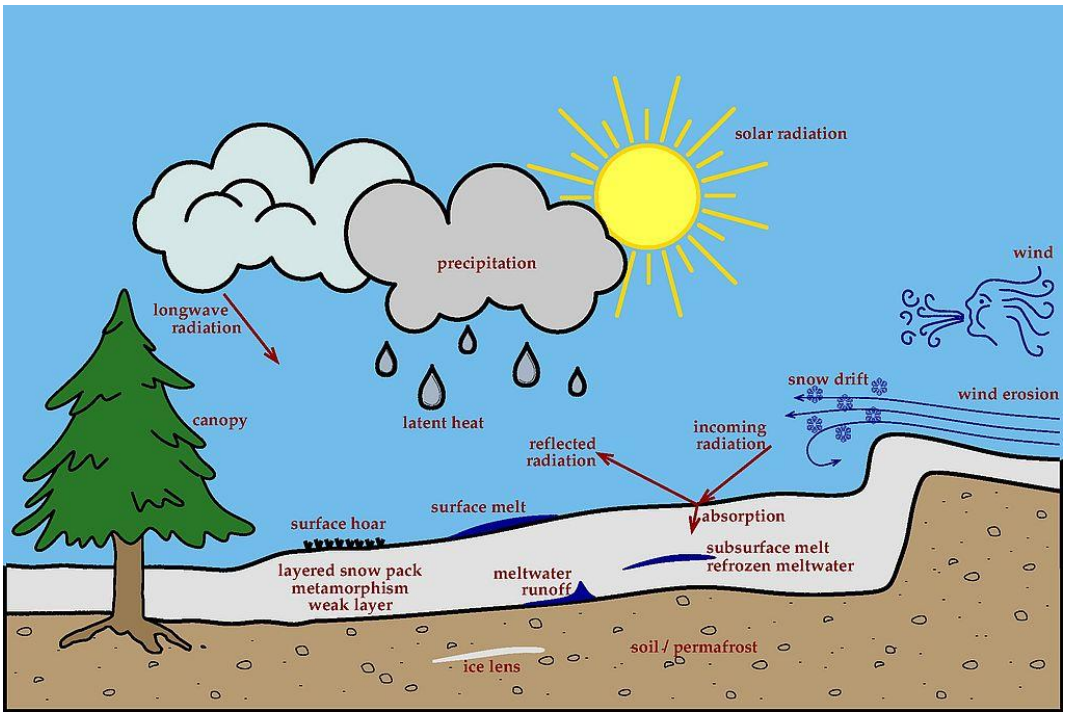

Figure 3: Overview of the main processes modelled by SNOWPACK. Image from [SLF, 2020].

The snowpack of the WFJ can be simulated using the data from the weather stations on the measurement site as input (air temperature, relative humidity, snow surface temperature, wind speed, short- and longwave radiation) [SLF, 2020], [Weber, 2017]. The SNOWPACK outputs are used for the analysis of each dataset. For the 2017 dataset, the output from the model run by [Trachsel, 2019] was used. For the 2020 datasets, SNOWPACK was run with a slightly different initialization, details are presented in appendix 7.4.1.

3.3. 2017 Dataset

The first dataset, referred to as the "2017 dataset", comes from the PhD thesis of Jürg Trachsel [Trachsel, 2019]. It consists of weekly 20 cm depth profiles collected on the WFJ (starting in February 2017). In addition, the 2017 dataset contains a continuous vapour isotopic composition measurement from the WFJ starting the 03.02.2017.

3.3.1. Snow isotope samples

The snow isotopic measurements consist of weekly 20 cm depth profiles with a 3 cm resolution between the 08.02.2017 and the 19.04.2017. In addition to each profile, 3 surface samples were collected and analysed (2 cm thickness). Figure 4 shows the profiles from February and March 2017 (plotted against manual HS). The high variability of HS during March makes the comparison from profile to profile

difficult as they correspond to different snow layers. In February, the HS variation is less pronounced and comparison between profiles might be possible. However, as shown by the sum of HN between profiles (green line in Figure 4), precipitation occurred and should not be neglected. Furthermore, compaction, sublimation and deposition from atmospheric vapour took place and should be considered while monitoring the snow isotopic composition of a given layer. Methodologies used to track a layer initially at the surface are presented in 3.3.5.

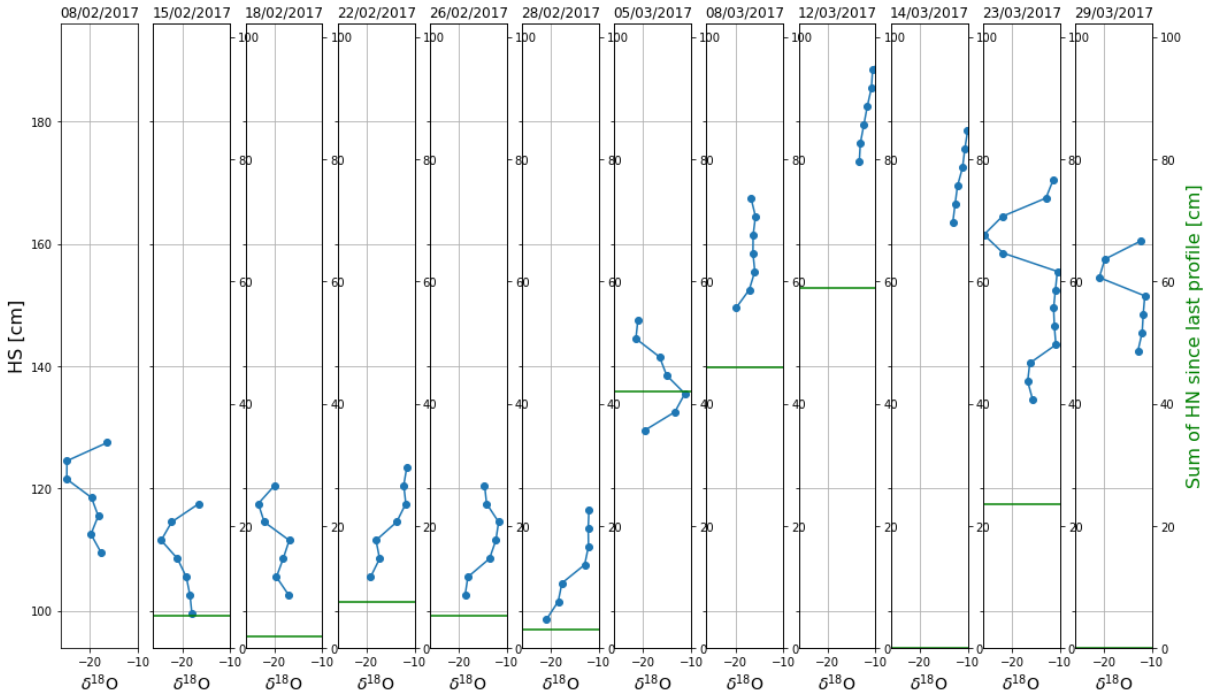

Figure 4: $\delta^{18}O$ (‰) profiles and new snow (HN) from the 2017 dataset. The green lines represent the sum of manually measured HN since the previous profile date (right axis). The profiles isotopic compositions are plotted against manually measured snow height (left axis).

3.3.2. Vapour isotopic composition

In 2017, vapour isotopic composition was obtained using a Picarro L2130-i placed on the WFJ, 2 m above the ground. The Picarro was calibrated daily during winter 2017 using three standards. A correction for the vapour mixing ratio was also applied. A more detailed description of the 2017 measurement campaign can be found in chapter 4 of [Trachsel, 2019] and in [Avak et al., 2019]. The air vapour isotopic composition for winter 2017 is presented and discussed in 4.1.1.

3.3.3. Snow and weather data

Meteorological data provided by [SLF, 2020], [Weber, 2017], and outputs from SNOWPACK run by [Trachsel, 2019] were used and compared to the measured snow isotopic composition. Details on some of those data are discussed below.

Snow height

The snow height (HS) is measured on the WFJ manually every morning and by automatic weather stations continuously. Those two HS measurements present a non-negligible difference (Figure 32 in appendix 7.3.1 illustrates this variation). The automatic measurements were used as SNOWPACK input and the modelled HS was forced toward their values (globally, the modelled and automatic HS are equal). Therefore, deviations between model and manual measurements are mainly due to differences

between manual and automatic measurements. To reach the targeted HS, the model can create or remove a layer of snow. This might create fictive precipitation during dry weather and the modelled new snow would be different from the measured HN. The significant difference between the manual measurements to the two other HS values (A mean difference during February and March 2017 of 10.25 cm is observed). This makes the layer tracking difficult as it will be discussed later.

Surface density

Density computed by SNOWPACK is used to calculate the snow water equivalent (SWE) of the snowpack, which helps track snow layers of interest. Globally, the modelled density is in good agreement with density derived from SMP measurements, but deviations can be found in some layers [Calonne et al., 2020]. SNOWPACK density at 1 cm depth is used as the snow surface density for the analysis of data from 2017.

New snow and temperature

To compare similar snow layer and observe a potential effect of sublimation, profiles without precipitation between sampling dates should be selected. Figure 5 shows the daily manual HN measurement (at 8:00 am) as well as the profiles dates. A period between the 23.03.2017 and the 29.03.2017 (4 sampling dates, including 2 when only surface samples were collected) can be selected. However, it should be highlighted that TA is above 0 °C inducing possible melt-refreeze processes. Therefore, it would be difficult to isolate sublimation since it is not the only explanation for changes in isotopic composition during this period. A discussion about those samples is done in 4.1.5.

Another option is to consider sublimation and deposition while a layer is at the surface. After burial, this layer could be tracked until the next profile is collected. Methodologies developed to explore this idea are presented in 3.3.5.

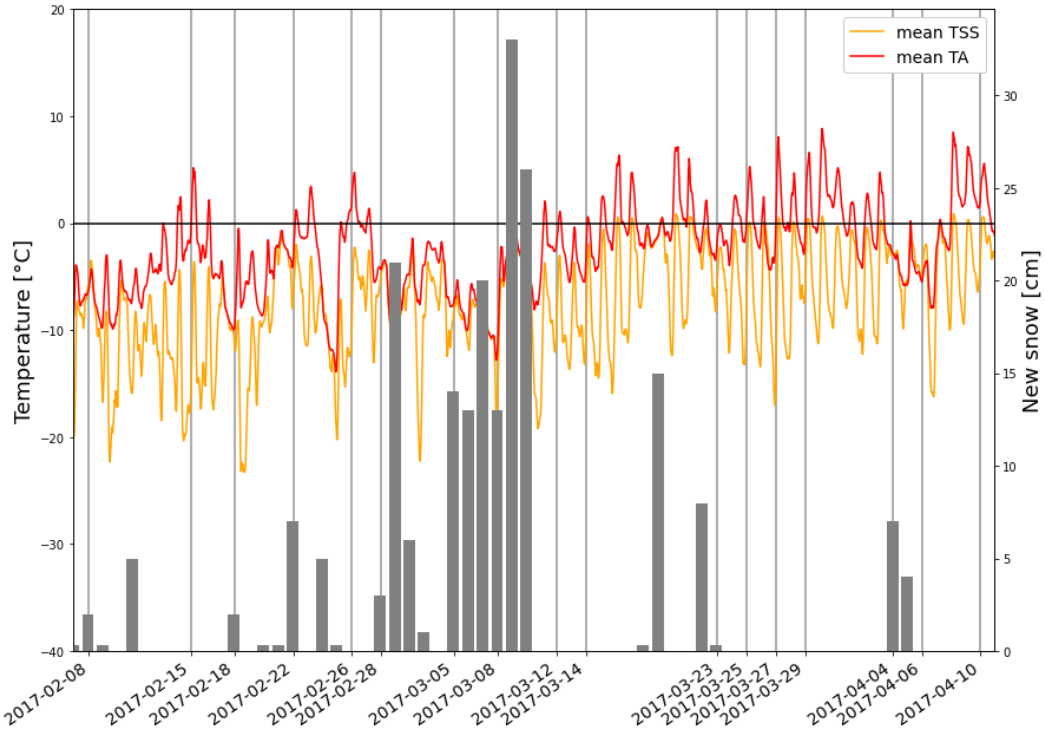

Figure 5: Manually measured new snow, air temperature, and snow surface temperature during the 2017 measurement campaign. The light grey verticals lines mark the dates when profiles (or surface samples) were collected.

3.3.4. Latent heat flux

To assess the effect of sublimation on the snow surface isotopic signal, an estimation of the latent heat exchange occurring between each sampling date should be calculated.

In case of precipitation occurring between sampling dates, only the latent heat exchange computed while the tracked layer is at the surface is considered to compare mini profiles. As soon as there is a new precipitation event, the latent heat exchange at the surface no longer concern the layer of interest. There would probably still be exchanges with the new snow layer, but there is no direct exchange with the atmosphere. As a first approach, it is assumed, that once buried, the snow isotopic composition does not change anymore. The date at which the layer is considered buried corresponds to the first date when the manual HN measurement gives at least 1 cm new snow (minus 12 hours since the measurement represents the last 24 hours). Several days are reported with HN=0.3 cm, usually corresponding to surface hoar deposition. Here, it is not considered as new snow but as atmospheric deposition.

The Sum of latent heat fluxes (Ql) are computed as:

$$Ql(t_{p1}, t_{p2}) = \sum_{i=p1}^{i=b} ql(t_i) * (t_i - t_{i-1}) \, [J\, m^{-2}] \tag{9}$$

Where b represents the time at which the layer is considered buried ($HN(t_b + 12h) \geq 1cm$), or if no precipitation occurred until the next profile date: $t_b=t_{p2}$, ql (W m^{-2}), is the latent heat flux at each SNOWPACK output timestep (t_i), t_{p1} and t_{p2} are the dates of the first and second profiles, respectively. The SNOWPACK output timestep (t_i-t_{i-1}) is of 3 hours for the 2017 dataset. Sum of negative and positive latent heat fluxes are also computed using (9) with only negative or positive ql, respectively.

In addition, SNOWPACK computes the sublimation and evaporation mass flux at each timestep. It allows to separate latent heat flux from sublimation (and solid deposition) to the one from evaporation (and liquid deposition). This is useful when the temperature gets above 0 °C. When sublimation and evaporation are summed, the results are very close to what could be obtained using the ql values.

3.3.5. Layer tracking

As already mentioned, precipitation occurred between most of the collected profiles in 2017. At each snowfall a new snow layer is at the surface, which makes the comparison between samples difficult. To monitor the isotopic composition of one sample originally at the surface, two methodologies were developed to track a layer after burial.

SWE conversion

Snow water equivalent (SWE) is an extensively used snowpack measurement. It represents the amount of water stored in the snowpack. SWE has the advantage of being independent of any compaction. Assuming negligible intra-snowpack vapour exchange, it is possible to calculate the SWE for different layers in the snowpack at a given time, and each layer should keep its SWE value until the melting season. Based on that, SWE can be calculated for the surface layer of a first profile, and the depth corresponding to this SWE on the second profile can be determined.

It must be noted that sublimation, evaporation, or deposition influence the SWE of the surface. Sublimation (and evaporation) up to about 1 kg m^{-2} representing 1 mm of SWE can be observed between profiles (visible in Figure 10, on p, 26). This value overestimates the potential error due to atmospheric exchanges because the layer of interest is no longer concerned by surface mass fluxes as soon as there

is precipitation. Furthermore, deposition compensates at least partly the reduction of SWE from sublimation and evaporation.

SWE for a layer L with a given height H, at time=t_k can be calculated using the following equation with ρ the density of snow or water and using ρ_{water} = 1000 kg m^{-3} :

$$SWE(L,t_1) = \int_{h=0}^{h=H} \rho_{snow}(h,t_k)\, dh * \frac{1}{\rho_{water}}\ [cm] \tag{10}$$

Using ρ_{snow} computed by SNOWPACK, at each time (t_k) each SNOWPACK layer (L_j) of height h_j can be converted to SWE (h_i the height of layer L_i in cm):

$$SWE(L_j,t_k) = \sum_{i=0}^{i=j} \rho_{snow}(h_i,t_k) * \frac{1}{\rho_{water}}\ [cm] \tag{11}$$

Knowing the height of a sample, the corresponding SWE can be determined using a linear interpolation from the SWE calculated for each SNOWPACK layer. The depth of each sample (D_{sample}) is available and can be converted to height using HS from manual or automatic measurements. As explained in 3.3.3, there is a significant difference between the automatic and manual HS measurements. This gives two distinct heights for each sample:

$$H_{sample}^{auto} = HS_{auto} - D_{sample}\ [cm] \tag{12}$$

$$H_{sample}^{manual} = HS_{manual} - D_{sample}\ [cm] \tag{13}$$

Since SNOWPACK heights correspond to HS_{auto}, a direct conversion to SWE is only possible using H_{sample}^{auto}. This conversion will be referred to as "*SWE conversion from automatic measurements*". To use the manual measurements, the height of each SNOWPACK layer should be adapted before the linear interpolation (otherwise the top samples are above the surface of the modelled snowpack). This second conversion will be referred to as "*SWE conversion from manual measurements*".

Various corrections for modelled heights and SWE have been tried and tested on monthly manual Hand Hardness (HH) profiles. HH allows to determine about 80% of the snow stratigraphy [Pielmeier and Schneebeli, 2003] and some of those layers can be observed over the whole season (called persistent layers hereafter) [Calonne et al., 2020]. Due to compaction, layers do not conserve the same height through the season. However, if the layers heights are converted to SWE, persistent layers should stay at relatively stable SWE values. The corrections for the modelled heights have been compared assuming that a good conversion would allow to retrieve similar HH against SWE profiles. The comparison is presented in appendix 7.3.2 and allowed to exclude some of the considered correction methods. It was decided to add a fictive layer with the surface density at the bottom of the modelled snow height. This allows to obtain the same HS as the manual measurements and some similarities between the HH against SWE profiles can be observed. Nevertheless, the method is far from perfect and potential error might come from this tracking method.

SNOWPACK layer tracking

The SWE conversion can present non-negligible differences depending on the methodology, and another approach using the layers created by SNOWPACK was tried. During precipitation, SNOWPACK creates layers of various thickness (usually between 1 and 4 cm) with specific snow properties (e.g. density, grain size, etc.). Each layer has a given identification number (elemID). During melt, layers at the surface are removed. The methodology presented here use the elemID of a first sample and retrieve its position on the next profile date.

Since the idea is to focus on surface fractionation processes, the surface layer of each profile is tracked until the next sampling date. Layers are added (or deleted) by step: For a threshold amount of precipitation (melt/sublimation), a layer is created (removed). Because of that, the top layer (representing the top of the snowpack) might be deleted during tracking even if sublimation is relatively small. For this reason, the second layer is tracked ($L_{tracked}$ hereafter). The difference between the height of $L_{tracked}$ ($H_{tracked}$) and the top of the snowpack is referred to as TH_{ini}: the initial thickness of $L_{tracked}$.

On the next profile date (t_{p2}), $H_{tracked}(t_{p2})$ is retrieved using elemID and can be corrected for TH_{ini} and for the fact that "surface" samples are centred at 1 cm depth. Only based on automatic measurement, the sample height $H_{sample}(t_{p2})$ can be calculated accounting for compaction with:

$$H_{sample}^{auto}(t_{p2}) = H_{tracked}(t_{p2}) + \frac{H_{tracked}(t_{p2})}{H_{tracked}(t_{p1})} * (TH_{ini} - 1)\ [cm] \quad (14)$$

$\frac{H_{tracked}(t_{p2})}{H_{tracked}(t_{p1})}$ is the ratio representing the simulated compaction of the snowpack under $L_{tracked}$ and will be referred to as the "compaction factor". A simple correction allows to consider the manual snow height measurements.

$$H_{sample}^{manual}(t_{p2}) = H_{tracked}(t_{p2}) + \frac{H_{tracked}(t_{p2})}{H_{tracked}(t_{p1})} * (TH_{ini} - 1\ ) + HS_{manual}(t_{p1}) - H_{auto}(t_{p1})\ [cm] \quad (15)$$

In (15), it is debatable whether the correction ($HS_{manual}(t_{p1})$-$HS_{auto}(t_{p1})$) should be multiplied by the compaction factor. First, it could be expected that the whole snowpack is compacted and the difference between the 2 measurements should be as well (as in (16)). By contrast, if the difference comes from systematic errors, or from an already very dense deep layer, the equation written as in (15) would make more sense. This difference in methodology can make a change of 1 or 2 cm, which already highly influences the estimation of the isotopic composition at the next profile.

$$H_{sample}^{manual}(t_{p2}) = H_{tracked}(t_{p2}) + \frac{H_{tracked}(t_{p2})}{H_{tracked}(t_{p1})} * (TH_{ini} - 1 + HS_{manual}(t_{p1}) - H_{auto}(t_{p1}))\ [cm] \quad (16)$$

Depths corresponding to H_{sample} (D_{sample}) can then be determined by:

$$D_{sample}^{auto}(t_{p2}) = HS_{auto}(t_{p2}) - H_{sample}^{auto}(t_{p2}) \quad and \quad D_{sample}^{manual}(t_{p2}) = HS_{manual}(t_{p2}) - H_{sample}^{manual}(t_{p2}) \quad (17)$$

The tracking is illustrated in Figure 6. If two profiles are not linked, the tracked layer was supressed of the SNOWPACK simulation between those two dates. This can happen because of melt or strong sublimation, which would mean that comparison between those samples is impossible. A comparison and discussion on the different tracking methods is done in 4.1.2.

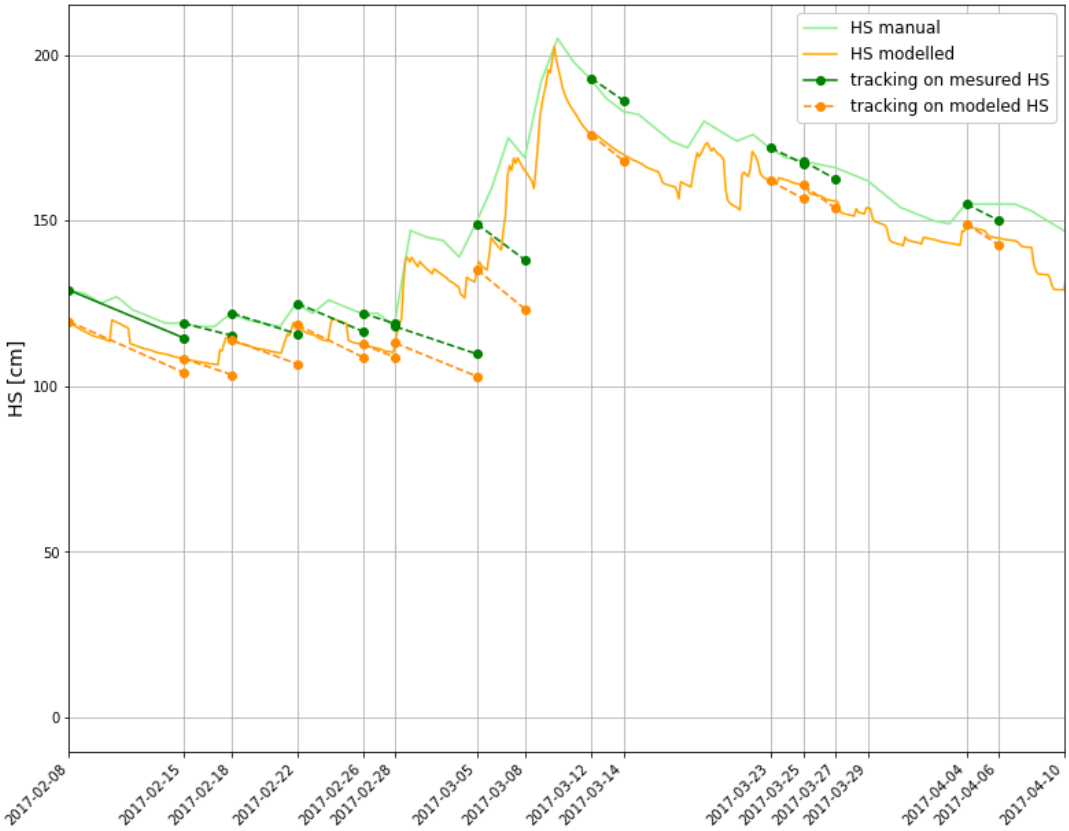

Figure 6: Tracking SNOWPACK layers with elemID. The green dotted lines show the tracking using the compaction simulated by SNOWPACK and the manually measured snow height calculated as H_{sample}^{manual} in (16). The orange dotted lines correspond to tracking using only the modelled height as for H_{sample}^{auto} in (14).

The SNOWPACK layer tracking method also allows to follow the evolution of snow density and grain size of a layer. For those parameters, no correction for height was attempted and only the tracked elemID is used. Variations of the snow density and grain size can be compared to changes in the isotopic signal.

Profile selection

Once the depth of the tracked layer at the second profile date is known, the new isotopic composition of that layer can be determined with a weighted mean of the two nearest samples. This gives an estimation of the change in isotopic composition happening between the two sampling dates.

While tracking layers, it is also possible to select the most interesting profiles. To have an idea of the influence of sublimation on snow isotopic composition, profiles supposedly mainly affected by sublimation and deposition should be selected. First, to separate the fractionation from sublimation to the one from melt-refreeze processes, only profiles between which TSS is constantly below -0.5 °C are kept. Second, to focus on surface processes, the tracked layer must be at least 30% of the time at the surface. Finally, the layer must be trackable. This selection allows to keep 6 profiles (5 in February and 1 in March). These data are used for a comparison with the latent heat flux and with the simplified model (presented in 3.6).

3.4. January 2020 Dataset

The second dataset analysed in this thesis is referred to as “January 2020 dataset”. It contains 3 daily surface snow samples for 12 consecutive days. On the top of it, air vapour isotopic composition was measured by the Piccaro placed on the WFJ in 2017.

3.4.1. Snow isotope samples

Snow surface samples were collected in January 2020 with the same methodology as in [Trachsel, 2019]. Three snow surface samples (2 cm thickness) were collected daily during 12 consecutive days (18.01.2020-29.01.2020). In addition, a 20 cm depth mini profile with 3 cm resolution was taken on the first day (18.01.2020). After collection in hermetically closed individual plastic tubes of 50 ml, the samples were stored in the -20 °C cold room at the SLF, Davos. The snow samples isotopic composition analysis was done in December 2020 at the WSL-Zentrallabor with an "LGR Off-Axis Integrated Cavity Output Liquid Water Isotope Analyzer" (LGR hereafter). Details on the snow isotopic composition analysis method are given in appendix 7.1.

3.4.2. Vapour isotopic composition

During winter 2019-2020, the Picarro installed on the WFJ in 2017 was still running, but not calibrated. Only a post-measurement correction based on the air vapour mixing ratio could be done. This correction is the same as the one developed for the results presented in [Trachsel, 2019] (2017 dataset). The procedure to define the correction using a dew point generator is described in [Aemisegger et al., 2012][1]. Details on this correction are given in appendix 7.1.3.

It should be noted that corrections for mixing ratio ($[H_2O]$) are also dependent on the isotopic composition itself [Thurnherr et al., 2020], and a correction that would also account for δD or $\delta^{18}O$ instead of only $[H_2O]$ would be more accurate. However, this would require a new dewpoint experiment with additional standards. Such a modification of the correction would only have a small impact on the results presented here.

3.4.3. Snow and weather data

Similarly to the 2017 dataset, meteorological data provided by [SLF, 2020] and outputs from SNOWPACK were used and compared to the snow isotopic composition. Details on some of those data are discussed below.

Surface density

Because snow surface samples are collected with a constant thickness (2 cm), the measured effect of deposition and sublimation depends on the snow density. For example, the effect of fractionating deposition will be more "diluted" in a very dense surface layer. Therefore, a good estimation of the density is important when comparing snow surface samples. Density computed by SNOWPACK on the very surface is not always very accurate. To determine snow density, a density cutter is often used. Nevertheless, this technique is not precise with light snow as it gets compacted during the measurements [Proksch et al., 2016]. During January (and December) 2020, SMP measurements were done on the WFJ. Those data were used to compute snow density with the procedure from [Proksch et al., 2015] explained in appendix 7.2. However, those density measurements are also less precise for light snow [Proksch et al., 2015], and results have to be used cautiously. A comparison with SNOWPACK density values is presented in appendix 7.2. This comparison helped select a surface density approximation that seemed coherent. The SNOWPACK density at 5 cm depth was selected as the surface density for the January 2020 analysis. Those surface density values are used with the simplified model (see chapter 3.6) and can have a significant effect.

[1] The correction is specific to each individual device, and it must be noted that the one used for the Picarro placed on the WFJ is different to the one presented in [Aemisegger et al., 2012].

New snow

Daily manual new snow measurements allow to see when precipitation occurred. Even small snowfalls of 1 cm day^{-1} have a strong impact on the measured surface isotopic composition (the thickness of the sample is ~2 cm). Figure 7 shows that snowfalls were registered before the 20.01.2020 and after the 25.01.2020. Therefore, further analysis will focus on the dates in between. The air temperature rose slightly above 0°C, during that period. However, the snow surface stayed well below 0°C the whole time and it seems reasonable to assume that there was no melting.

For days with precipitation, a comparison between the snow surface and the vapour isotopic composition can give information on whether falling snow is in isotopic equilibrium with the surrounding vapour. The manually measured SWE of the new snow (taken at the same time as the HN measurement) can be used to assess more precisely the mass and density of the new snow.

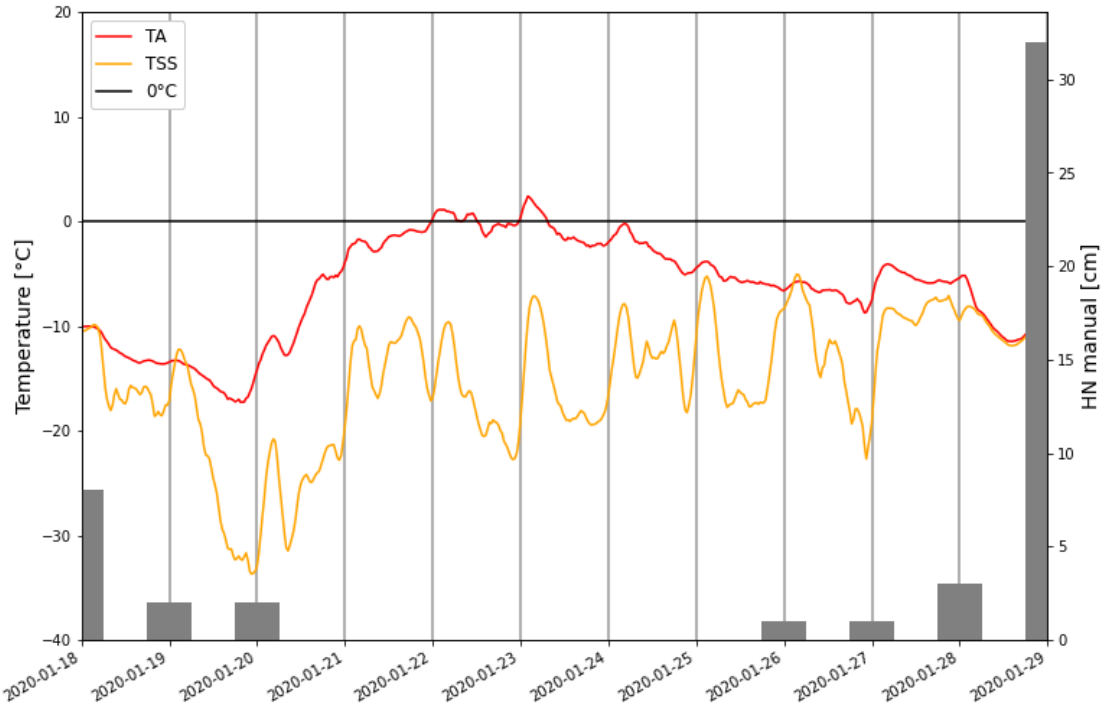

Figure 7: Manually measured new snow, air temperature, and snow surface temperature during January 2020.

3.4.4. Latent heat flux

An important parameter for the latent heat flux computed by SNOWPACK is the surface boundary condition (BC). When Neumann BC is selected, the computed heat fluxes serve as boundary condition. When Dirichlet BC is chosen, the snow surface temperature is fixed by the measured TSS. This influences the heat flux computation [Morin et al., 2020]. Both BC approaches were compared over the period of interest and show similar behaviours (the comparison is illustrated in appendix 7.4.1). Neumann BC gives a globally more negative latent heat flux, and the difference comes from the use of the Monin-Obukhov theory. The vapour pressure at the snow surface is needed and considered at saturation. The saturation vapour pressure is directly related to TSS and therefore to the choice of the BC. When Neumann BC is used, TSS is calculated from the energy balance and is influenced by the variability of the measured short and long wave radiations. The latent heat flux would be more negative with Neumann BC if the computed TSS is higher than the measured one. Since TSS is available and considered reliable, Dirichlet BC was used (as in [Schmucki et al., 2014] or [Stössel et al., 2010]), for TSS < -1 °C.

Another way to obtain latent heat fluxes value is to use sonic anemometer measurements. Since these devices are already placed on the WFJ, the latent heat flux from SNOWPACK could be compared. Unfortunately, data from sonic anemometers were not available during the periods studied in this work. They would present a great improvement for future sampling campaigns. Nevertheless, studies from [Stössel et al., 2008], [Stössel et al., 2010] showed that SNOWPACK gives a reliable estimation of the latent heat flux on the WFJ.

The computed latent heat flux is compared to changes in snow surface isotopic composition. This allows to observe potential effects from sublimation and/or deposition. The simplified model (presented in 3.6) also requires an estimation of the latent heat exchange.

3.5. December 2020 Dataset

The December 2020 dataset consists of samples collected as part of this thesis. This sub-chapter gives a description of the measurement campaign.

3.5.1. Measurement campaign

The point of this measurement campaign is to focus on surface snow isotopic signal change during a period without precipitation. For that, samples of two different thicknesses (~2 cm and ~1 cm) were collected twice a day in two different locations on the WFJ for 8 consecutive days (14.12.2020-21.12.2020). In addition, mini profiles were collected every two days.

Sampling sites

All the samples were collected on the WFJ. Two sampling sites were chosen in order to capture potential changes in isotopic signal due to a higher wind exposition. Stronger wind is expected to potentially transports snow, which would modify the snow surface layer. In addition, it increases the latent heat exchange.

The first site considered as **wind sheltered** is situated next to the WFJ measurement field and protected by a small hill on the South-East. The second site is considered as **wind exposed** and situated on the small hill on the South-East of the wind sheltered site. A map is available in appendix 7.5.1.

Surface snow sample

Two different types of snow surface samples were collected: **The 2 cm surface samples** were collected similarly to the 2017 and January 2020 datasets. They were directly collected in 50 ml plastic tubes of 3 cm diameter, where the top ~2 cm was filled with snow from the surface. Because of the circular entrance of the tube (a picture is available in appendix 7.5.1), the 2 cm thickness is not uniformly collected (more snow is collected on the top 1 cm than below). However, this method was kept because it can be compared to the other datasets. Moreover, it is easy to reproduce and to avoid contamination of the samples.

The 1 cm surface samples were collected using a spatula. The idea was to collect a uniform 1 cm layer. For that, ledges were put on each side of the spatula (the width between the ledges corresponds to the diameter of the plastic tube). Pictures are available in appendix 7.5.1. The 1 cm snow samples were then stored in 50 ml plastic tubes. The transfer from the spatula to the tube is relatively difficult, and a non-uniform 1 cm thickness sample is to be expected if the whole amount of snow on the spatula does not end up in the tube.

Twice a day (morning (around 8:00) and afternoon (around 16:00)), three of each of the surface sample were collected on each site (24 surface samples per day). This was done for 8 consecutive days (14.12.2020-21.12.2020), corresponding to a period (almost) without precipitation.

Mini profiles

Mini profiles similar to the ones collected for the 2017 dataset [Trachsel, 2019] were taken on each site every 2 days. 14.12.2020-22.12.2020, (10 mini profiles).

Those profiles have a 3 cm resolution over 20 cm depth (7 samples). The top samples are corresponding to the top ~2 cm like the 2 cm surface samples. Collection was done using the 50 ml plastic tubes and a template allowing to place each of the tube relatively precisely (+/- 0.5 cm). Pictures in Figure 8 help visualize the procedure.

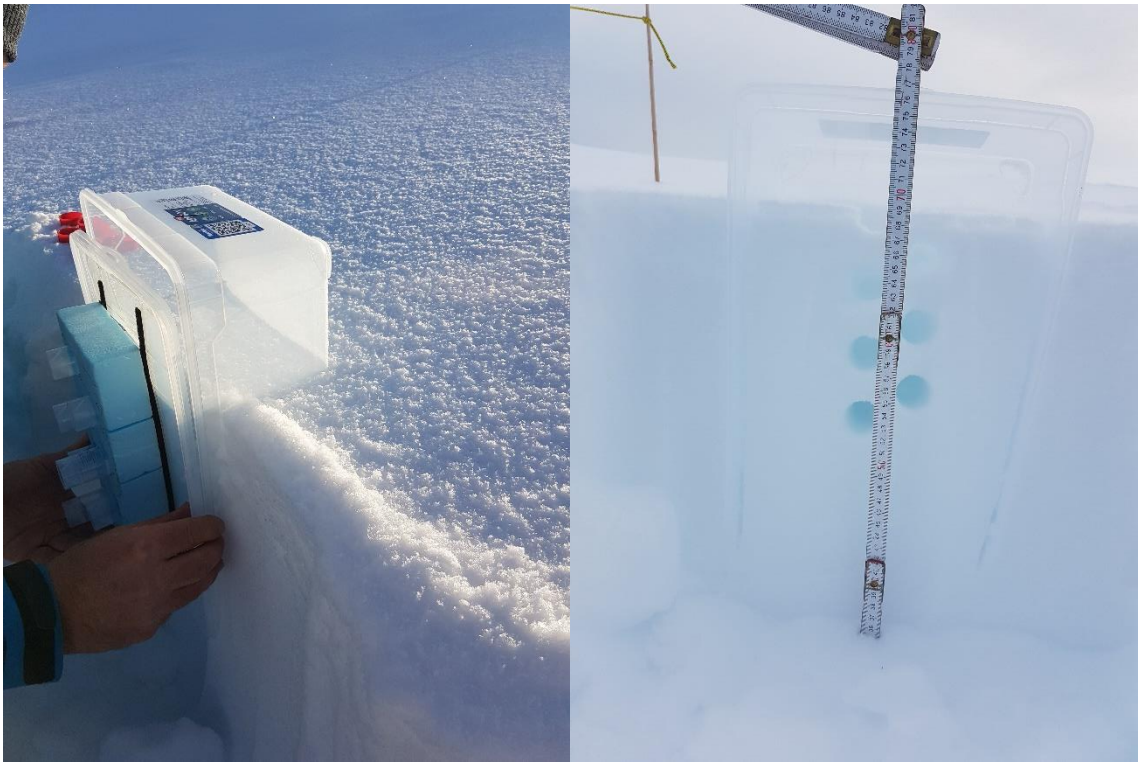

Figure 8: Pictures of the mini profile template (left) and of the mini profile after removal of the tubes (right).

Snowfall signal

On each day following precipitation, new snow was collected in the morning (starting the 05.12.2020). This can allow to observe potential post-depositional isotopic changes and assess the variations of the snowfall isotopic signals. For large snowfalls, a cylinder was used to collect a constant amount over the whole depth of new snow. The snow was then stored in sealed plastic bags. For smaller snowfall (up to ~9 cm), the 50 ml plastic tubes could be used.

After the precipitation-free period (on the 22.12.2020), the new snow (9 cm) was collected one last time together with two mini profiles and the usual surface samples (1 and 2 cm). This can help assess whether the new snow as a uniform isotopic composition over depth and space. The mini profiles might allow to observe an influence of the precipitation on the old snow isotopic composition.

Complementary measurements

In addition to the snow samples, **snow height** (HS) was measured daily on both sites (wind sheltered, and wind exposed) by probing. Two other probes were left (one on each site) and the indicated snow height values were registered daily.

On the wind sheltered site, a **camera** was installed and took a picture every 10 minutes during the following dates: 15.12.2020 11:00 - 17.12.2020 11:00 and 20.12.2020 14:00- 22.12.2020 14:00. A

failure of the memory card is responsible for the gap in-between. The pictures help identify potential snow deposition, snow transported by the wind or precipitation.

3.5.2. Snow surface changes

A quick overview of the meteorological and snow surface conditions observed during the sampling campaign is presented in Figure 9. It includes observations from the camera and HS measurements on the wind sheltered site. In addition, wind velocity TA and TSS are plotted because of their direct influence on the snow surface.

The observations from the camera allow to classify different periods: if (almost) no change of the snow surface is visible, it is classified as “calm and dry” (green background in Figure 9); if small changes of the surface are visible, but the main features remain similar, it is classified as “possible snowfall” [2] (orange in Figure 9); If changes of the snow surface are easily visible, it is classified as “visible new snow” (red in Figure 9). The field observations done while collecting the snow samples correspond well to what could be said from the camera.

[2] Wind could also explain small changes. However, from the wind velocity, HN measurements and field observations, those periods are more likely to be influenced by very small snowfalls.

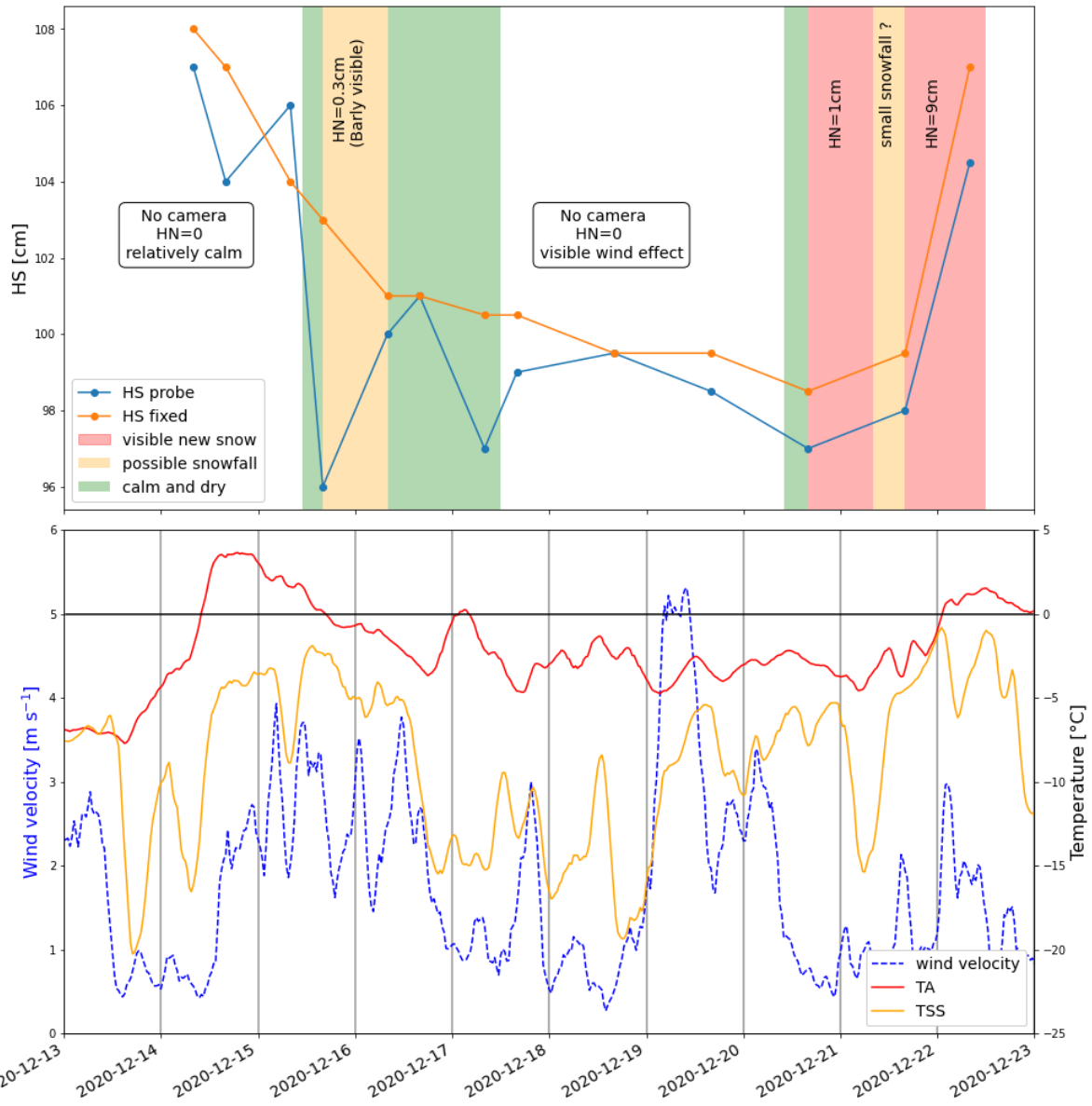

Figure 9: overview of the snow surface conditions during the December 2020 sampling campaign. On the first panel, the HS measured on the wind sheltered site are plotted: the blue line (HS probe) corresponds to probing on a random position of the side of the site. The orange line (HS fixed) is the value surveyed on the fixed probe (constant position). The sub-plot background colours (red, orange, green) correspond to observations from the camera (more details are given in the text). The second panel presents the wind velocity and temperature measured on the WFJ and averaged with a 3-hours moving window.

Before the camera was installed (on the 15.12.2020), very small wind effects were observed. Nevertheless, they can probably be neglected for this analysis (a few particles were drifting, and a very small and loose wind crust could be observed).

The new snow of 3 mm registered on the 16.12.2020, could have a small impact on the next samples. From the camera, there is almost no visible change of the snow surface. The very thin and light new snow might have been blown away before the light was good enough to compare the snow surface from two pictures (around 9:40 am). The pictures used for this remark are shown in appendix 7.5.2.

During the period without camera (17 to 20 of December) no precipitation was registered. However, surface hoar was observed on the 18.12.2020 and 19.12.2020 (~ 3 mm and ~ 5 mm, respectively). In addition, relatively strong wind influenced the snow surface on the 19.12.2020.

During the evening of the 20.12.2020, small snowfalls were observed and influenced the snow surface (registered as 1 cm HN and visible on the camera). Samples collected on the 21.12.2020 should be analysed considering this. The snowfall (9 cm HN) from the night of the 21-22 of December totally renewed the snow surface.

Globally, the snow surface is relatively unchanged between the 14.12.2020 and the 20.12.2020. Analysis of the snow isotopic signal should not be impacted by new snow (apart possibly on the 16.12.2020 in the morning). Wind drifted snow can have an impact and could explain a potential change in the signal on the 19.12.2020.

3.6. Equilibrium fractionation model

To estimate the expected effect of an equilibrium fractionation situation, a very simplified model was developed. The details are given for the model used for the 2017 dataset. Small adaptation for the surface samples of the 2020 datasets, are presented afterward.

3.6.1. Simplified model

A 2 cm thick snow layer corresponding to the surface sample of a first profile is considered well mixed. Its isotopic composition is only modified by equilibrium fractionation from sublimation or deposition. The model is basically solving the following equation:

$$\frac{\partial N_i}{\partial t} = DEP_i(t) - SUB_i(t) \qquad i = H_2O, HDO, H_2^{18}O \tag{18}$$

With N_i the number of molecules of i in the 2 cm surface layer, DEP_i and SUB_i, the number of molecules of i deposited and sublimated.

The model computes the evolution of the mass of the 2 cm surface layer and its isotopic composition written δ^{18}_{mod} (for $\delta^{18}O$) at each timestep (t_i) until burial. The same approach can be used for HDO (not presented here). Burial time (t_{burial}) is defined as the first time 1 cm of new snow is manually measured (minus 12 hours, like for the latent heat flux computation discussed in 3.3.4). The change in mass (m) of the 2 cm thick layer due to sublimation or deposition can be written as:

$$\frac{\partial m}{\partial t} = ql(t) * L_{sub}(TSS(t)) \quad [kg\, m^{-2} s^{-1}] \tag{19}$$

The mass exchanged at each timestep (m_{exch}) can be computed using dt corresponding to the output timestep of SNOWPACK (3 hours for the 2017 dataset and 30 minutes for the 2020 datasets):

$$m_{exch}(t_i) = ql(t_i) * L_{sub}\big(TSS(t_i)\big) * dt \quad [kg\, m^{-2}] \tag{20}$$

With L_{sub} (J kg^{-1}), the latent heat of sublimation as a function of the snow surface temperature (TSS °C), computed using an empirical quadratic fitting based on [Yau and Rogers, 1996]:

$$L_{sub}(T) = (2834.1 - 0.29 * T - (0.004 * T^2)) * 1000 \ [J\, kg^{-1}] \tag{21}$$

The initial mass of the modelled layer $m(t_{p1})$ is calculated using ρ_1 kg m^{-3} the snow density at 1 cm depth and d the thickness of the surface layer (2 cm):

$$m(t_{p1}) = \rho_1(t_{p1}) * d \ \ [kg\ m^{-2}] \tag{22}$$

The new mass at each timestep is calculated as:

$$m(t_i) = m(t_{i-1}) + \ m_{exch}(t_i) \ \ [kg\ m^{-2}] \tag{23}$$

The initial isotopic composition ($\delta^{18}_{mod}(t_{p1})$) is known from the average of the 4 surface isotopic measurements. δ^{18}_{mod} is updated at each timestep. **In case of deposition** (positive latent heat flux and mass exchange), the mean measured vapour isotopic composition [3] of each timestep is used and assumed constant (during that timestep). For simplicity, the mean molecular weights of the surface layer and of the exchanged mass are considered equal:

$$\frac{\sum_i \ N_{i,mod} * M_i}{\sum_i \ N_{i,mod}} \cong \frac{\sum_i \ N_{i,exch} * M_i}{\sum_i \ N_{i,exch}} \qquad i = H_2O, HDO, H_2^{18}O \tag{24}$$

Where $N_{i,mod}$ and $N_{i,exch}$ are the number of molecules i in the modelled layer and the exchanged mass. M_i is the molecular weight of i. This simplification has a very small influence on the next equation: (e.g. for an isotopic composition of ($\delta^{18}O$ = -10 ‰, δD = -80 ‰) or of ($\delta^{18}O$ = -30 ‰, δD = -240 ‰), the relative mass difference is 5.8 * 10^{-4} %).

The isotopic composition computation for each timestep can be written as:

$$\delta^{18}_{mod}(t_i) = \frac{1}{m(t_i)} * \left(m(t_{i-1}) * \delta^{18}_{mod}(t_{i-1}) + \ m_{exch}(t_i) * \delta^{18}_{exch}(t_i)\right) \ [‰] \tag{25}$$

Where δ^{18}_{exch} is the isotopic composition of the exchanged (deposited) mass, that is calculated using (2),(5) and the equilibrium fractionation (α) given by [Ellehoj et al., 2013] in Table 2:

$$\delta^{18}_{exch}(t_i) = (\alpha^{18}_{s-v}(TSS(t_i)) * \left(\frac{\delta^{18}_{vap}(t_i)}{1000} + 1\right) - 1) * 1000 \ [\ ‰] \tag{26}$$

$\delta^{18}_{vap}(t_i)$ is the 3 hours average vapour isotopic composition (2 m above ground).

In case of sublimation (negative latent heat flux), and assuming sublimation at equilibrium with the "well mixed" layer (2 cm for $t=t_{p1}$), a Rayleigh distillation model can be used [Gat, 1996], [Sodemann, 2006]. Since the timesteps are relatively short (maximum 3 hours) and the mass exchanged during one timestep is relatively small compared to the mass of the sample, the mean molecular weight can be approximated as constant (N the total number of molecules in the layer):

$$\frac{N(t_i)}{N(t_{i-1})} \cong \frac{m(t_i)}{m(t_{i-1})} \tag{27}$$

Using (2),(6) and (27), the distillation model can be written in δ notation as:

[3]The air isotopic composition was measured for the 2017 and January 2020 datasets. For December 2020), deposition can be simulated as an addition of mass with the isotopic composition of the modelled snow surface layer.

$$\delta^{18}_{mod}(t_i) = (\delta^{18}_{mod}(t_{i-1}) + 1000) * \left(\frac{m(t_i)}{m(t_{i-1})}\right)^{\alpha^{18}_{v-s}(TSS(t_i))-1} - 1000\ [\text{‰}] \quad (28)$$

Because the assumption of a well-mixed 2 cm layer is discussable, the model can also be run using (25) and considering that the sublimation flux is captured in the air isotopic signal as:

$$\delta^{18}_{exch}(t_i) = \delta^{18}_{vap}(t_i) \quad (29)$$

However, assuming that the sublimation mass flux is the main vapour source 2 m above ground is also not very realistic. The well mixed assumption of 2 cm (as initial starting point of the model) comes from the thickness of the samples collected. For analysis, a sample is completely melted and mixed, and no data are available for thinner layers. If not specified differently, equation (28) is used. The use of a Rayleigh distillation model as in (28) or assuming a constant isotopic composition (during the timestep) as in (25) has a negligible impact because of the relatively small mass flux at each timestep compared to the mass of the sample.

Changes in isotopic composition are analysed in 4.1.4 and are simply calculated for each profile date as:

$$\delta^{18}_{difference} = \delta^{18}_{mod}(t_{burial}) - \delta^{18}_{mod}(t_{p1})\ [\text{‰}] \quad (30)$$

This model is very simplistic and aims to assess what changes in isotopic signal could be expected from equilibrium fractionation with sublimation and deposition. Differences with measurements are to be expected.

3.6.2. Modified model

A very similar model was used for the surface samples of March 2017 and for the January 2020. A simplification is possible as no precipitation occurred between the samples, so the time of burial do not need to be considered and the total latent heat exchange occurring between two sampling dates can be used (t_{burial}=$t_{next\ sample}$).

All the surface samples have a thickness of 2 cm, which might not represent the exact same layer at each date. Effects from compaction and sublimation can be partly accounted for by adding a contribution from the layer below the surface. This was tried at the end of the simulation (at t=t_{p2} corresponding to the next sampling date).

$$\delta^{18}_{mod}(final) = \frac{1}{m(t_{p2}) + m_{LL}} * \left(m(t_{p2}) * \delta^{18}_{mod}(t_{p2}) + m_{LL} * \delta^{18}_{lower\ layer}\right)\ [\text{‰}] \quad (31)$$

With m_{LL} the mass exchanged with the lower layer, computed as:

$$m_{LL} = \rho_1(t_{p2}) * d - m(t_{p2})\ [kg\ m^{-2}] \quad (32)$$

The equation (31) is only used if m_{LL}>0.

The isotopic composition of the lower layer must be approximated with the available data. This is explained for each dataset in the next sub-chapters. Each dataset has been tested using the model with and without the contribution from the lower layer. They are referred to as the modified model and the simplified model, respectively.

March 2017

For March 2017, on the first and last dates of the 4 surface samples considered, mini profiles were collected. This allows to have an idea of the isotopic signal evolution below the surface. The isotopic composition of the lower layer is determined as followed.

The lower layer is assumed to have an isotopic composition corresponding the average of the top sample (0-2 cm depth, written δ_{1cm}) and the second sample (2-5 cm depth, written $\delta_{3.5cm}$). This layer is assumed to follow a linear change between the two profiles (23.03.2017 written D0 and 29.03.2017 written D6). Using D the number of days since D0, it can be written as:

$$\delta^{18}_{lower\ layer}(D) = (6 - D) * \frac{\delta^{18}_{1cm}(D0) + \delta^{18}_{3.5cm}(D0)}{2} + D * \left(\frac{\delta^{18}_{1cm}(D6) + \delta^{18}_{3.5cm}(D6)}{2}\right) [‰] \quad (33)$$

The contribution is then added to the model result using (31).

January 2020

In January 2020, snowfalls of 2 cm day^{-1} occurred during the two days following the first measurements. The snow layers corresponding to the first and second surface samples were buried and can give an approximation of the isotopic composition below the surface. The lower layer isotopic composition is defined as the average of the surface samples form the two first days of measurements. In other words:

$$\delta^{18}_{lower\ layer} = \frac{\delta^{18}_{1cm}(18) + \delta^{18}_{1cm}(19)}{2} [‰] \quad (34)$$

With $\delta^{18}_{1cm}(18), \delta^{18}_{1cm}(19)$ the mean snow surface isotopic composition measured on the 18.01.2020 and 19.01.2020, respectively.

In a second time, the model was modified to consider the small precipitation at the beginning and at the end of the sampling campaign as deposition. This was simply done by considering the precipitation at isotopic equilibrium with the measured vapour isotopic composition. The equilibrium fractionation factor was calculated using the mean TA of the day. The mass deposited was defined by the manually measured SWE of new snow. For 2 cm of new snow, the snow surface is considered completely renewed, and the model result is replaced by the estimated snowfall composition. For 1 cm of new snow half of the surface layer is considered renewed.

4. Results and discussion

This chapter presents the results from each dataset separately. A discussion is done in 4.1 for the 2017 dataset and in 4.2 for the January 2020 dataset.

4.1. 2017 Dataset

This sub-chapter presents the results obtained with the 2017 dataset. Their validity and significance are discussed. Finally, some details on what would help assess the effect of sublimation on snow isotopic composition during a new measurement campaign are given.

4.1.1. Results overview

This sub-chapter is an overview of the snow and air isotopic composition measurements of 2017. They are compared to meteorological data and snow properties to identify potential processes affecting the snow surface isotopic signal. Figure 10 allows this comparison and details about the plotted data are given below.

Data presentation

In the top panel of Figure 10, the snow surface isotopic composition is the average of the 4 surface samples collected with each profile. The air isotopic composition is averaged between the two profile dates (what is referred to as air isotopic composition, is the isotopic composition of vapour contained in the air). Due to unreliable vapour isotopic measurements between the 4 and 13 of March 2017, there is a gap between the 05.03.2017 and 12.03.2017 profiles. Air vapour mixing ratio ([H_2O] air in ppmv) is also averaged between two profiles.

Equilibrium values for snow (snow that would be at equilibrium with the measured vapour isotopic composition) are calculated using the fractionation factor (α) from [Ellehoj et al., 2013] presented in Table 2 (chapter 2.3). α is calculated at each time step (using TSS of that time step) and converted to δ values using equations (5) and (2). Finally, the δ values are averaged between the two profile dates. Equilibrium values for air (vapour that would be at equilibrium with the measured snow isotopic composition) are calculated similarly.

In the second panel, snow density, grain size and wind speed are averaged between two profiles dates. Snow density and grain size come from SNOWPACK, where values at 1 cm depth have been selected.

In the third panel, mass changes are computed from the mass fluxes provided by SNOWPACK and integrated between two profile dates. The sublimation and evaporation mass fluxes are used, which means that “sublimated mass” includes the mass lost by evaporation. This becomes significant when temperatures rise above 0 °C and must be kept in mind as fractionation might occur because of melt/refreeze or evaporation processes rather than sublimation.

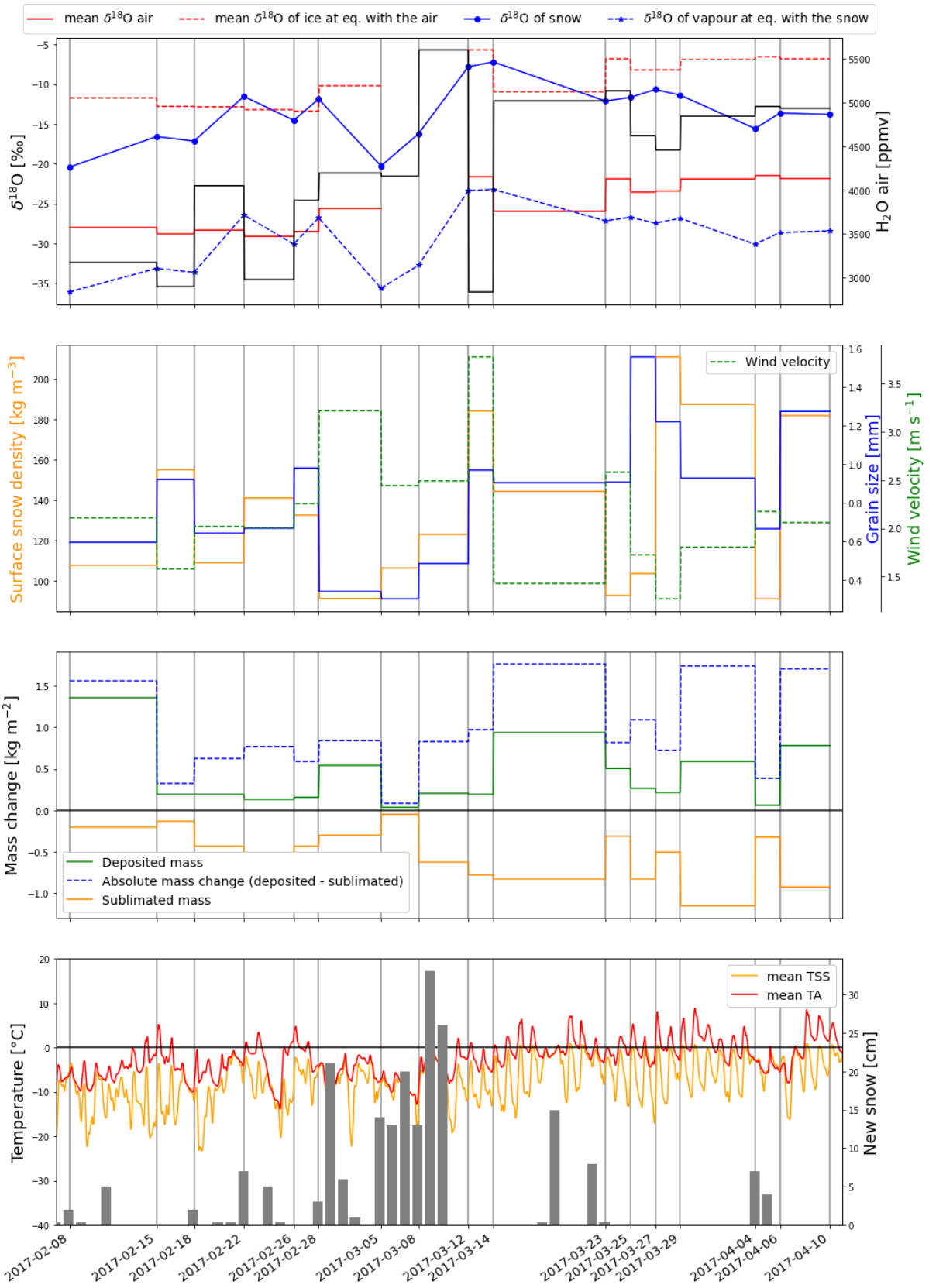

Figure 10: Meteorological data summary. Step functions represent average or sum between two profiles. Where there is no legend, the colour of the line is the same as the one of the corresponding axis. The light grey verticals lines mark the dates when profiles (or surface samples) were collected. Please, see the text for more details.

First observations

On the first panel of Figure 10, the comparison of the calculated equilibrium and measured values shows that air and snow are relatively close to equilibrium for $\delta^{18}O$. Globally, snow is slightly depleted compared to an equilibrium situation with the fractionation factor from [Ellehoj et al., 2013]. If fractionation occurs during deposition, it will result in a small overall isotopic enrichment of the snow surface. On the contrary, a depletion would be expected if deposition was a non-fractionating process.

On the second panel, snow surface density and grain size, which are linked to snow metamorphism processes [Colbeck, 1982], seem behave relatively similarly to the changes in the surface snow isotopic composition. Lighter, more recent snow, with smaller grain size is usually more depleted. Both processes are probably linked to the age of the snow surface and to the surface heat exchanges. A more detailed analysis should be done as Figure 10 is only a coarse overview and the distinction between each of the processes is difficult. This is quickly discussed later in this chapter, but no clear connection between snow surface metamorphism and isotopic change could be determined.

On the third panel, there is no evidence of a link between mass exchanges and evolution of the surface isotopic composition. However, new precipitations create new surface layers with different isotopic compositions. The isotopic signal of a given snow layer is mainly driven by the source of air moisture at the origin of the precipitation [Trachsel, 2019]. Therefore, the layer tracking methods (presented in 3.3.5) should be used to assess the changes in the snow isotopic signal.

4.1.2. Layer tracking comparison

The different layer-tracking methods are compared in the sub-chapter. It allows a first comparison between snow isotopic profiles.

SWE conversion

The two SWE conversions allow to compare isotopic profiles. Only the profiles from February are plotted in Figure 11 and Figure 12. Those are the most interesting profiles as temperatures are below 0 °C most of the time, and SWE values are very similar allowing comparisons. Due to increased precipitation in March, most of the profiles collected afterward cannot be compared.

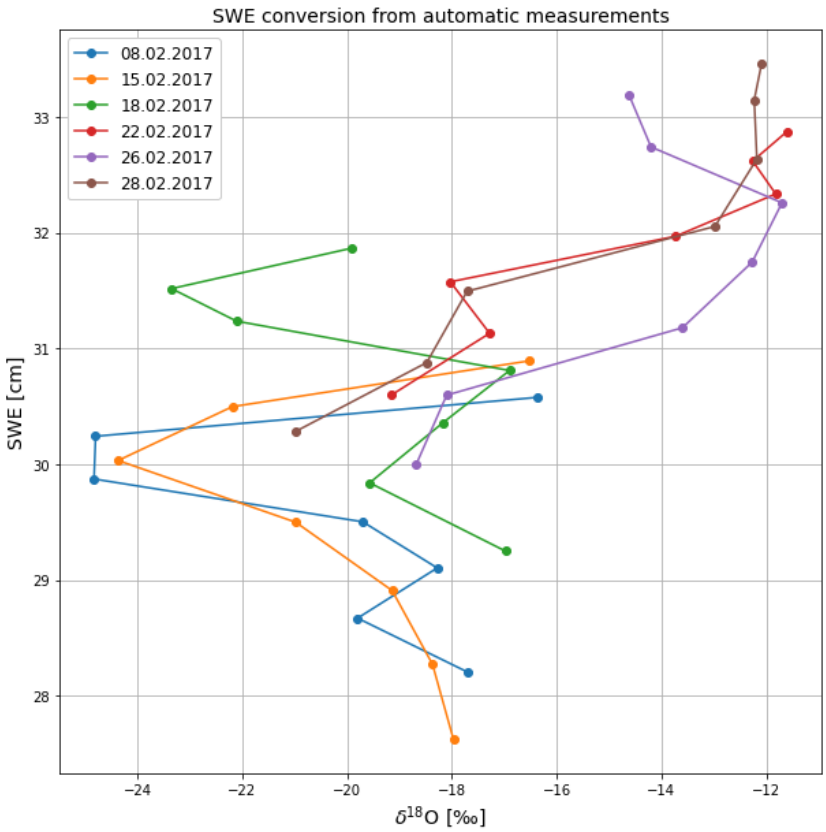

Figure 11: $\delta^{18}O$ Isotopic profiles (‰) against SWE. SWE obtained using the conversion from automatic measurements. Each dot represents one sample.

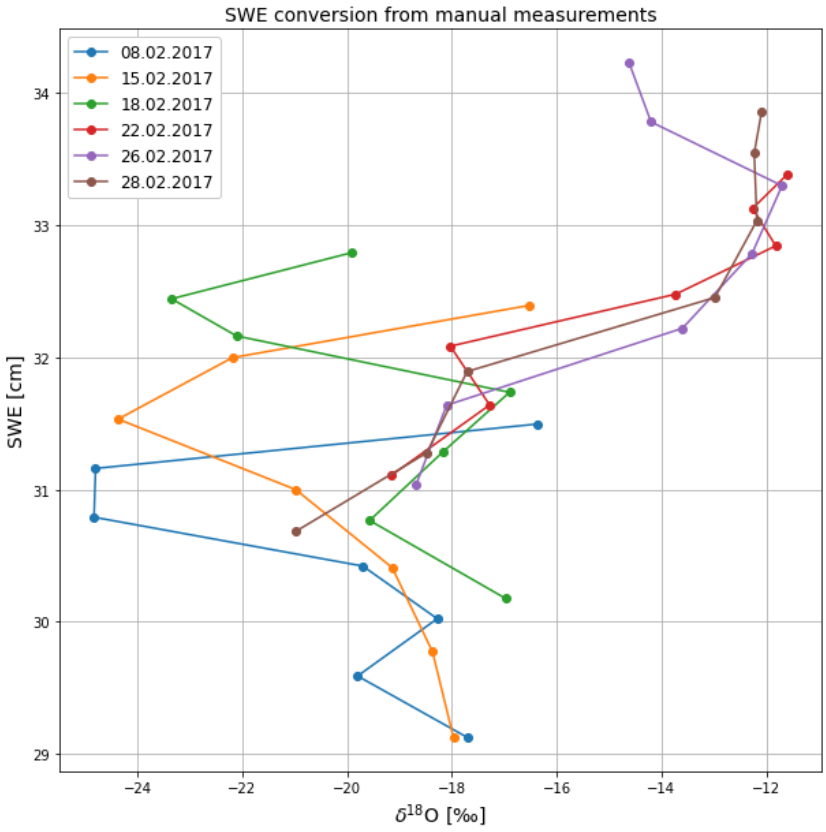

Figure 12: $\delta^{18}O$ isotopic profile (‰) against SWE. SWE obtained using the conversion from manual measurements (correction). Each dot represents a sample.

As it can be observed in Figure 11 and in Figure 12, the two conversion methods give different results. Tracking isotopic composition of a given sample from one profile to the next is significantly different using one conversion to SWE or the other. A comparison of the variations in $\delta^{18}O$ is done for both methods and some incoherencies are listed below:

For SWE conversion from manual measurements (Figure 12), the decrease of SWE between the 26 and 28 of February is probably inaccurate. In Figure 10, sublimation and evaporation represent about 0.5 kg m^{-2}, corresponding to 0.5 mm of SWE (or using a snow density of 100 kg m^{-3} to 0.5 cm of snow). This is clearly less than the approximately 3.5mm SWE decrease plotted on Figure 12.

In addition, the three first profiles are relatively similar, but seem to get shifted toward higher SWE. If vapor transport in the snowpack, deposition or fractionating sublimation could explain a smoothing or some variations, the changes in isotopic composition is sometime significant here (The surface $\delta^{18}O$ of the 08.02.2017 changes by more than -6 ‰ when tracked until the 15.02.2017). Those changes probably cannot be solely explained by fractionating sublimation and deposition (an estimation of the potential effect of fractionating sublimation and deposition is done using the simplified model in 4.1.4).

For SWE conversion from automatic measurements (Figure 11), the 18.02.2017 profile is plotted with 3 samples taken above the surface profile of 15.02.2017, which would correspond to 9 cm of new snow. This is not coherent with the manual measurements reporting 2 cm of new snow between those two dates. This most likely comes from the difference between the manual and automatic measurements. As mentioned in 3.3.3, the modelled HS is forced toward the automatic measurements and might create fictive snow in order to reach the target height.

Overall, one method does not show strong advantages compared to the other. The main problem comes from the differences between automatic and manual HS as well as between modelled precipitation and manually measured HN. In future studies, a high resolution density profile of the snowpack could be determined using a SMP [Calonne et al., 2020] for each profile date. The computation of SWE from density with heights corresponding exactly to the ones of the isotopic profiles would avoid the problems mentioned above.

Nonetheless, it must be noted that the main features of Figure 11 and Figure 12 are similar: the 8, 15 and 18 of February profiles are clearly more depleted compared to the 22, 26 and 28 of February profiles. The new snow falling between the 18.02.2017 and the 22.02.2017 is probably enriched in ^{18}O compared to the surface of the snow (new snow and air isotopic composition are visible on Figure 10). Similarly, new snow could explain the depletion of the surface isotopic composition between the 22 and 26 of February. An enrichment seems to occur afterward (until the 28.02.2017) as the depleted surface layer is not retrievable anymore. This could come from fractionating sublimation, deposition or wind blowing the surface snow away. The fact that the 3 last profiles of February do not reach value as low as -24 [‰] like the 3 first ones could come from a global enrichment or smoothing of the snowpack. However, it is also possible that the depleted layers are simply buried deeper than what was measured.

SNOWPACK layer tracking

The results from the SNOWPACK layer-tracking are presented here. The depths, D^{auto}_{sample} and D^{manual}_{sample} are plotted together with manually measured HN in Figure 13.

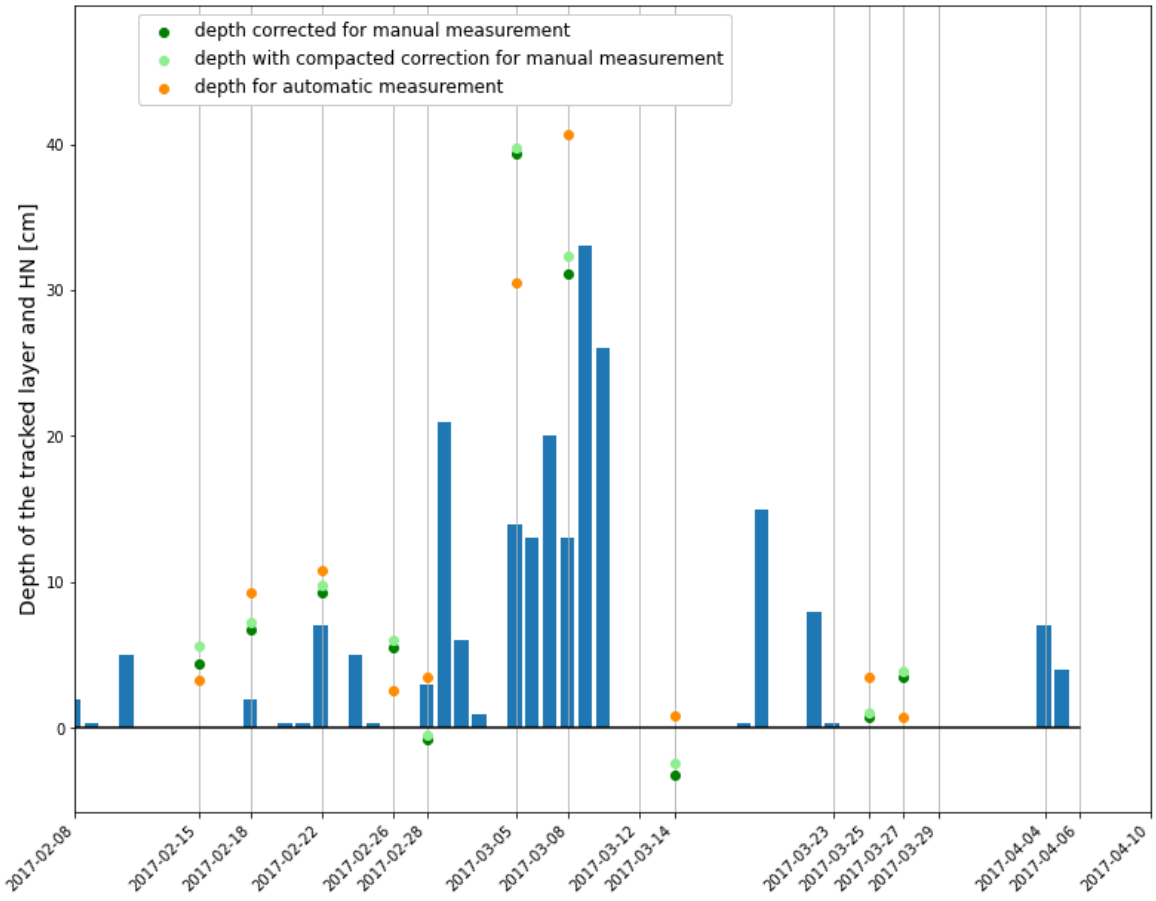

Figure 13: Depth of the tracked layers based on modelled HS (corresponding to automatic HS, D_{sample}^{auto} $[cm]$) in orange. Depth of the tracked layers corrected for manual measurements in green (D_{sample}^{manual} $[cm]$). Light-green dots correspond to computations with (16)(compacted correction) and dark-green to (15). The bars represent manually measured HN cm.

As expected, each method gives a different depth. None of them is completely coherent with what could be expected based on the HN measurements. By creating new snow to reach the automatic measurement SNOWPACK can burry a layer, which would affect D_{sample}^{auto}. Alternatively, if compaction is overestimated (underestimated) by the model, the D_{sample}^{manual} will be computed deeper (shallower). This might explain the negative D_{sample}^{manual} on the 14.03.2017. One aspect is also that the ground is not perfectly flat. The negative depth could be due to snow removed at the manual measurement position (i.e. sublimation, evaporation, or wind drift) or to snow added at the automatic measurement station (i.e. deposition or wind drift).

Methods comparison

Each method was used to estimate the depth of a sample that was initially at the surface. The results are summarized in Figure 14. As already written, each method gives a different result, which influences the estimated change in isotopic composition.

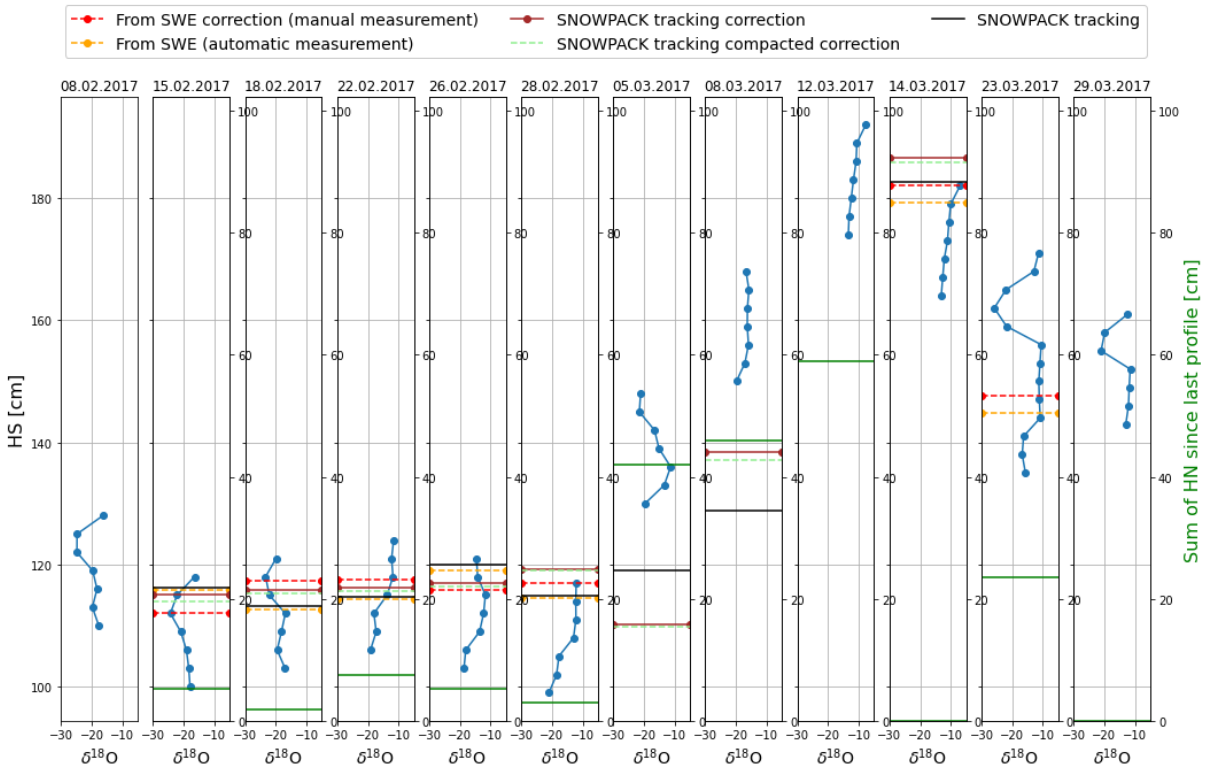

Figure 14: Isotopic profiles with estimated height of the previous surface sample (left axis). In the legend: "Correction" refers to the correction used to reach manual snow height measurements. "From SWE" refers to a method using SWE conversion, "SNOWPACK" to the SNOWPACK layer-tracking method, "compacted correction" to the use of equation (16), and "correction" to (15). Solid green lines show the sum of HN since the previous profile (right axis). $\delta^{18}O$ (x axes) is in [‰].

Figure 15 allows to compare the variations of the estimated isotopic composition changes between the five methods. The differences can be significant for some of the profiles and the choice of the method might have a stronger impact than what could be expected from fractionating sublimation. As stated before, the choice of the method is not straightforward as each of them presents different uncertainties and assumptions. The two methods that are not corrected are highly dependent on the simulated HS. As the model is forced toward the automatic measurements it might create new layers when there is no precipitation, which would have a strong impact on the estimated depth (and the change in isotopic composition). Unfortunately, the corrections done to use the manual measurements are also dependent on the modelled HS because it influences the compaction and density of the snowpack. Moreover, the corrections are directly derived from the modelled HS and vary for each profile. The point of those corrected methods comes from the fact that isotopic profiles are taken manually and the HS at the top of the profile corresponds to the manually measured HS.

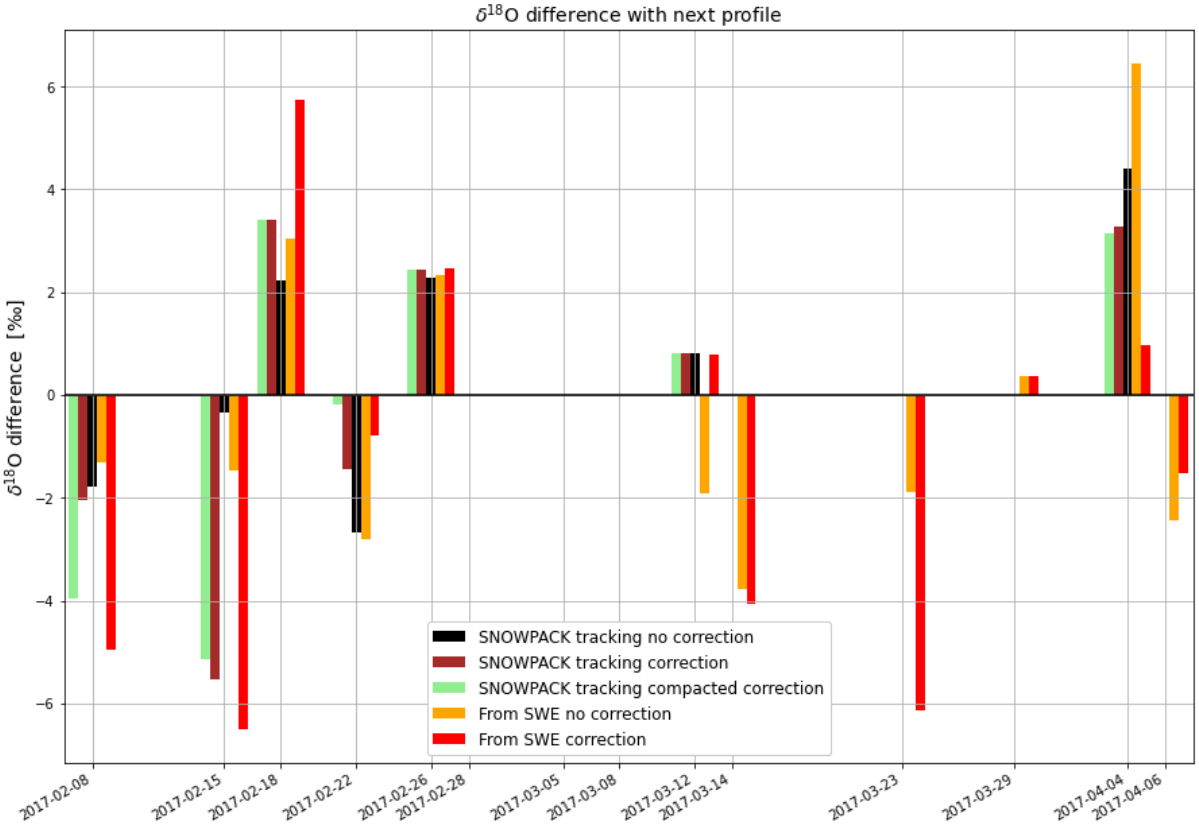

Figure 15: $\delta^{18}O$ (‰) change estimated with each of the presented tracking method. In the legend: "Correction" refers to the correction used to reach manual snow height measurements. "From SWE" refers to a method using SWE, "SNOWPACK to a SNOWPACK layer-tracking method, "compacted correction" to the use of equation (16), and just "correction" to (15). The date where the bars are centred corresponds to the date when the surface sample was collected, and the difference is computed with the tracked value at the next profile date. (i.e. the bars on the 08.02.2017 correspond to the $\delta^{18}O$ change between the 08.02.2017 and 15.02.2017). Each profile date is represented by a light grey vertical line. If the estimated depth is larger than 20 cm (the mini-profile thickness), the isotopic change is not plotted. Similarly, if the tracked layer was removed during the SNOWPACK simulation, the profile is ignored for the SNOWPACK tracking method.

4.1.3. Latent heat flux and isotopic change

Simple scatter plots of the changes in isotopic composition are presented in this sub-chapter. It helps assess whether the snow surface isotopic composition is linked to the latent heat flux. A plot selecting only the negative latent heat flux focusses on sublimation whereas one with only the positive latent heat flux shows the effect of the deposition. Since the theme of this work is the influence of sublimation on snow isotopic composition, details are given for the negative latent heat flux analysis.

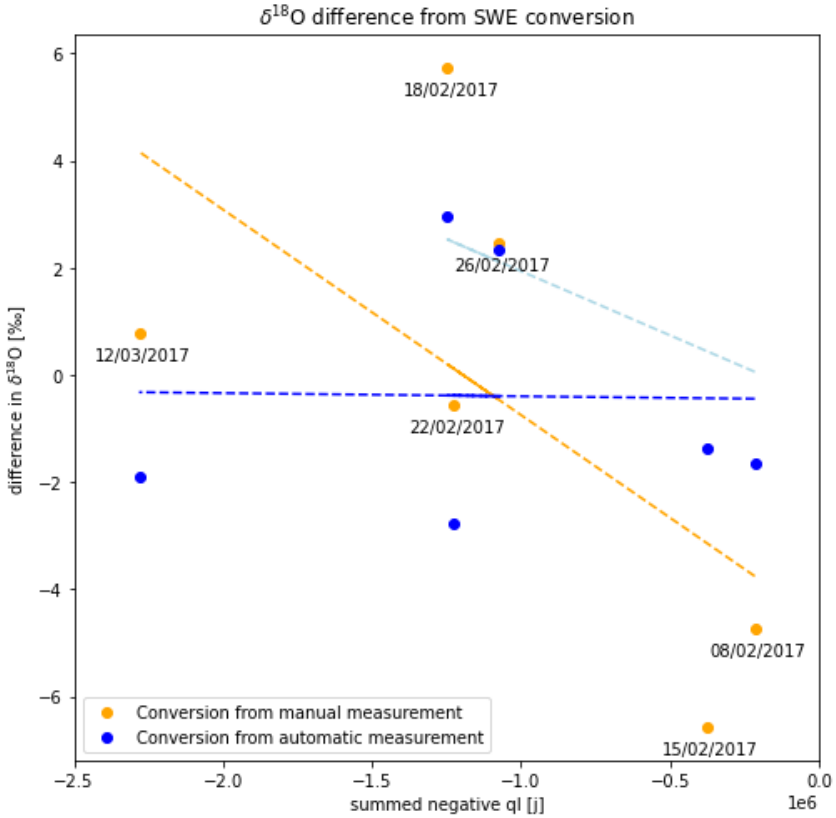

Figure 16: Difference in $\delta^{18}O$ (‰) using tracking with SWE conversion from manual measurements (orange) and automatic measurements (blue) against the negative latent heat exchange (J) (while the tracked sample was at the surface). The dates are shown for the conversion from manual measurements only. However, only the difference in $\delta^{18}O$ (y axis) is changing and both methods can be compared as the x-axis values are the same. The dashed lines are least square error linear regressions. The colours are the same as the corresponding dots. The light-blue dashed line is a linear regression for the automatic measurement ignoring the 12.03.2017 value. Please see text for more details and regression slopes.

In Figure 16, it is again possible to see the large differences between the tracking methods. Due to this high variability, interpretations are very difficult and of low confidence. The least square error linear fitting for the manual measurements might indicate a correlation between the sublimation (negative latent heat flux) and the change in isotopic composition (slope of $-3.83*10^{-6}$ ‰ j^{-1}). However, due to the insufficient number of values, no clear conclusion is possible. Additionally, using the SWE conversion from the automatic measurements no link is visible (slope of $-0.06*10^{-6}$ ‰ j^{-1}). The isotopic composition changes of the 22.02.2017 and the 12.03.2017 show decreases in $\delta^{18}O$ for strongly negative latent heat exchanges. For the 12.03.2017, the conversion from automatic measurements is the only method predicting that the sample gets buried. Moreover, no precipitation was observed, so this point should perhaps be ignored. Another regression line (in light blue) is shown without the 12.03.2017 and might indicate an influence of sublimation toward isotopic enrichment (slope of $-2.39*10^{-6}$ ‰ j^{-1}).

For the 22.02.2017, the tracking method might also give wrong information, but there is no strong evidence to support that. The 22.02.2017 sample is from freshly fallen snow and is buried on the 24.02.2017. The two snow events probably had different isotopic compositions, grain sizes and specific surface areas. Relatively strong exchanges by vapour transfer in the snowpack might have occurred and influenced the snow isotopic profile like it was observed in the experiment of [Schindler, 2020].

For completeness, the same plot is shown using the SNOWPACK layer tracking In Figure 17.

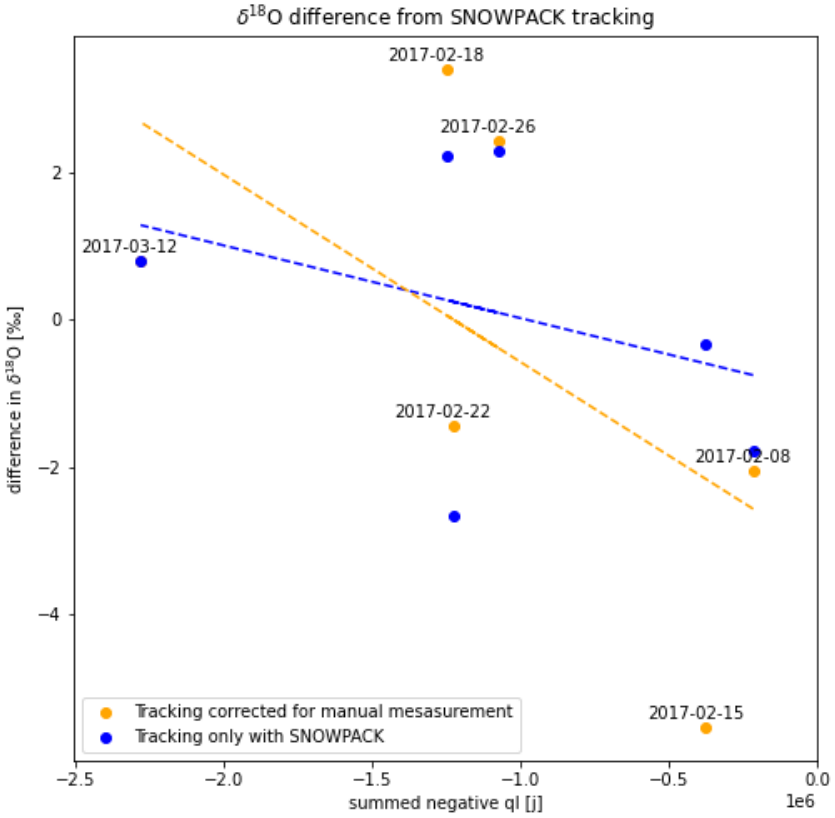

Figure 17: Difference in $\delta^{18}O$ (‰) from the SNOWPACK layer-tracking with correction for manual measurements (blue) and without correction (orange) against the negative latent heat exchange (J) (while the tracked sample was at the surface). The dates are shown only for the tracking with correction for manual measurements. However, only the difference in $\delta^{18}O$ (y axis) is changing and both methods can be compared as the x-axis values are the same. The dashed lines are least square error linear regressions. The colours are the same as the corresponding dots.

As it could be expected, Figure 17 is similar to Figure 16. Again, differences in the methodology show large variations and any tendency should be interpreted cautiously. Both regressions lines have negative slopes (for corrected tracking the slope is $-2.54 * 10^{-6}$ ‰ j^{-1}, and using automatic measurements, the slope is $-0.99 * 10^{-6}$ ‰ j^{-1}). No clear conclusion can be done, but the general trend would indicate that for a more negative latent heat exchange, an enrichment (or smaller depletion) could be expected.

A similar trend could be expected for deposition as more positive latent heat flux would increase deposition with a selection of the heavier SWIs contained in the vapour. However, no link could be found. It must be noted that deposition depends on the composition of the vapour and a very depleted vapour could also decrease the isotopic composition of the surface snow. In addition, if sublimation was the dominant process, the trend due to deposition would be hidden. A similar analysis was done for the absolute latent heat flux (positive ql – negative ql). Results are comparable to the negative latent heat flux plots. Because of the redundant information and high uncertainty already discussed those plots are not shown here.

The negative latent heat flux analysis might indicate fractionating sublimation. This can motivate further studies were the tracking methodology would not have an impact as dominant as here. Obviously, it is also difficult to separate the different processes. For example, snow metamorphism is dependent on the age of the snow at the surface. In addition, vapour transport in the snowpack would have a different effect depending on the isotopic composition of the neighbouring layers. Finally, deposition is dependent on the vapour isotopic composition, which should also be considered. This last point is discussed using the simplified model in the next sub-chapter (4.1.4). Potential processes linked to other snow parameters were tested (the list of those parameters is presented in appendix 7.3.3), but nothing clear could be found.

4.1.4. Simplified model

The simplified model (presented in chapter 3.6) allows to estimate the expected changes in isotopic composition due to fractionating sublimation and deposition. As described, it does not consider any intra snowpack processes and contains strong assumptions such as the well mixed surface layer of initially 2 cm. It was developed to allow a comparison with the collected 2 cm sample.

Figure 18 compares the modelled change in isotopic signal to what is deduced from tracking using SWE conversion from manual measurements. As already discussed, the tracking method highly influences the results, but the model is independent of that (using a different tracking method changes the x-axis values, but not the model results). Each tracking method has been plotted against the model results, but no clear link could be found so only one is shown.

An enrichment is always modelled. This was expected as fractionating sublimation of the well mixed layer is considered and can only cause an enrichment of the solid phase. The deposition could be modelled as a depletion in case of strongly depleted water vapour in the air. Yet, as it can be seen on Figure 10, vapour is close to equilibrium with snow or slightly enriched (compared to equilibrium with snow).

The (sometimes-strong) depletion estimated by the tracking does not match with the model. One explanation could come from the oversimplification of the model, which is ignoring the vapour exchange between the layers in the snowpack and with the new snow (after burial). The tracking method also has high uncertainty and depletion is probably overestimated in some cases (see Figure 15, e.g. on the 15.02.2017, the method used here estimates more depletion than the others). Furthermore, the thickness of a sample is always of 3 cm (2 cm at the surface) and the tracking estimates the new isotopic composition based the two nearest samples. Because of the relatively high variability of the isotopic signal with depth, this can strongly influence the estimated change in isotopic composition. On the contrary, the model only considers one layer with no influence of the neighbouring one.

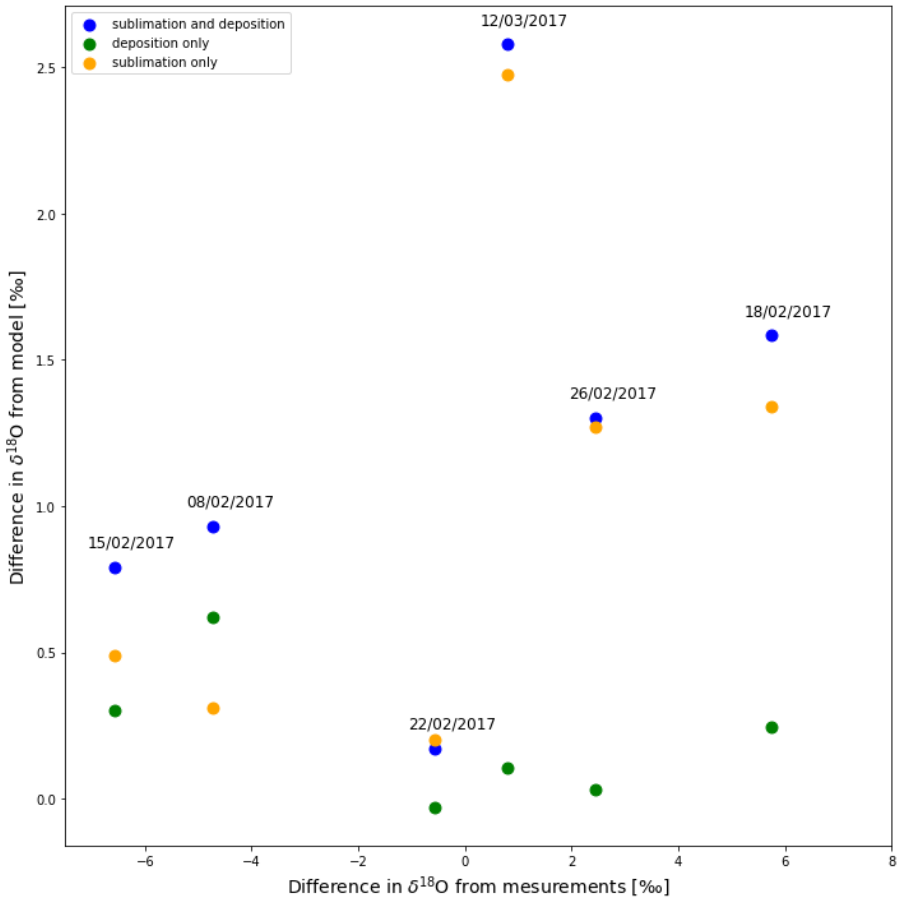

Figure 18: Simplified model results plotted against differences in $\delta^{18}O$ estimated by SWE conversion from manual measurements (as the orange dots in Figure 16). The dates are only shown for the combined modelled effects (deposition and sublimation), but each effect can be compared because they have the same x-axis coordinate.

The model has also been run considering that sublimation has the composition of the measured vapour isotopic composition. This has a very small effect on the results, which could be expected as the air is close to isotopic equilibrium with snow (see Figure 10).

The modelled differences in $\delta^{18}O$ are directly linked to the initial layer thickness and density. Thinner layers would be more influenced because the enrichment by deposition is not changed but the signal is less diluted. The modelled sublimation would be affected by a change in layer thickness, but there would still be a globally stronger enrichment for smaller layers (because there is less dilution of the fractionating sublimation effect). The model was developed to be compared to the measurements, but for more precise estimations, it would be interesting to determine the thickness influenced by sublimation and deposition, which could be considered as "well-mixed". The estimation of diffusion in firn from [Johnsen et al., 2000] could be adapted. Nevertheless, effort should probably first be put toward a better tracking or more field data with a higher temporal resolution.

4.1.5. March surface samples

The four selected dates of March 2017 present an interesting case as no precipitation occurred during that period. The surface values can be compared without the problematic tracking uncertainty. However, it must be kept in mind that due to compaction and possible melt, the constant sampling thickness does not always represent the exact same layer. In this sub-chapter the simplified model is used to compare measurements with the change in signal that could be expected from equilibrium fractionation. The model is then slightly modified. First, the equilibrium fractionation assumption is quickly discussed.

Equilibrium fractionation assumption

The model presented in chapter 3.6 assumes equilibrium fractionation. However, if the net latent heat flux is not null, sublimation and evaporation are non-equilibrium processes (see 2.4). It is possible to assess the importance of the kinetic effects by comparing the linear regression of $\delta^{18}O$ and δD as it is done in Figure 19.

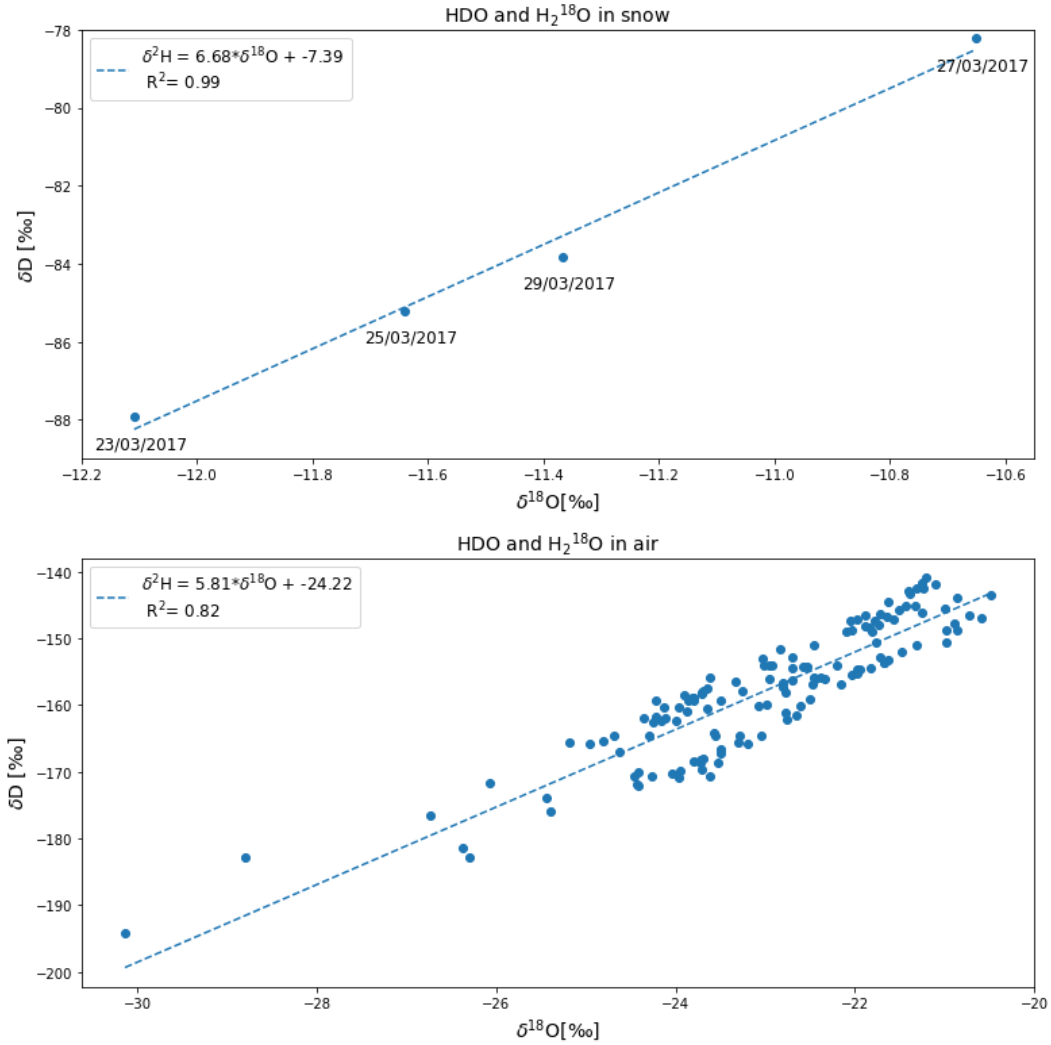

Figure 19: $\delta^{18}O$ and δD relations from measurements of the snow surface and vapour. Vapour data come from hourly average (from the Piccaro placed on the WFJ). Snow data come from the 4 days when surface samples were collected.

As a start, it must be noted that the number of snow samples is low, and the remarks done here should be validated with a bigger dataset. The slope between each sample is relatively constant and the linear regression gives a good fit. A slope of 6.68 is different from the one of the GMWL (slope of 8). Therefore, the d-excess is varying from date to date, which could indicate kinetic fractionation. However, the constant slope implies a similar behaviour between $\delta^{18}O$ and δD. For this reason, only $\delta^{18}O$ is analysed hereafter as δD would show similar results. The importance of kinetic fractionation is difficult to assess since an air mass with vapour that experienced strong kinetic fractionation could be at the origin of this specific snow layer. The deviation from the GMWL is not necessarily due to post-depositional processes.

Air and snow $\delta D/\delta^{18}O$ slopes are close to equilibrium in this case: Using the equilibrium sublimation fractionation from [Ellehoj et al., 2013] and snow data with a slope of 6.68 , the slope of the vapour would be 5.86 (reversely, vapour data with a slope of 5.81 would give snow with a slope of 6.63).

Assuming equilibrium fractionation here seems a reasonable first approach. Nevertheless, if more samples were collected (with a higher frequency), it might be possible to assess potential post-depositional kinetic effects. [Moser and Stichler, 1974] observed changes in slope between morning and afternoon samples. They interpreted this result as sublimation with kinetic fractionation occurring during the day and equilibrium fractionation during deposition at night. This analysis would be more robust with measurements of the vapour isotopic composition as the arrival of a new air mass with a different $\delta D/\delta^{18}O$ ratio would also change the effect of deposition. In any cases, taking samples twice a day would help to separate the processes and allow to assess the validity of the equilibrium fractionation assumption more precisely.

Simplified model

To estimate the possible fractionation occurring during sublimation, the simplified model presented in 3.6 is used as a comparison. Figure 20 shows the isotopic signal variations as well as relevant data and the model results.

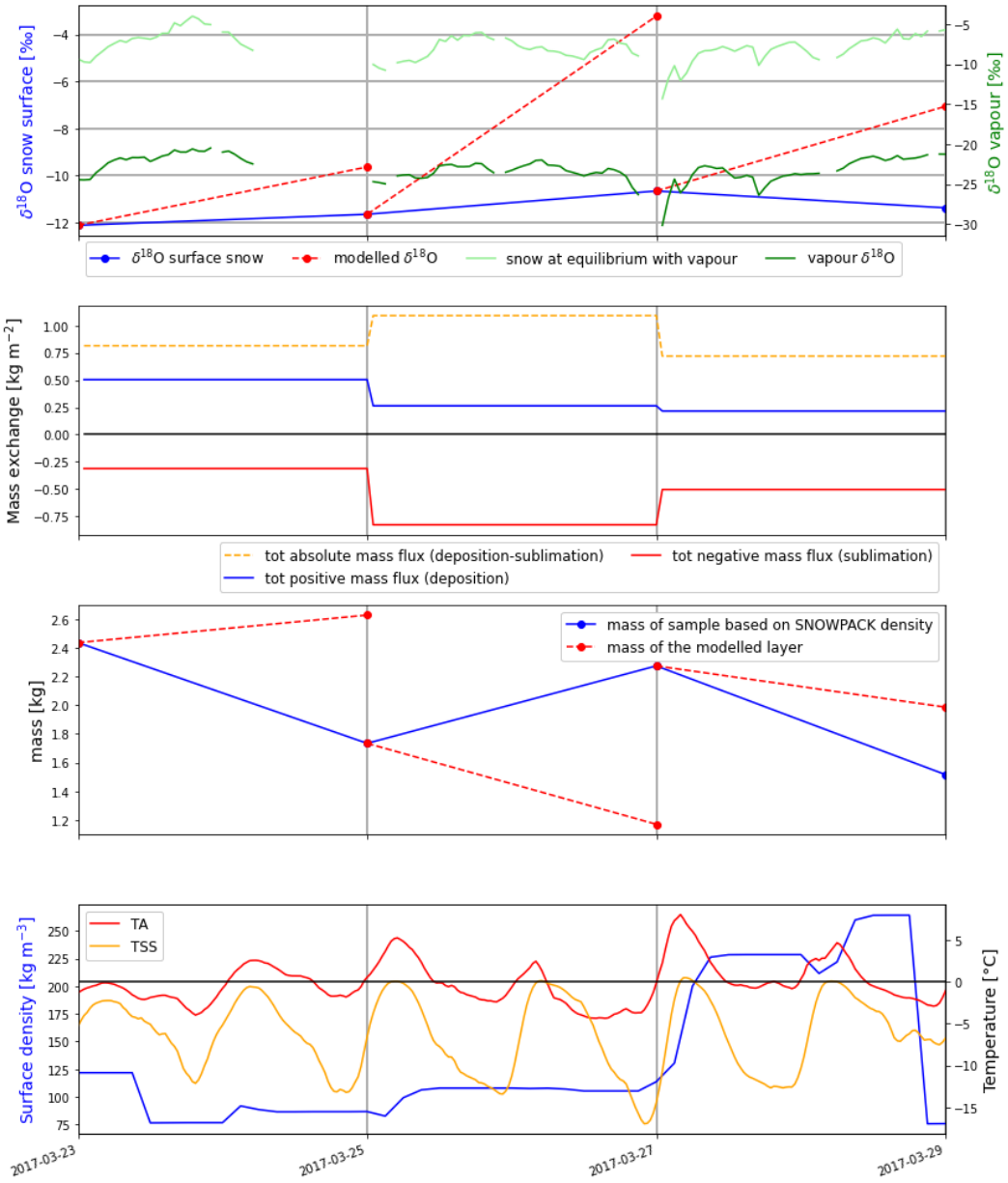

Figure 20: Simplified model results for March 2017 (first panel, left axis). The blue line represents the measured snow surface isotopic composition, and the red dashed line the model prediction. The right axis shows the measured vapour isotopic composition and the snow that would be at equilibrium with it. The second panel shows the mass flux computed by SNOWPACK. The third panel shows the estimated mass of the samples, and the mass of the modelled layer. The bottom panel shows the surface density (1 cm depth), TA and TSS (3 hours moving mean).

The measurements show a small enrichment of the snow surface for the 3 first samples and a depletion on the last sampling date (Figure 20 , first panel). The depletion observed on the 29.03.2017 probably comes from a lower layer that was buried before. This point is discussed later. The air temperature rises above 0 °C and TSS reaches 0 °C daily from the 25.03.2017 indicating probable melt. As each phase transition has a different effect and cannot be separated, the model is not appropriate for this situation and can only give an approximation of what could be expected. It gives a strongly overestimated enrichment, which might partly come from the choice of the mass exchange data (plotted on the second panel). The mass exchange is the addition of the evaporation and the sublimation. It is used to calculate fractionating sublimation/deposition. Yet, as soon as there is liquid water, the processes are different and there is probably liquid-solid fractionation. For a pendular system as here [Trachsel, 2019], the isotopic content of one sample is not influenced if there is no evaporation since the sample is completely melted before analysis. In case of complete refreeze without exchange with the atmosphere, the process

is neutral. However, in case of evaporation of part of the melted snow, the liquid water is probably enriched resulting in an enrichment of the snowpack when refreezing. By curiosity, the same plot has been computed using only the sublimation mass exchange and is presented in appendix 7.3.4.

Ignoring the evaporative mass exchange is very debatable because fractionation is probably occurring during evaporation of melted snow. It highly reduces the mass exchange and modelled isotopic enrichment for days with high temperature (after the 25.03.2017). However, it has little impact before the 25.03.2017 and an overestimation is still modelled there. As it only improves result of one interval, the mass exchange from evaporation should probably be included. This would mean that either the mass exchange or the influence of phase change on snow isotopic composition is overestimated. It is also possible that the thickness of the layer influenced by surface processes is underestimated. To give an order of idea, the model was run dividing the mass exchange by 6 (Figure 21). This factor 6 is given here as a rough estimation to have a model matching the measures but it should not be considered as a result.

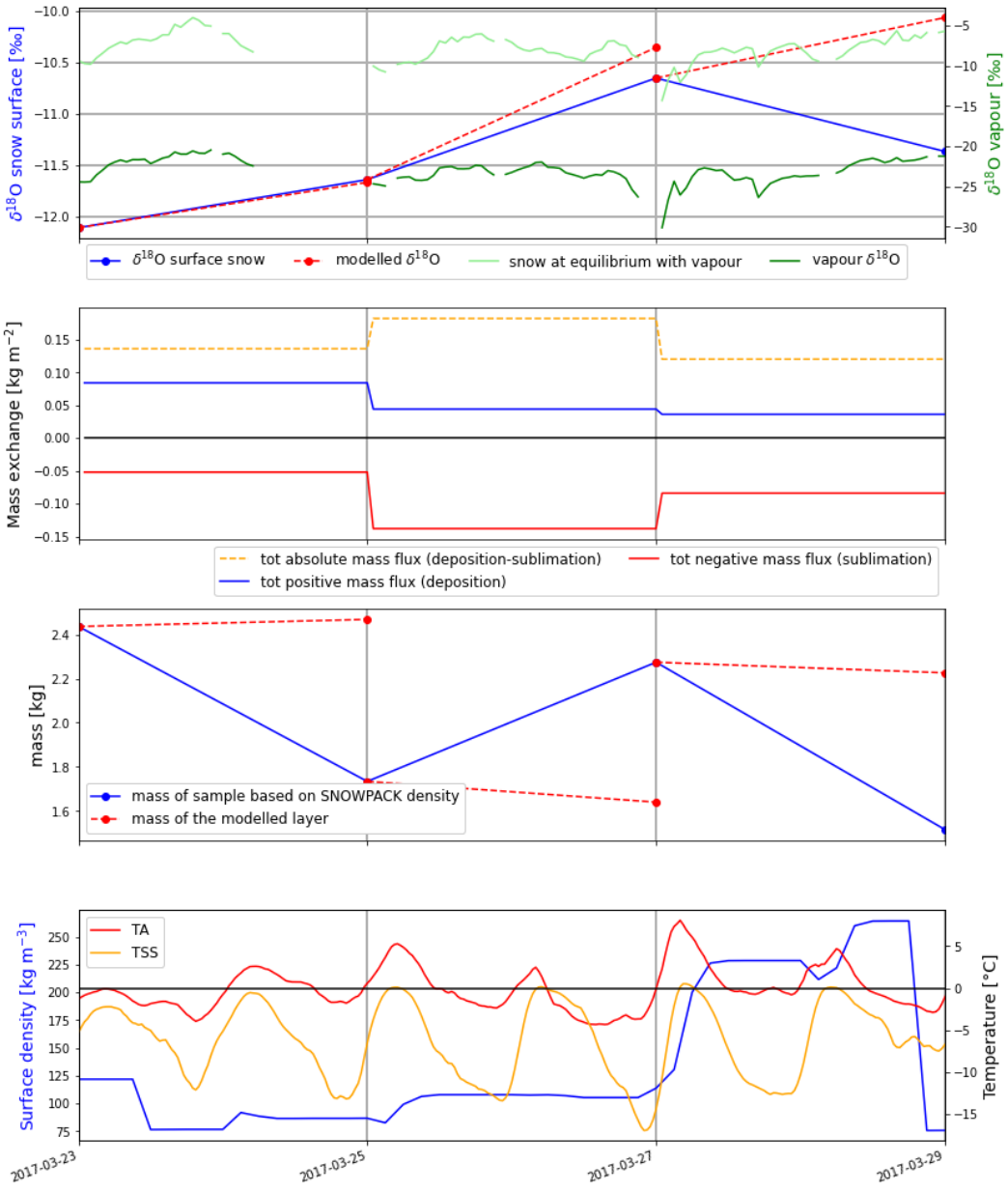

Figure 21: Same as Figure 20 but dividing the mass flux by 6.

The fact that the model in Figure 21 shows more coherent results could indicate the following: (i) The mass exchange is overestimated by a factor of about 6, (ii) The assumption of equilibrium fractionation with the formula from [Ellehoj et al., 2013] gives excessive enrichment estimations, (iii) The thickness of the layer influenced by surface exchanges is about 12 cm (6*2 cm), diluting the enrichment, (iv) intra-snowpack vapour or liquid water exchanges, reduce the enrichment of the surface, (v) The samples collected do not correspond to the same layer from date to date (i.e. because of compaction) and surface enrichment is not well captured because of a potentially depleted layer deeper. (vi) Only the very surface of the snow is enriched (opposite of (iii)) and part of it is completely evaporated (as in the layer-by-layer theory). This would only allow to capture part of the effect of fractionating sublimation.

This factor 6 is probably (partially) explained by a combination of the above-mentioned reasons. A factor 6 error for (i), (ii) or (iii) alone does not seem to be reasonable, but each reason could contribute to part of the overestimation from Figure 20. (i) or (vi) could also mean that layer-by-layer fractionation occurs about ⅚ of the time and equilibrium fractionation should be considered only for the remaining ⅙. Potential non-equilibrium fractionation could also play a role. As discussed before, kinetic effects are difficult to assess, but should be relatively small. (iv) is not considered for this model as the assumption was that surface processes would be dominant. Nevertheless, it should be considered in more complete models. (v) is potentially an important process: As shown on the third panel of Figure 20, the masses of the samples are not matching the modelled masses of the layers. Figure 22 shows that samples collected deeper are more depleted. It must also be noted that the density (plotted on the lower panel of the figures above) gives uncertainty in the estimation of the mass of each sample. No precipitation occurred during this period but the density (always at 1 cm depth) is sometime decreasing. This does not seem reasonable especially when observing the strong drop between the 28 and 29 of March. Probably, SNOWPACK is adding new snow of low density to reach the measured HS from the automatic station.

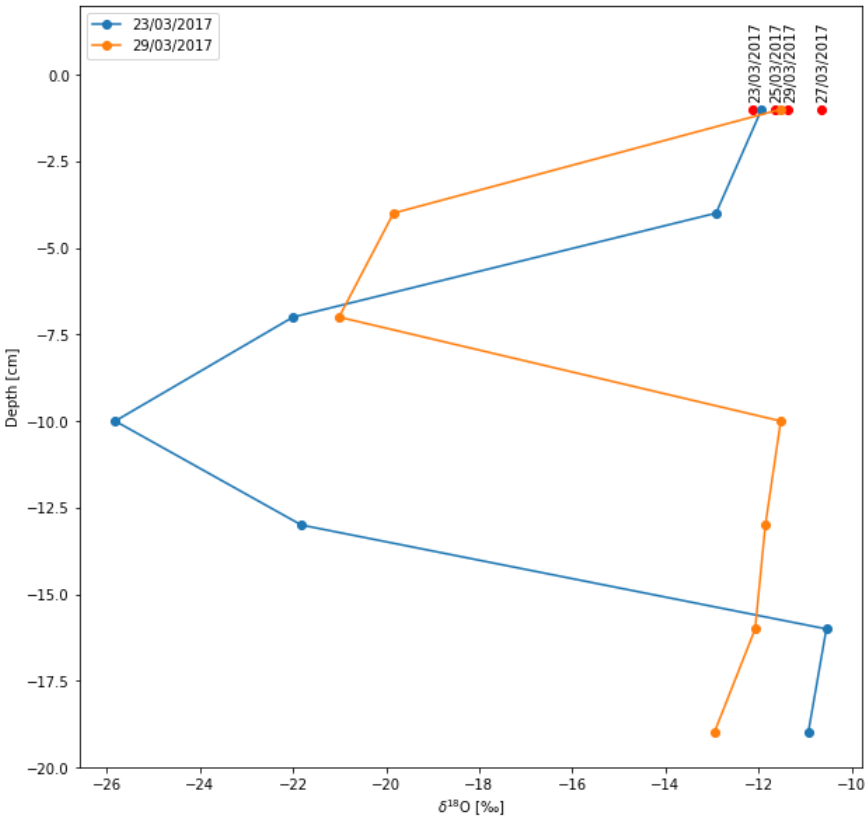

Figure 22: Isotopic profiles from the 23 and 29 of March 2017 and the 4 surface samples taken during that period (red dots). The red dots present the same values as in Figure 20 top panel (3 samples each time). The tops of the profiles are plotted as the average of the top of each profile and the 3 additional samples (average of 4 samples).

Figure 22 shows the evolution of the isotopic signal between the two profiles. There seems to be a shift upward, which can be due to the melt of a first layer of snow and (or) compaction. The 29.03.2017 profile is smoothed compared to the 23.03.2017. This might come from vapour exchange within the snowpack. Compaction might also have an impact as the 3 cm thick samples (2 cm at the surface) probably do not represent the same snow layer on the two profiles. A sample of compacted snow on the 29 of March can include a mixt of two samples from the 23.03.2017.

Modified model

To do a better comparison between the model and the samples, masses can be estimated from the maximum density occurring between the 23.03.2017 and the date of interest. It is possible to include the contribution from a lower layer in the model so that similar snow thicknesses are compared. A contribution of a deeper layer is added to the model when the next sample is heavier than the modelled mass.

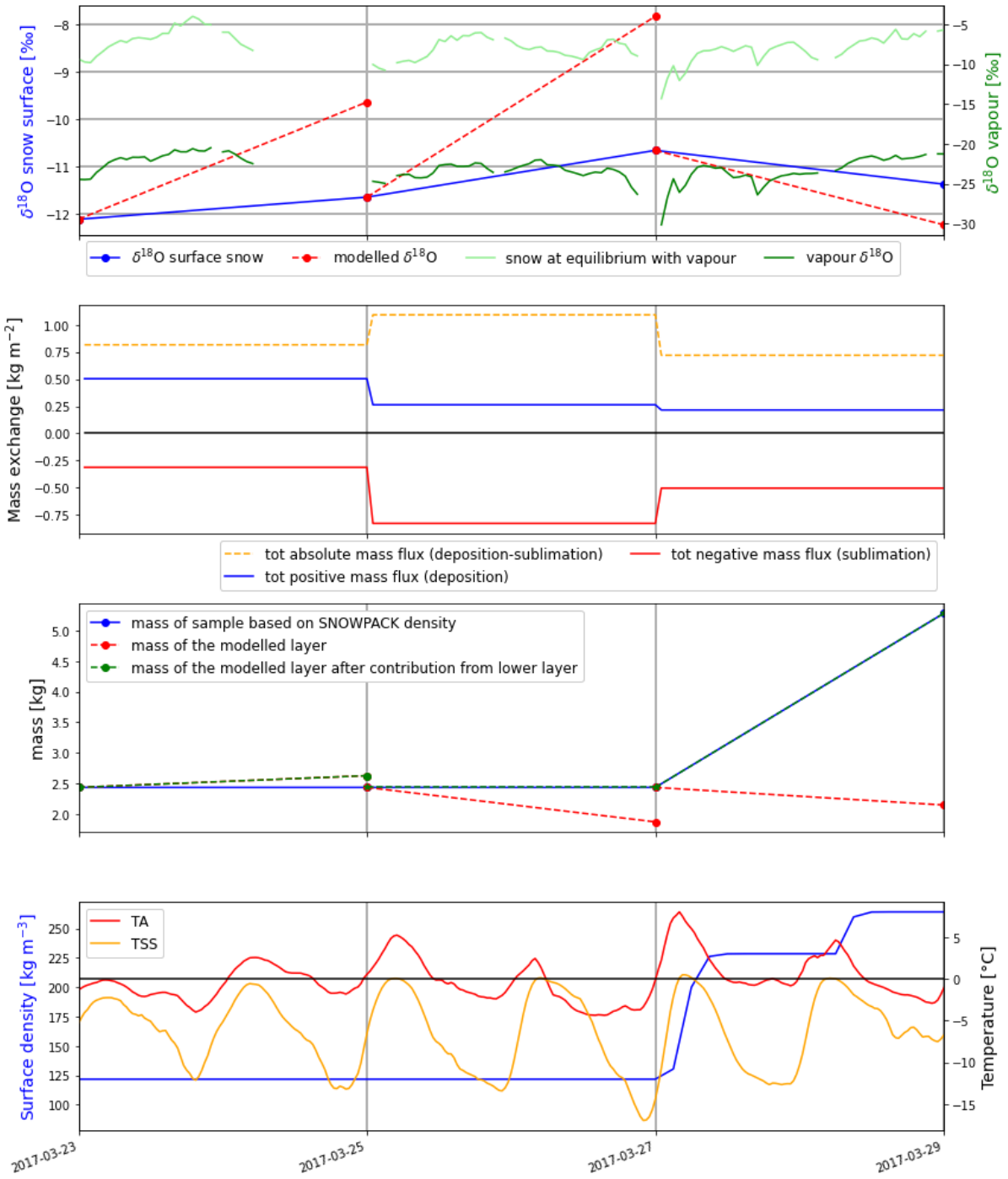

Figure 23: Same as in Figure 20, but including contribution from lower layer and considering only increasing density.

The modified model gives slightly more coherent results. Modelled changes in the isotopic signal are again overestimated but have a similar tendency compared to the observation. This is particularly visible for the 29.03.2017 where surface melt and compaction have probably increased the surface density. The 2 cm thickness of the 29.03.2017 likely includes a depleted snow layer that was previously deeper. For future studies, the compaction and the contribution from lower layers should be considered when collecting surface samples of constant thickness.

The effect of mass changes between each sample is also important to consider since there is no clear information on the thickness influenced by surface sublimation and deposition. If it only has an effect over the top 1 cm, the 2 cm samples would give a diluted signal change. This would not be a significant problem assuming constant density (modelled fractionating sublimation would be slightly different, but

changes would be reasonable for the enrichment estimated here). However, when compaction occurs, the signal change is more diluted because the mass of the sample is larger for a similar surface exchange.

A quick sensitivity analysis was also done for the modified model. A division by factor 5 of the latent heat flux give the best results. The plot is visible in appendix 7.3.4.

The results of March 2017 are interesting and give a first idea of surface effects. This analysis shows the importance of compaction and the potential influence of lower layers on surface measurements. This should be considered for future studies. Yet, the number of samples is too low, and the careful analysis of the results presented here does not allow to have a quantitative conclusion on the significance of fractionation occurring during sublimation. In addition, with temperatures above 0°C, additional post-depositional processes should be considered.

Collecting samples following a consequent snowfall would probably reduce the variability of the snow isotopic composition over depth. Selecting a period with air and snow temperatures below 0°C would allow to focus on sublimation effects. Finally, a more complete model could also simulate the evolution of the isotopic signal within the snowpack and improve the lower layer contribution estimation. This would also help separate the different processes and obtain a better estimation of the effect of sublimation.

4.2. January 2020 Dataset

This sub-chapter presents the results obtained from the January 2020 dataset. First, a discussion on the isotopic signal variation of air and snow is presented. The simplified model is then used to assess potential effects of sublimation.

4.2.1. Results overview

The results from the analysis of the snow samples for δD and $\delta^{18}O$ are presented in Figure 24. An overview from snow and air isotopic composition, the SNOWPACK simulation results, and meteorological data is presented in Figure 25. This allows a first discussion on the variation of the snow isotopic signal.

In Figure 24, a global enrichment of the snow surface can be observed between the 18 and the 27 of January. The sharp depletion of the snow surface after that day can be explained by a snowfall completely renewing the snow surface. The error bars show the minimum and maximum value among the three daily samples. The variation is within the uncertainty of the measurements done with the LGR for $\delta^{18}O$, but not for δD [4]. The differences in the δD values might partly come from spatial variability (samples were collected about one meter apart). However, it might also come from the sampling or melting and transfer procedure. The uncertainty from the lab analysis or the sampling procedure still allows to see the global enrichment between the 18.01.2020 and the 27.01.2020.

[4] The uncertainty of the measurement done with the LGR is ± 1‰ for $\delta^{18}O$ and ± 2‰ for δD, from the Test report of the WSL-Zentrallabor.

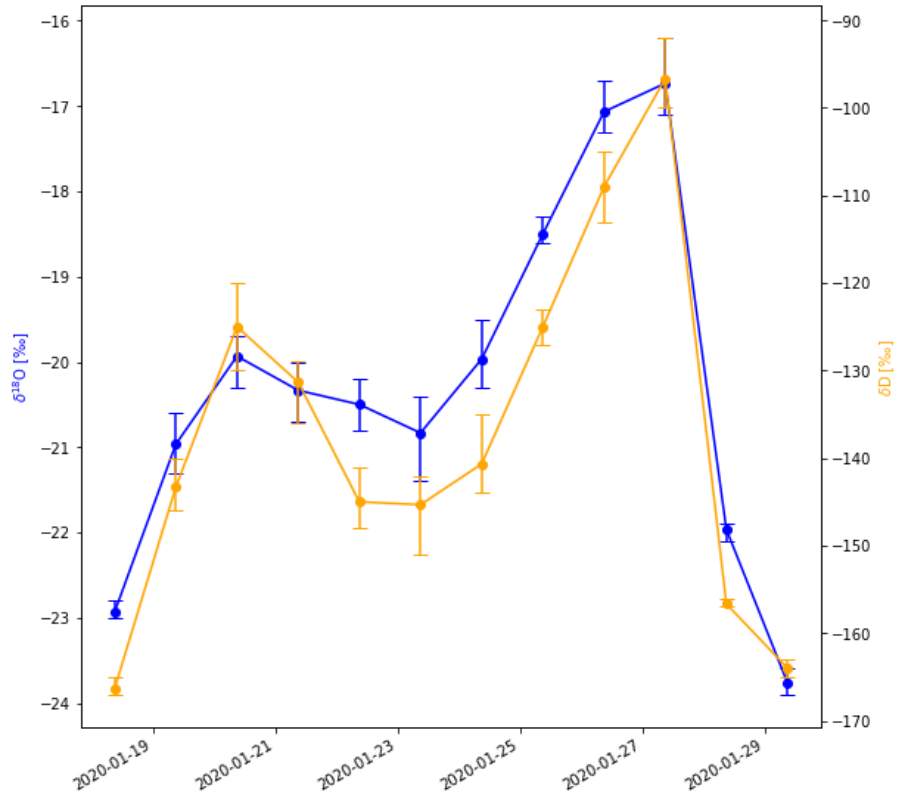

Figure 24: snow isotopic composition: $\delta^{18}O$ in blue (left axis) and δD in orange (right axis). The dots represent the mean value of the 3 daily surface samples. The error bars show the minimum and the maximum value among those 3 samples.

Figure 25 aims to compare the variation of the isotopic signal with other parameters. On the first panel, the equilibrium values (snow at equilibrium with vapour and vapour at equilibrium with air) are calculated with the equilibrium fractionation factor from [Ellehoj et al., 2013]. The two y-axes should be highlighted: On the left for the snow and snow at equilibrium with vapour (blue) and on the right for the vapour values (green). This shows that the vapour is globally enriched (~10 [‰] on average between the 18.01.2020 and the 29.01.2020) compared to equilibrium with snow. This is a different situation to what was observed with the 2017 dataset. In case of deposition of vapor on the snow surface, an enrichment is to be expected. This might already be visible on this plot as days with enriched vapour seem to be followed by an enrichment of the snow surface. This probably shows an influence of the atmosphere on the snow surface isotopic composition, which could come from deposition (the top panel of Figure 26 in the next sub-chapter might better illustrate that).

Surface snow enrichment can be observed between 18 and 20 of January and between the 23 and the 27 of January. The first enrichment period is marked by small snowfalls (~2 cm on 19 and 20 of January) affecting (or replacing) the top 2 cm of the snowpack. The samples are probably mainly consisting of freshly fallen snow.

Between the two snow-enrichment periods (between the 20 to the 23 of January), a small decrease in the snow surface isotopic composition can be observed. Almost no deposition is computed during that time. This might show that deposition has a non-negligible effect on the snow surface isotopic signal. The relatively depleted vapour isotopic signal during that period might partly come from depleted vapour originating from snow sublimation. This would only be possible with fractionating sublimation since snow isotopic composition is more enriched compared to vapour. The fact that snow shows depletion, does not support fractionating sublimation, but the potential enrichment from sublimation could be compensated by other processes like vapour exchange with deeper snow layers.

The second enrichment period (23-27 of January) starts without precipitation. The 23.01.2020 is a day with relatively large sublimation. Deposition is occurring on the 24.01.2020 and probably induces an enrichment of the snow surface. Small snowfalls (~1 cm day^{-1}) occur on the following days and affect the snow surface isotopic composition. Globally, deposition seems to be linked to enrichment, but it is difficult to make a conclusion because of the unknow effect of the new snow.

After the 27 of January, comparisons with the previous samples are impossible because of the stronger precipitation and the probable effect of the wind. The new snow is clearly more depleted than what was previously at the surface. It is also more depleted than the equilibrium with vapour isotopic composition, which is showing that the measured vapour isotopic signal does not correspond to equilibrium with the falling snow.

A comment on the effect of the wind can be done here. After deposition, blowing wind can easily remove a surface hoar layer. This could be responsible for a depletion of the snow surface since the deposited layer is probably enriched compare to the bulk 2 cm sample. Stronger wind usually induces more sublimation and it might be difficult to differentiate the effect of the two processes. Similarly, drifted snow can induce depletion or enrichment and burry or remove the layer initially at the surface. The snow redistribution effect was already considered as a significant post-depositional process in [Epstein et al., 1963]. For modelling, it would require more information on the spatial variability of the snow surface isotopic composition and a better resolution of the isotopic variation trough depth. Nevertheless, during the January 2020 sampling campaign, mean hourly wind velocity were mostly under 4 m s^{-1} until the 27.01.2020. 4 m s^{-1} is a threshold [5] for snow redistribution [Vionnet, 2012]. Therefore, snow redistribution is probably not the main factor affecting the surface isotopic composition before the 27.01.2020. It is still possible that part of the depletion is due to a wind gust removing some of the enriched snow at the surface. To monitor the wind transport and the variation of the snow surface, a camera or a particle counter could be installed for futures studies.

[5] The threshold of 4 m s^{-1} corresponds to hourly mean wind velocity measured 5 m above ground. This corresponds to the minimum velocity for displacement of very light and fresh snow.

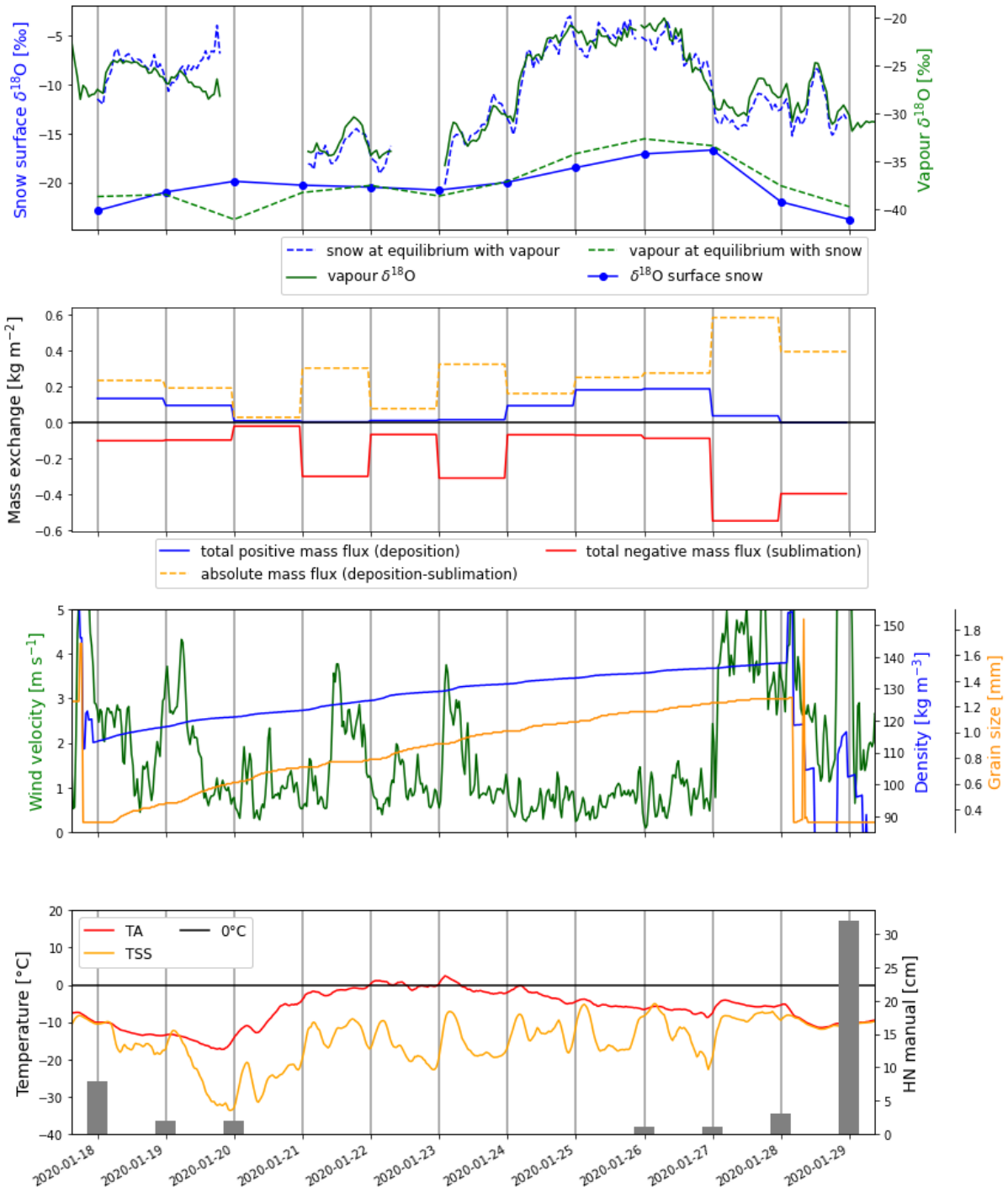

Figure 25: Overview of the data from January 2020. Air and snow isotopic analysis on the first panel. The SNOWPACK outputs: Mass exchange on the second panel and grain size and surface density on the third panel. Wind speed (1 hour moving mean), TA and TSS (3 hours moving mean) come from automatic weather stations on the WFJ. HN comes from the daily manual measurements (at 08:00 am).

Figure 25 allows to see a probable effect of deposition on the snow isotopic composition. The enriched vapour compared to the equilibrium with snow is coherent with this idea. Effect of sublimation is not clear, and further analysis is done using the simplified model in the next sub-chapter. Linear regressions between the change in isotopic composition of the snow and the computed latent heat fluxes are presented in appendix 7.4.2. They also show a probable effect from deposition, but not from sublimation. The precipitation probably influenced the snow surface isotopic composition and the comparison between the samples taken before the 20.01.2020 and after the 25.01.2020 is difficult.

4.2.2. Simplified model

The simplified model (presented in 3.6) allows to give an order of idea of the effect of fractionating sublimation and/or deposition. A first run accounting for fractionating sublimation and deposition is presented in Figure 26.

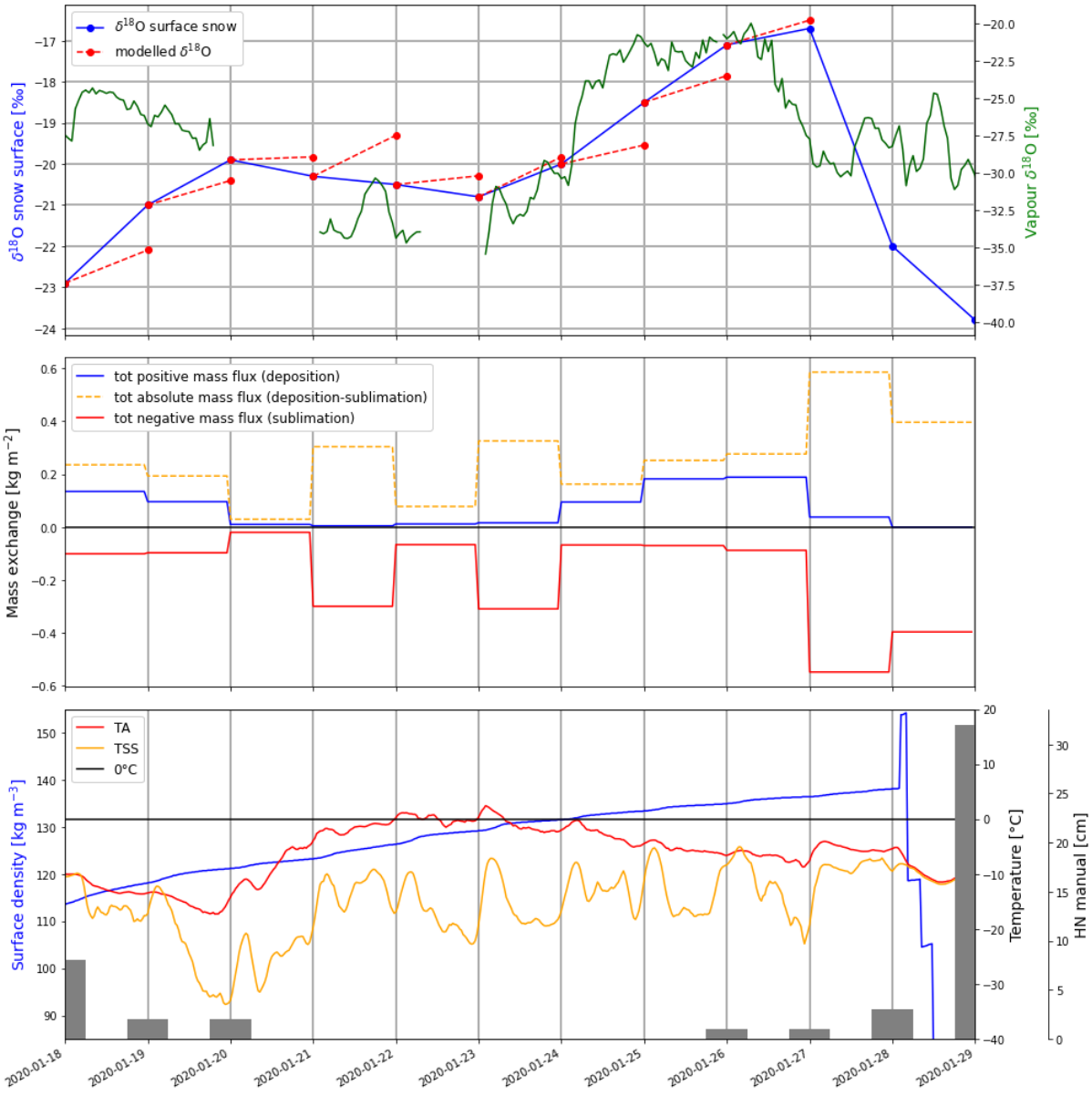

Figure 26: Results of the simplified model for January 2020. In blue the measured snow isotopic composition and in red the results of the model. The measured vapour isotopic composition is plotted on the right axis of the first panel. The other parameters come from the SNOWPACK simulation or weather stations on the WFJ (as in Figure 25).

The results of the model (Figure 26) do not fit well with the measured surface values. As already discussed in the previous sub-chapter, new snow falling before the 20.01.2020 and after the 25.01.2020 is probably the dominant process and effects of sublimation or deposition are negligible in comparison. Still, the period without precipitation is not well predicted either. The model can only predict a depletion from deposition of very depleted vapour, and in this case, the vapour is enriched compared to equilibrium with snow.

As the discussion from the previous chapter suggested that sublimation might not induce surface snow enrichment, the model was run only accounting for deposition. The results are presented in appendix

7.4.3, but they do not show better results. The model might underestimate the effect of deposition. If surface hoar is deposited, it influences the layers of snow contained in each sample. A surface hoar layer can have a thickness of several millimetres and stay during sublimation as it emits long wave radiation maintaining it cold (the incoming short wave is absorbed below) [Hachikubo and Akitaya, 1996]. This can maintain the enriched deposited layer from day to day and sublimation would come from a more depleted, deeper layer.

Precipitation could be considered as deposition. This has a very strong effect on the model as 2 cm of new snow totally renews the snow surface (1 cm renews half of it). The model was run assuming that the snowfall is at equilibrium with the measured vapour isotopic composition (for the mean air temperature of that day). The plot is shown in appendix 7.4.3. Days with precipitation are modelled with an excessive enrichment coming from the enriched measured vapour isotopic composition discussed before. By curiosity, the formula from [Ellehoj et al., 2013] was modified and reducing the fractionating effect of phase changes gives relatively good results for days with precipitation (plot also in appendix 7.4.3). However, other reasons than a poor equilibrium fractionation constant could explain why the falling snow is not at equilibrium with the measured vapour. Probably, the vapour isotopic composition at the altitude where the precipitation was formed is different to the one measured two meters above ground, and the falling snow do not reach equilibrium with the surrounding air. The Piccaro not being calibrated might also shift the vapour isotopic composition values. Finally, a potential overestimation of the amount of new snow collected in the surface samples might come from the centimetre precision of the HN measurements. The vapour at the origin of the precipitation could be estimated using back trajectories (for example as in [Steen-Larsen et al., 2011]), but this goes beyond the scope of this thesis.

4.2.3. Modified model

Like for the 2017 dataset, a modified model including potential effect of compaction during samples collection was used. Due to the snow falling during the two first measurement days, the buried surfaces of the 18 and 19 of January 2020 were used to determine the lower layer isotopic composition.

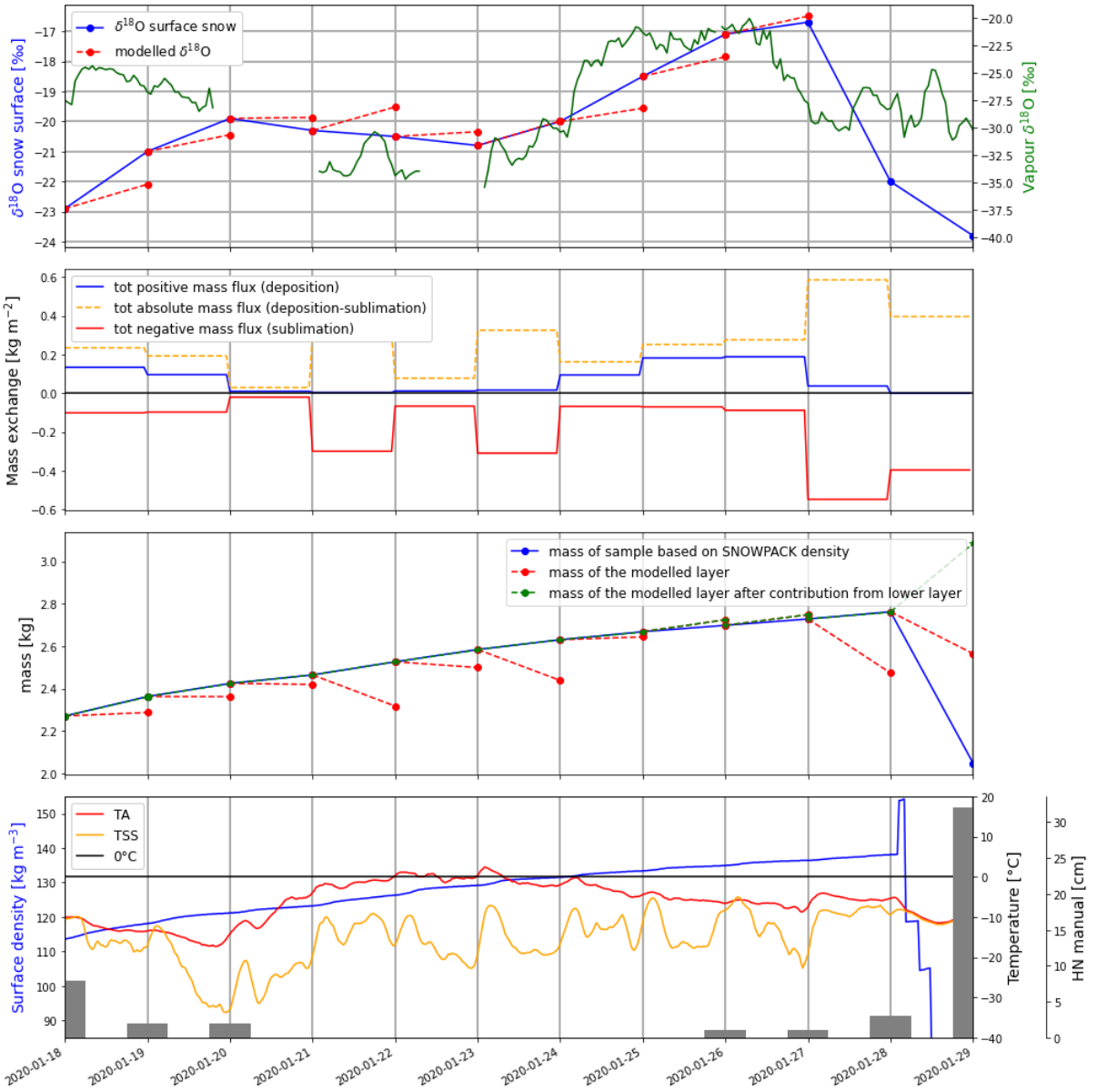

Figure 27: Modified model for January 2020. The third panel shows the mass of each sample estimated using the surface density. The red dashed lines show the modelled masses not accounting for the lower layer contribution. The estimated sample mass is plotted in blue (the blue line is mostly covered by the corrected modelled mass in green).

The modified model gives relatively close results compared to the simplified model. For days without precipitation, results are slightly better because less enrichment is modelled during the depletion period (20 to 23 of January). The day with relatively strong sublimation and enrichment (23-24 of January) is still correctly estimated. The following day is almost not affected because deposited mass compensates the sublimated mass and the contribution from the lower layer is very small.

The modified model was also run assuming non-fractionating sublimation. This allows to reduce the modelled enrichment during the depletion period (and even simulate a small depletion). However, the days when enrichment is measured do not fit at all (the plot is available in appendix 7.4.4).

Unfortunately, the model does not give clear information on whether snow surface sublimation is a fractionating process (during January 2020). It is very probable that multiple processes not included in the model are influencing the surface isotopic composition. During the 5 days without precipitation, 3 of them show a depletion of the snow surface, which cannot be reproduced by the simplified model. Including the contribution from the lower layer gives slightly improved results. Yet, high uncertainty

remains in the isotopic composition of the lower layer and on the fraction of the 2 cm thickness this contribution represents. Additional mini profiles could partly solve this problem allowing to track some of the deeper layers and giving information on the isotopic composition just below the surface.

Potential error could come from the latent heat flux computation. This could be verified in future studies using sonic anemometers, but the expected difference is relatively small since SNOWPACK was found to compute reliable latent heat flux for the WFJ [Stössel et al., 2008].

The air isotopic composition could be more accurate if calibrations using standards were done daily. A better post-measurement correction could also be defined (as it was discussed in 3.4.2), but would require additional lab experiments with that specific Picarro. Finally, the model could be improved by including intra-snowpack processes and an estimation of the thickness of the deposited layer (surface hoar).

4.3. December 2020 Dataset

Unfortunately, the results from the December 2020 measurement campaign could not be analysed during this thesis. The measurements of the snow isotopic composition at the WSL Zentrallabor was postponed due to a technical problem of the LGR.

Nevertheless, these results will be used in a forthcoming study. The high sampling frequency and the fact that the snow surface remained relatively unchanged during the campaign should allow an interesting analysis.

5. Conclusion and outlook

During this thesis, two layer-tracking methods based on SWE estimates and SNOWPACK simulations have been developed and helped to interpret the data from 2017. The analysis of surface samples from March 2017 and January 2020 gave a first idea of the surface isotopic signal changes, and the potential influence of various post-depositional processes.

The coarse time resolution of the 2017 dataset renders the profiles comparison difficult. The analysis done by [Trachsel, 2019] already exploits this dataset using the whole profiles depth and tracking frontal passages. He showed that snow isotopic composition is mainly defined by the history of the vapour at the origin of the precipitation. This can create strong differences between the layers of the snowpack.

The analysis of post depositional processes requires a precise tracking of snow layers to be able to compare samples containing snow from the same precipitation event. The methodologies developed exploring this idea and presented here, contain significant uncertainties. Large differences in the monitoring of snow isotopic composition arise from the choice of the layer-tracking method. It prevents to formulate a clear conclusion on which processes influence the isotopic signal. An improvement of the tracking methods could be done by collecting snow density data (for example using a SMP). However, the high resolution needed to assess the significance of post-depositional processes like fractionating sublimation would not necessarily be attained.

The surface samples from March 2017 and January 2020 allowed to observe the evolution of the snow isotopic composition during periods without precipitation. It was found that fractionation probably occurs during deposition, but its significance during sublimation remains unclear. Depending on which processes affect the snow surface isotopic composition, the possible effect of sublimation could be concealed. An estimation of the wind transported snow and intra-snowpack vapour exchanges could allow to separate the different processes.

The thickness affected by surface sublimation depends on the snow properties, and the assumption of a well-mixed 2 cm surface layer is debatable when modelling the expected fractionating sublimation effect. A determination of the depth from which the surface sublimation mass flux is originating would clearly improve the model and allow to design better samples collection campaigns.

For the analysis of samples of constant thickness, attention should be paid to snow compaction. If the effects due to surface exchanges are mainly captured by a layer thinner than the sample, a varying density (and sample mass) would influence the dilution of these effects. On the opposite, if the surface exchanges influence a thicker layer, only a part of the effects would be captured in the surface sample. In this case, deeper samples should also be collected. In addition, compaction, sublimation, and deposition influence which snow layers are contained in a "surface" sample. This directly affects the measured isotopic composition and can lead to wrong conclusions when comparing surface samples from different days.

The analysis done during this thesis allowed to understand the difficulties in the assessment of the effects of sublimation on snow isotopic composition. The significance of fractionation during sublimation is still ambiguous and calls for additional samples collection and analysis. A better measurement campaign for a period without precipitation would be as follows. It would include samples collections several times per day of various thicknesses and at multiple depths. In addition, a calibrated device should be used to measure the vapour isotopic composition and a camera and/or a snow particle counter installed and employed to monitor the snow surface. If possible, precise snow density measurements should be collected. The December 2020 dataset includes part of those requirements. The forthcoming results will probably help assess the effect of sublimation on snow isotopic composition.

6. Acknowledgments

I would like to thank the following people, who have helped me undertake this research:

Dr. Pirmin Philipp Ebner for sharing his expertise on stable water isotope in snow, and his very useful feedbacks.

Dr. Jürg Trachsel for his great advices and help during field work.

Prof. Michael Lehning for his guidance and valuable insights in snow science.

Dr. Alec Van Herwijnen for building and installing the camera on the WFJ.

Michael Haugeneder, Stephanie Mayer, and Fabian Wolfsperger for collecting samples in December 2020.

Matthias Jaggi for a nice introduction to the cold lab and information on the SMP data.

Dr. Franziska Aemisegger for the help and information about vapour isotopic composition measurements.

7. Appendix

7.1. Isotopic composition analysis

7.1.1. Sample preparation

To measure snow isotopic composition, the samples must be melted and transferred to appropriate vials. The samples were collected in 50 ml plastic tubes and stored in the SLF cold lab (-20 °C). The transfer to the vials is done following the same procedure as in [Trachsel, 2019]. The tubes filled with snow were taken out of the cold room until complete melting within the closed plastic tubes (about 3 hours). The resulting water was transferred to 1.5 ml vials suitable for a liquid water isotopic composition measurement. This was done while wearing clean plastic gloves and a chirurgical mask. The procedure includes the following steps:

- The melted sample is shaken by hand for about 10 seconds in the closed plastic container.
- The micropipette (200 [µl]) tip is changed.
- The 50 ml plastic container is opened.
- The micropipette is filled and emptied (waste) 3x with the sample water to remove possible contamination of the tip.
- The 1.5 ml vial is filled using the micropipette and closed hermetically. Depending on the amount of melted snow, the vials are sometimes only half filled.
- The plastic container is closed.

After the transfer, the plastic tubes were put back in the -20 °C cold room. The whole procedure was done within a day to avoid possible fractionation of the melted snow while in the plastic container. The vials were sent to the WSL Zentrallabor, Birmensdorf by post. Due to a technical problem of the measuring device, the prepared January 2020 vials had to be stored (sealed with paraffin) for approximately one month at 13.5 °C.

7.1.2. Laboratory Analysis

The snow isotopic composition measurements from the 2020 samples were done at the WSL Zentrallabor, Birmensdorf using an “LGR Off-Axis Integrated Cavity Output Liquid Water Isotope Analyzer” (LGR hereafter). This is a different device than the two “Picarro cavity ringdown spectrometers L2130-i” (Picarro hereafter) used for the 2017 dataset and the air vapour isotopic composition measurements.

The LGR and the Picarro use different laser absorption spectroscopy methods. However, they give generally comparable results [Maruyama and Tada, 2014], [Aemisegger et al., 2012], [Berman et al., 2020]. For comparison between air and snow data or between the 2017 and 2020 datasets, a small variation might still come from the different measurement techniques. The d-excess might be more impacted by the change in device as it is very sensitive to small differences in $\delta^{18}O$ [Aemisegger et al., 2012]. Nonetheless, this should not strongly influence the trends observed.

7.1.3. Vapour isotopic composition correction.

The vapour isotopic composition measured by the Picarro situated on the WFJ had to be corrected. During winter 2017, the Picarro was calibrated daily using three standards. This was not done in January 2020 and the calibration cannot be done afterward. However, it is still possible to use a correction for variability in vapour mixing ratio. The correction is specific to this device and was defined for the 2017 measurement campaign. The correction was determined using a dew point generator and the procedure is descried in [Aemisegger et al., 2012]. As the correction is specific to each individual device, it must

be noted that the one used for the Picarro placed on the WFJ is different to the one presented in [Aemisegger et al., 2012] only the method is the same). The data processing is explained here.

First, all the data flagged by the Picarro are removed and data are arranged with a constant 1 second timestep using a linear interpolation.

Second, the mixing ratio ([H_2O]) measured by the Picarro is corrected following the linear fitting from the dewpoint generator experiment done in 2017.

$$[H_2O]_{corr} = [H_2O]_{raw} * 0.761754685542 - 290.809057321 \quad (35)$$

The $\delta^{18}O$ values can then be determined with:

$$\delta^{18}O_{corr} = \delta^{18}O_{raw} - (a * [H_2O]^3_{corr} + b * [H_2O]^2_{corr} + c * [H_2O]_{corr} + d) \quad (36)$$

With: a=1.26696736*10^{-12}; b=-3.80193873*10^{-8}; c=4.52829463*10^{-4}; d=-2.35816850

And the δD values with:

$$\delta D = \delta D_{raw} - (a * [H_2O]^3_{corr} + b * [H_2O]^2_{corr} + c * [H_2O]_{corr} + d) \quad (37)$$

With a=1.02789068*10^{-11}; b=-3.79501488*10^{-7}; c=5.82680750*10^{-3}; d=-35.2638974

Finally, the data are averaged for different timesteps (1minute, 10 minutes, 1 hour) using a weighted mean with the vapour mixing ratio. This allows to have the main air vapour isotopic signal over the time of average. For examples, for the 1-minute average, the corrected δ values ($\delta^{18}O$ or δD) are computed for each minute as:

$$\delta_{60\,\mathrm{sec}\,average} = (\sum_{s=0}^{60} \delta_i * [H_2O]_i) / \sum_{s=0}^{60} [H_2O]_i \quad (38)$$

7.2. Density comparison and SMP measurements

Density derived from the SnowMicroPen (SMP) have been used and compared to the ones computed by SNOWPACK. The procedure to derive density from the measured force needed to penetrate the snow is described in [Proksch et al., 2015] and has been defined using microcomputed tomography. The "snowmicropyn" Python package (https://snowmicropyn.readthedocs.io/en/latest/) was also developed from the work of [Proksch et al., 2015] and allows to compute relatively easily the snow density from the SMP raw data.

During this thesis, the densities from SMP for January and December 2020 have been computed. Seven profiles were taken every day. For each of them, the distance to the surface of the snowpack is retrieved using the algorithm from the "snowmicropyn" package. In case of surprising values (distance to the surface of less than 7 cm or more than 25 cm), the profile is skipped. The remaining profiles should have relatively similar distance to the surface. A variation of a few centimetres for days with fresh snow is to be expected because the device is placed on skis and the snow under them gets compacted during each measurement. The densities values of the remaining profiles are then averaged for each depth (1.25 mm resolution). In addition, an average over 1 cm is done (i.e. the SMP density at 1 cm represents the average density between 0.5 and 1.5 cm).

7.2.1. January 2020

Figure 28 shows the densities from the SMP at different depths for the January 2020 period. As expected, density globally increases with depth. No clear compaction is visible during the period without precipitation (20.01.2020-25.01.2020), and the variations might be due to measurements inaccuracy or poor distance to surface estimation. Alternance of relatively dense and light snowfall could explain those variations before the 20.01.2020 and after the 25.01.2020. Surface hoar deposition could also affect the 1 cm density, but the effect at 5 cm should be very low.

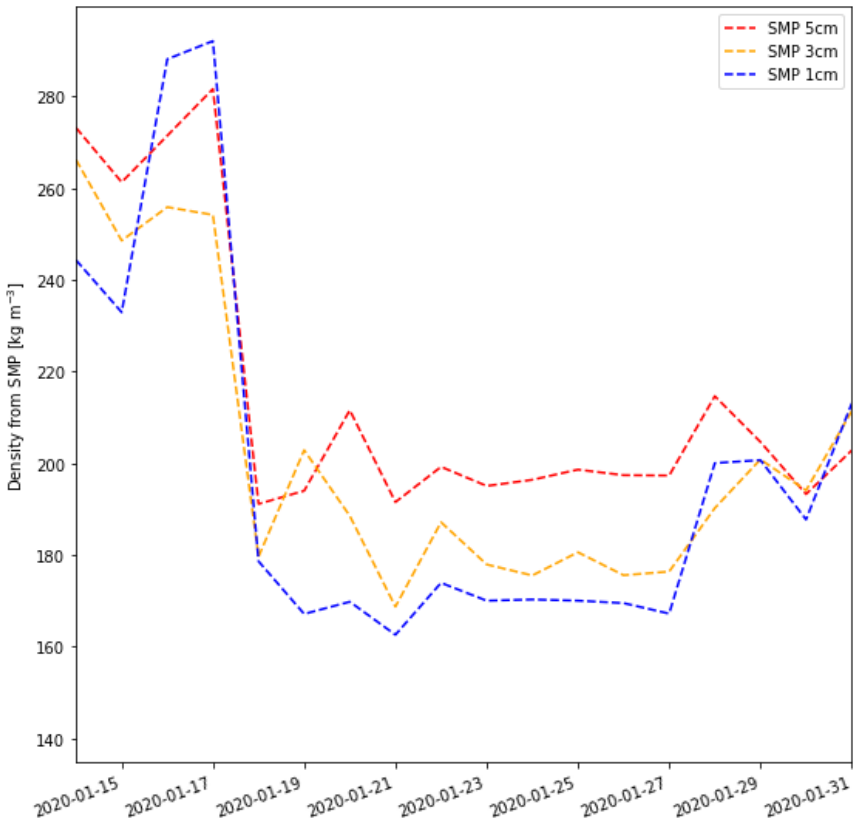

Figure 28: Density from SMP. Comparison of different depth (1, 3 and 5 cm)

A comparison with SNOWPACK density values is presented for 1, 3, and 5 cm depth in Figure 29. The snow density in SNOWPACK can be modelled using different parametrization. Two of them were compared (“ZWART” and “LEHNING_NEW”) together with data from the SMP at 1, 3 and 5 cm depth.

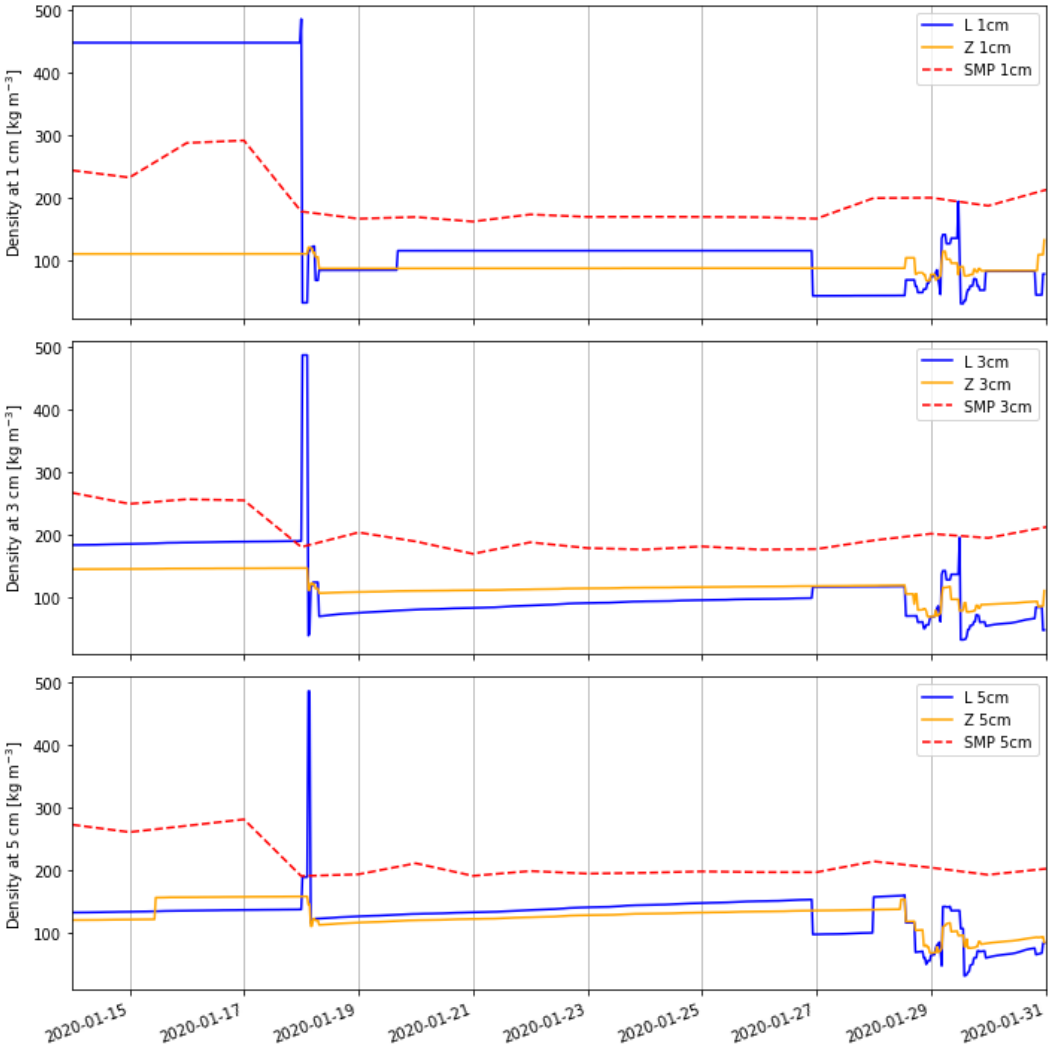

Figure 29: Density comparison between SMP density and two SNOWPACK density parametrization "LEHNING_NEW" (L) and "ZWART" (Z) For January 2020.

Figure 29 shows that SMP density values are globally higher than the ones from SNOWPACK. It is difficult to assess which method is closest to reality. In any cases, the density is shown as relatively constant over the period without precipitation (20.01.2020-25.01.2020). The ZWART parametrization shows a constant value of 84.9 kg m^{-3} at 1 cm depth, which might be too light. The LEHNING_NEW parametrization shows some very abrupt changes in density at 1 cm depth. The steep decreases can be explained by small snowfall. The abrupt increases might come from the surface layer being suddenly removed from the simulation or re-freezing occurring at the surface. A deeper layer should probably be considered for more stability.

The SMP seems to overestimate the surface density. Snowfall occurred between the 18 and the 20 and between the 26 and 31 of January with densities of about 100 kg m^{-3} (1 cm HN corresponds to 1 mm SWE of HN). None of those precipitation seems to be captured by the SMP, which is always giving value above 160 kg m^{-3} at 1 cm depth.

The probable overestimation of the SMP measurements and the abrupt changes in LEHNING_NEW can have a relatively strong effects when using the simplified (or modified) model (presented in 3.6) as it would change the mass of the layer influenced by sublimation. The density modelled by the ZWART parametrization at 5 cm depth can be a good compromise. It shows a smooth increase in density from 113 to 138 kg m^{-3} (18.01.2020-28.01.2020), which seems more realistic than the very low modelled density at 1 cm. Those values (at 5 cm) are still lower than the 1 cm SMP values.

7.2.2. December 2020

In December 2020, no precipitation occurred (or less than 1 cm day^{-1}) between the 14.12.2020 and the 21.12.2020. The SMP densities at different depths (Figure 30) do not show any clear trend during that period and the variations probably come from the distance to surface estimation. The formation of a crust could also explain the sudden peak in the density at 1 cm the 20.12.2020. It must also be noted that the sensor was broken on the 14.12.2020 and had to be changed. This could also have an impact on the sensitivity of the device.

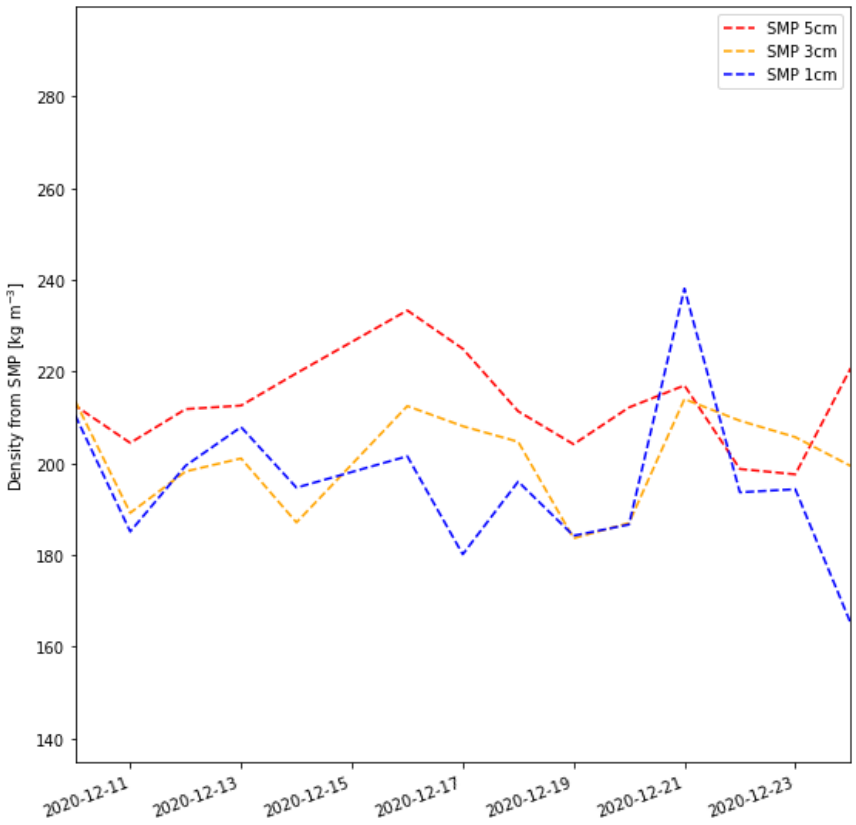

Figure 30: SMP density comparison for December 2020

Like for January 2020, the density from SNOWPACK was compared to the one from the SMP. Again, the SMP values are higher and some abrupt changes can be observed with both SNOWPACK density parametrizations. Looking at the manually measured HN and SWE (of HN), a density of about 100 kg m^{-3} could be approximated (~1 mm SWE for ~1 cm snow). As snow gets older and more compacted, a higher value could be expected. However, small snowfalls (e.g. 5 cm the 13.12.2020 at 8:00 am) are not reported from the SMP measurements to have a density below 180 kg m^{-3}. Therefore, an overestimation from the SMP is expected.

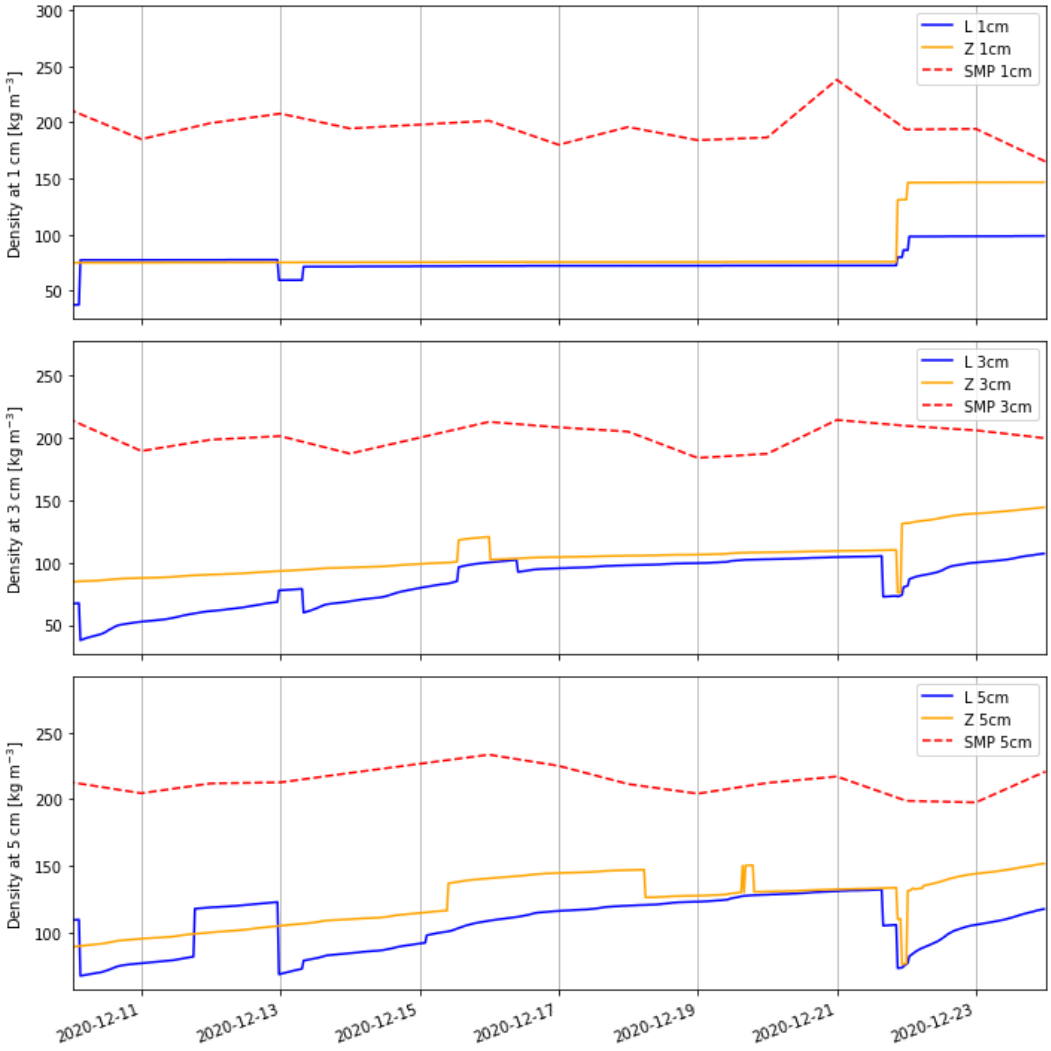

Figure 31: Density comparison between SMP density results and two SNOWPACK parametrization "LEHNING_NEW" (L) and "ZWART" (Z). For December 2020.

Like for January 2020, the SMP and SNOWPACK give different results. A choice is not straightforward and, the ZWART parametrization at 5 cm depth is used as surface density to be consistent with the January 2020 dataset. The two "bumps" visible between the 14.12.2020 and the 21.12.2020 on the third panel of Figure 31 might be problematic. This could be removed by taking the mean value or using a linear change during the period without precipitation.

7.3. 2017 Dataset

The additional material for the 2017 dataset is available in this section.

7.3.1. Manual and automatic HS

The plot below illustrates the difference between the manual and automatic snow height (HS) measurements. The modelled HS values are forced toward the automatic measurements.

Figure 32 Snow height (HS) comparison between model, manual and automatic HS measurements

7.3.2. SWE conversion for manual measurements

Various corrections for modelled height and SWE have been tried and tested on monthly manual Hand Hardness (HH) profiles. HH allows to determine about 80% of the snow stratigraphy [Pielmeier and Schneebeli, 2003] and some of those layers can be observed over the whole season (called persistent layer hereafter) [Calonne et al., 2020]. Due to compaction, layers do not stay at the same height through the season. However, if the layers heights are converted to SWE, persistent layers should stay at a relatively stable SWE value. The Corrections for modelled height have been compared, assuming that a good conversion allows to retrieve similar HH values for the same SWE. This was done to have an idea of the best correction method. However, HH are subject to variability from observer to observer [Pielmeier and Schneebeli, 2003] and not all layers are persistent, thus this testing is not sufficient to validate nor refute a correction method.

The main idea is to compare whether it is preferable to add a **F**ictive **L**ayer (FL) at the bottom of the modelled snowpack or **D**istribute the snow height **D**ifference (DD) over the whole profile. (FL) and (DD) height corrections are defined with the following equations.

$$HS_{diff} = HS_{manual} - HS_{auto} \tag{39}$$

$$(FL):\ h_j^{corrected} = h_j^{modelled} + HS_{diff} \tag{40}$$

$$(DD):\ h_j^{corrected} = h_j^{modelled} * (1 + \frac{HS_{diff}}{HS_{auto}}) \tag{41}$$

A second question concerning the correction of the SWE values was set. The difference in SWE could be written as:

$$SWE_{diff} = HS_{diff} * \frac{\rho_{snow}}{\rho_{water}}\ [cm] \tag{42}$$

The SWE correction could again be spread over the whole snowpack depth or added as a fictive bottom layer. In addition, the choice of ρ_{snow} is discussable.

First, it could be assumed that the difference in snow height occurs over the whole depth and the average density of the snowpack should be used (**a**verage **d**ensity, ad). Second, it could be assumed that differences come from surface processes influencing the model and observation dissimilarities (**s**urface **d**ensity, sd). This seems reasonable as profiles are compared with one-week difference, and changes in HS_{diff} resulting in changes in SWE_{diff} would probably occur on the surface. The low surface density compared to the rest of the snowpack also prevents excessive correction due to small inaccuracies in snow height measurements (manual or automatic). Finally, it is possible to simply not correct the SWE values ($\rho_{snow} = 0$). This would be assuming that the SWE is accurately modelled by SNOWPACK and heights are corrected just to reach the manual measurements. However, this has small interest compared to using directly H_{sample}^{auto} instead of H_{sample}^{manual} in (12).

HH profile from each correction method were compared graphically but no clear conclusion could be done. (FL ad) gives uncoherent results and should not be used.(FL sd), (DD ad) and (DD sd) give very similar results and a choice is not straightforward. The main interest is on the top 20 cm of the snowpack, where (FL) and (DD) are relatively similar (at 20 cm depth of a 120 cm snowpack, there is a 16.7% change in the correction). In the end, (FL sd) has been chosen because it keeps the snow surface density as modelled by SNOWPACK (a fixed fictive layer at the bottom just shifts the values). This is not realistic as the fictive layer changes in thickness and density from date to date. This should not be used for tracking layers deeper in the snowpack. Nevertheless, it is deemed reasonable as a first approach for layers close to the surface. Figure 33 shows the HH profiles with the height of each layer as measured during sampling. Figure 34 shows the conversion of the HS from Figure 33 to SWE.

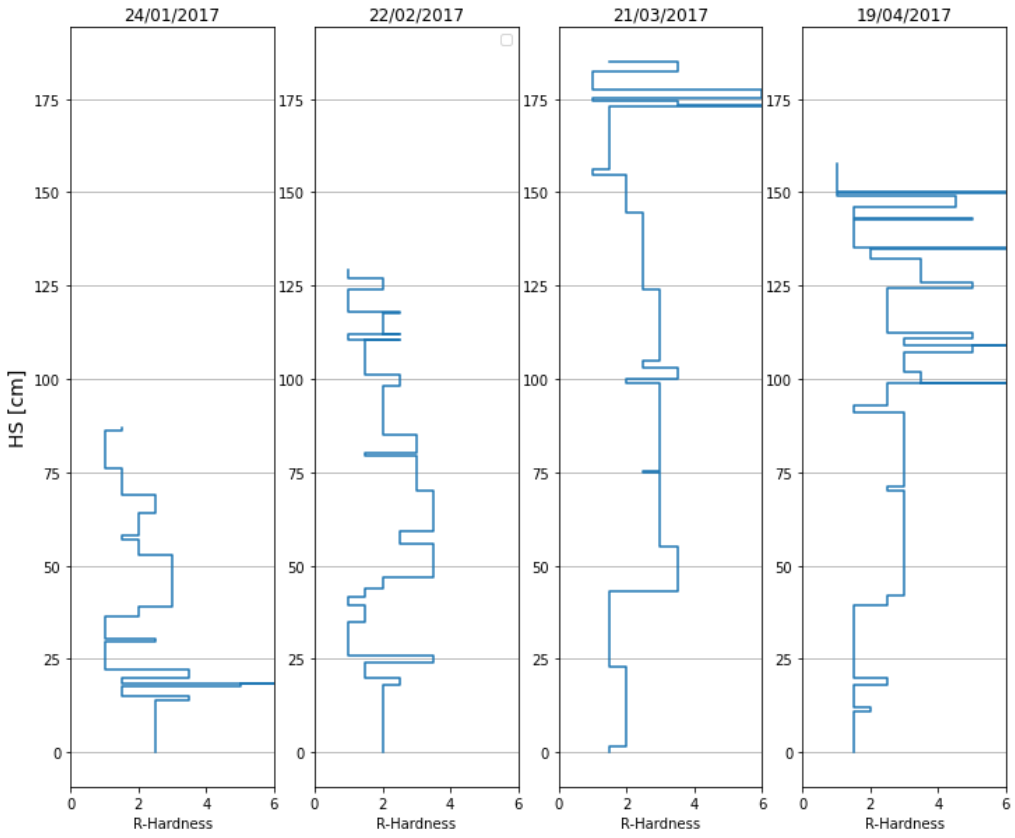

Figure 33: Hand Hardness (HH) profiles against the manually measured height of each layer (HS)

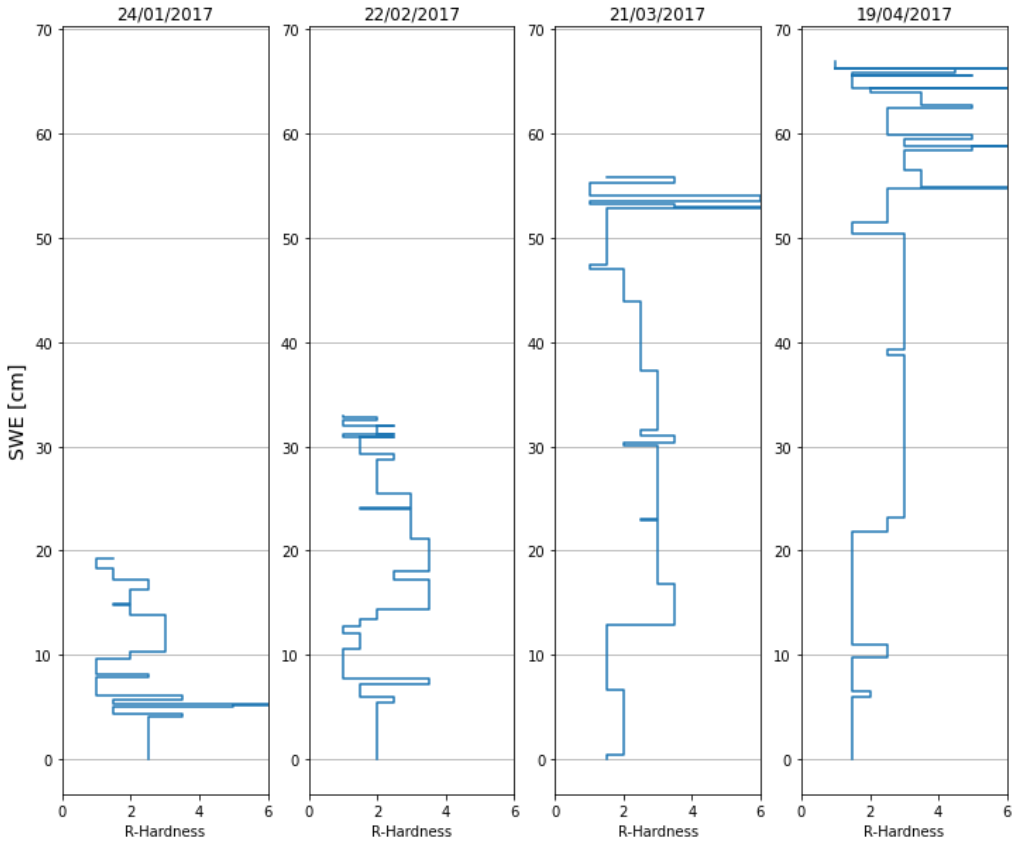

Figure 34: Hand Hardness (HH) profiles, with measured layer height converted to SWE using (FL sd)

The SWE conversion allow to retrieve a layer at a given SWE since it removes changes in layer thickness due to compaction. As stated before, it is not expected to retrieve all layers since some are not persistent and profiles were taken by different observers only once a month. On Figure 34, it is possible to observe similar patterns at relatively close SWE. The conversion is clearly not perfect as shifts between some layers can be observed. This shows a potential source of error when this method is used for layer tracking. Nevertheless, results are not completely incoherent and the use of HH profiles allowed to compare correction methods and select a reasonable one.

7.3.3. Other possible relationship

Similar analysis to what is presented in 4.1.3 was done using additional parameters. The idea was to reveal potential explanations for snow isotopic changes. The variations of the following parameters were compared to changes in isotopic composition.

- Snow surface density
- Tracked layer density
- Surface Grain size
- Tracked layer Grain size
- Isotopic composition of new snow (above the tracked layer)
- Time at the surface / buried

Various combination including several of those parameters were attempted. However, no clear link could be found. There are probably multiple processes involved, and each of them is influenced differently by several of the above-mentioned factors. For a better understanding, stronger statistical methods are needed here. This was not attempted for the 2017 dataset because of the low reliability of

the estimated isotopic composition changes. In addition, the tracking uncertainties also influence the values of several of the above-mentioned parameters. A separation of each of the processes during laboratory studies could give more a precise estimation of their respective significance. Finally, a model including fractionation during snow metamorphism and vapour exchange trough the snowpack could be tested on a similar dataset. However, the modelled layer heights must match the ones from the samples.

7.3.4. March 2017 surface samples

Additional results for the March 2017 analysis are presented here.

Simplified model

The figure below shows the results from the simplified model run. The mass exchanged by evaporation is ignored (only sublimation and dry deposition are considered).

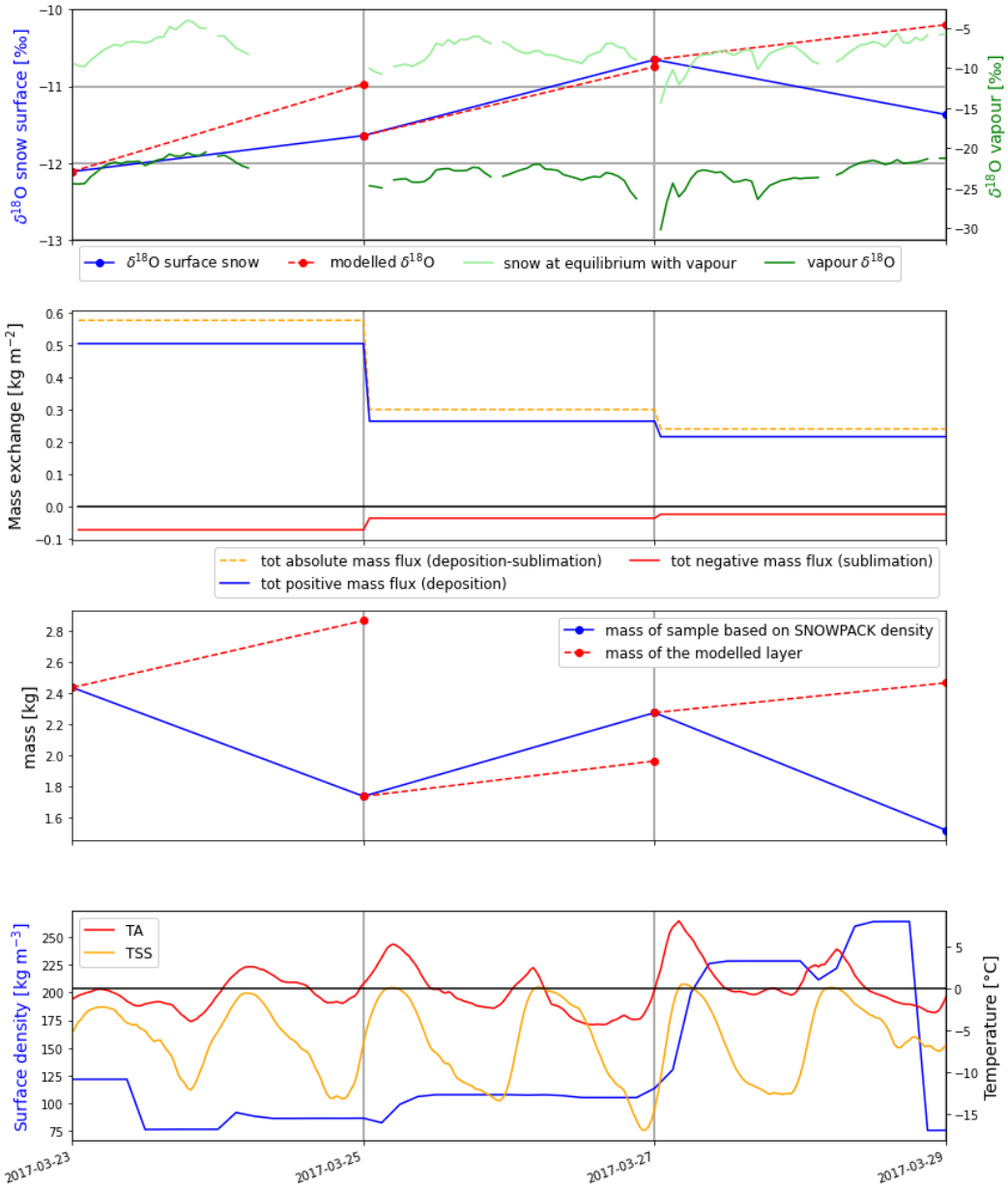

Figure 35: Simplified model results (same as in Figure 20), but only considering sublimation (and dry deposition).

Figure 35 is ignoring the evaporative mass exchange, which is a very debatable assumption. As the mass flux is reduced, the overestimated enrichment observed in Figure 20 is less visible. The first interval (23.03-25.03) is almost not influenced by the removal of mass by evaporation and the model still shows an overestimation. In opposite, the second interval (25.03-27.03) is strongly modified as TSS reaches 0°C and evaporation becomes significant. Ignoring evaporation, results in an underestimation of the mass exchange and a diminution of the modelled isotopic enrichment. From this, it is probable that the mass exchange from evaporation should be included. However, it would mean that either the mass exchange or the influence of phase change is overestimated.

Modified model for March 2017 with reduced mass exchange

The figure below presents the modified model run (like Figure 23). It includes a contribution from the lower layer and an only increasing density. The mass exchange is divided by **5** to show the order of magnitude of the overestimation of the enrichment from the model.

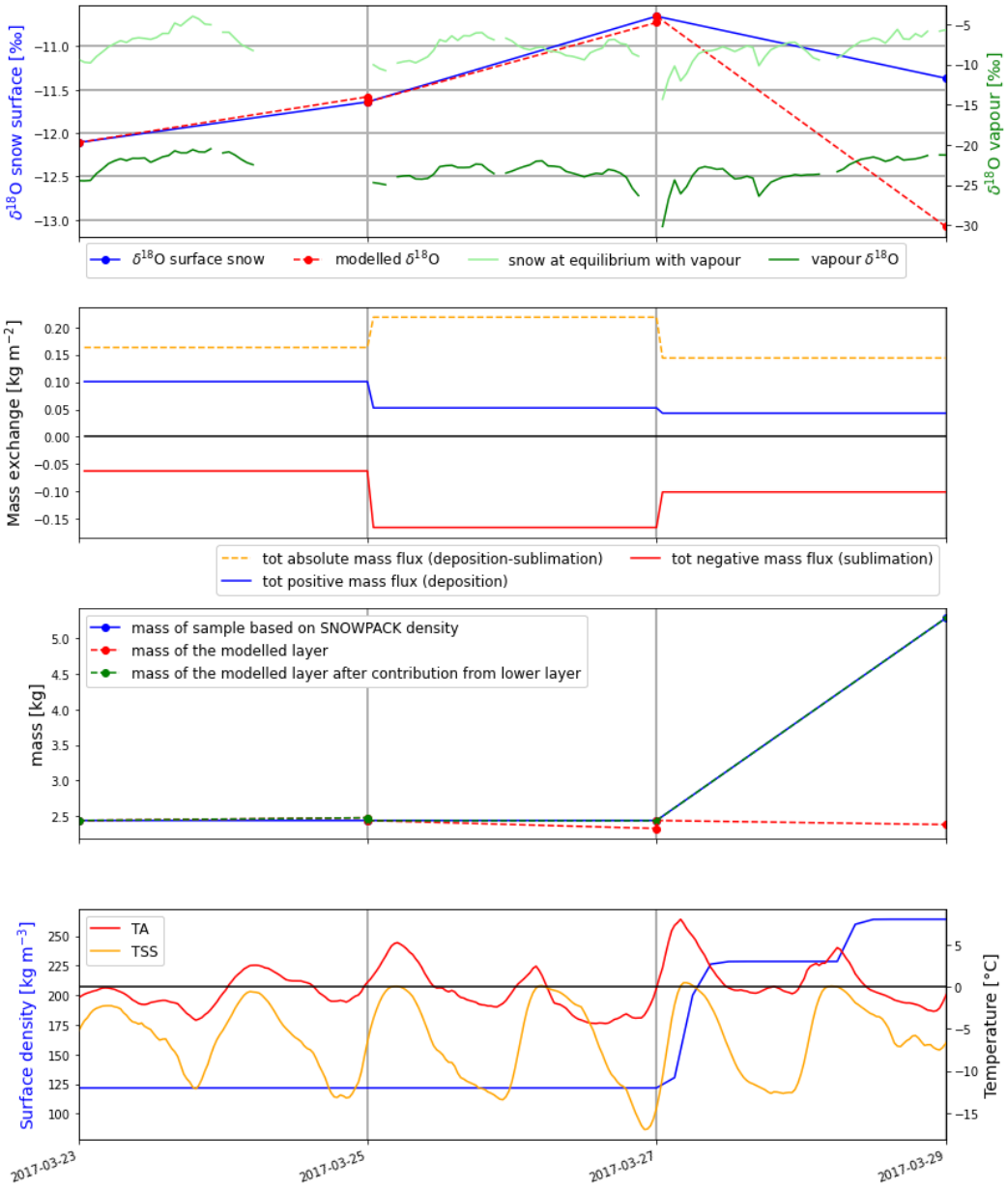

Figure 36 Modified model results (like Figure 27), but dividing the mass flux by 5.

7.4. January 2020 Dataset

The additional material for the January 2020 dataset is available in this section.

7.4.1. SNOWPACK model

SNOWPACK was run to have an estimation of the latent heat flux and surface density. The model was initialized with a configuration very similar to the one available in [Weber, 2017]. Some details are discussed below.

Model initialization

The modelled snow height was forced toward the automatic measurements like for the 2017 simulation. In this case, a difference with the manual measurements is not as problematic since tracking is not needed for this dataset because it includes a period without precipitation. Yet, it might be problematic for the density estimation of the surface. Two density parametrizations ("ZWART" and "LEHNING_NEW") were tested and already compared in 7.2. The model was run for smaller output timestep than in 2017 (30 minutes) to avoid excessive compensation of positive and negative latent heat fluxes. SNOWPACK allows to simulate the soil below the snow, and this is used as a lower boundary condition with a spin-up of 1.5 years.

Latent heat fluxes

The SNOWPACK latent heat flux outputs from two different initializations are compared here. Latent heat flux using Neumann BC or Dirichlet BC are plotted in Figure 37. The data come from SNOWPACK outputs with 30 minutes timestep (computation timestep of 15 minutes) and have been smoothed with 3 a hours moving mean. The computed latent heat fluxes using different boundary condition are relatively similar. Globally Neuman BC gives more negative values, which would increase the estimated sublimation mass flux.

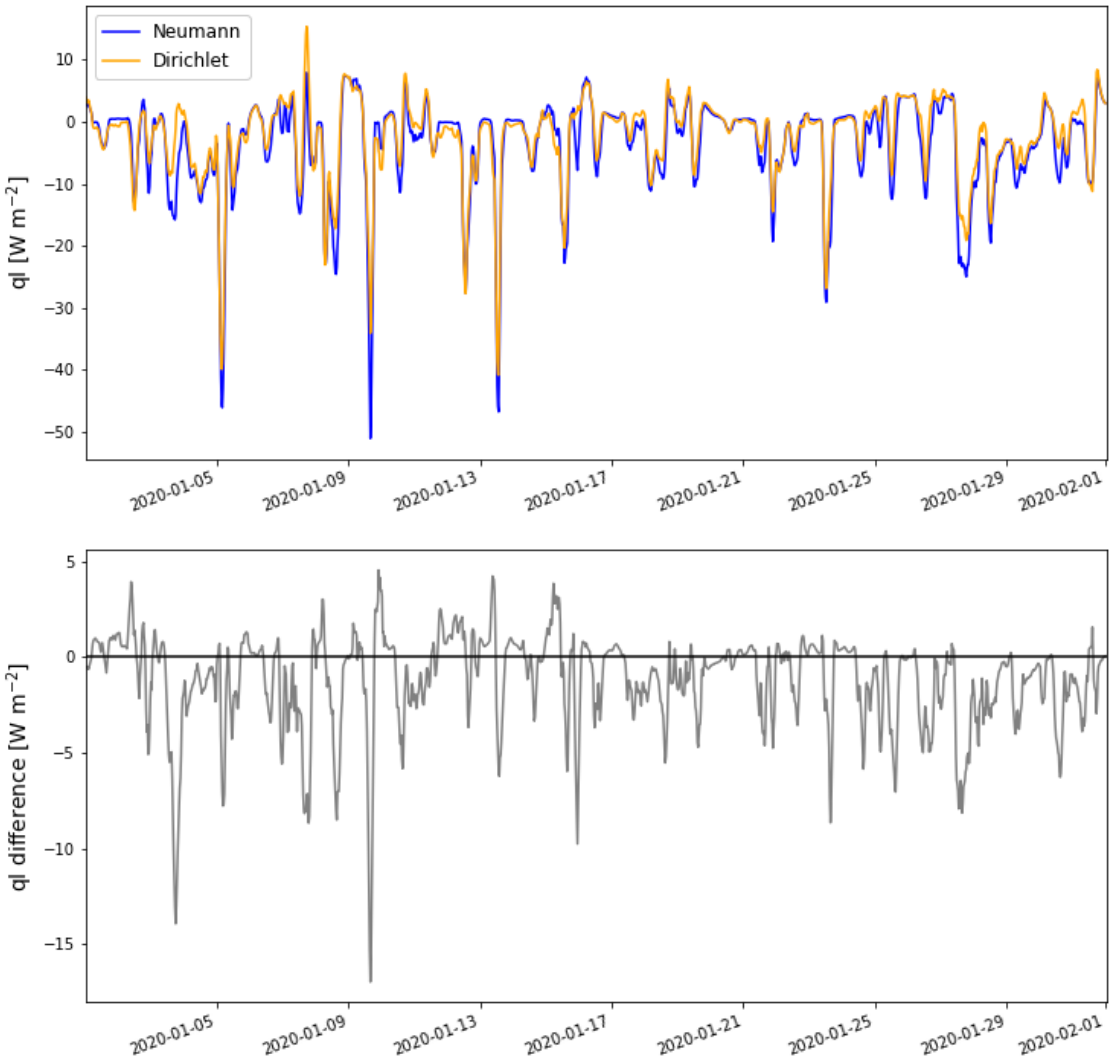

Figure 37: latent heat flux comparison using Dirichlet or Neuman BC. The difference is computed as: Neumann - Dirichlet.

7.4.2. Latent heat flux and change in isotopic signal

Linear regressions between the computed latent heat fluxes and the changes in snow isotopic composition are plotted on the figure below. Figure 38 shows a possible relationship between deposition (positive ql) and enrichment of the snow surface. Negative latent heat flux does not seem to be related to a change in surface snow isotopic composition. This analysis could help find a dominant process influencing the snow surface isotopic composition. However, for secondary processes, their effect can be hidden or compensated and not visible in a simple linear regression. The number of samples is in any case too low for a robust conclusion from linear regressions.

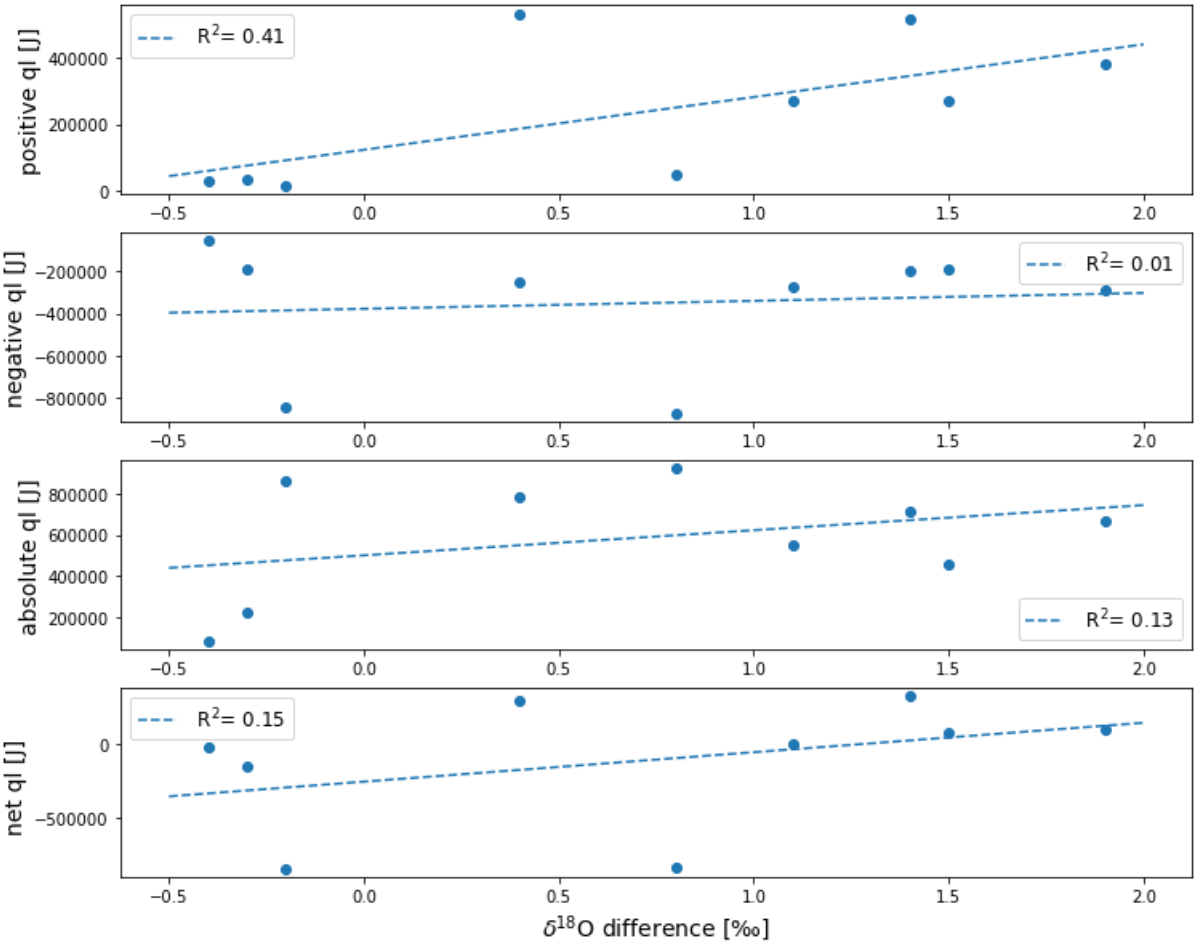

Figure 38: linear regression between changes in isotopic composition of the snow surface and the sum of latent heat fluxes (ql) between each sampling date.

7.4.3. Simplified model

Small modifications were done to the simplified model and use for the analysis of the January 2020 dataset.

Deposition only

For the January 2020 dataset, the simplified model was run accounting only for deposition. The results are presented in Figure 39 below. The effect of deposition is modelled as a very small enrichment. Deposition is probably not the only process influencing the snow surface isotopic composition, but the model might underestimate its effect.

During deposition, surface hoar can grow by several millimetres [Jamieson and Schweizer, 2000]. It influences the amount of snow collected in each sample (e.g. 3 mm of surface hoar represents 15% of the 2 cm thick sample). The next sample will therefore have 3 mm less of the old snow. This partial renewal of the surface also affects the mass of each sample. Sublimation often does not remove the surface hoar layer. This is due to long wave radiation from the surface hoar layer maintaining it cold while the incoming short wave radiation is absorbed below [Hachikubo and Akitaya, 1996]. This is not considered in the simplified modelled, which assumes a well-mixed 2 cm layer.

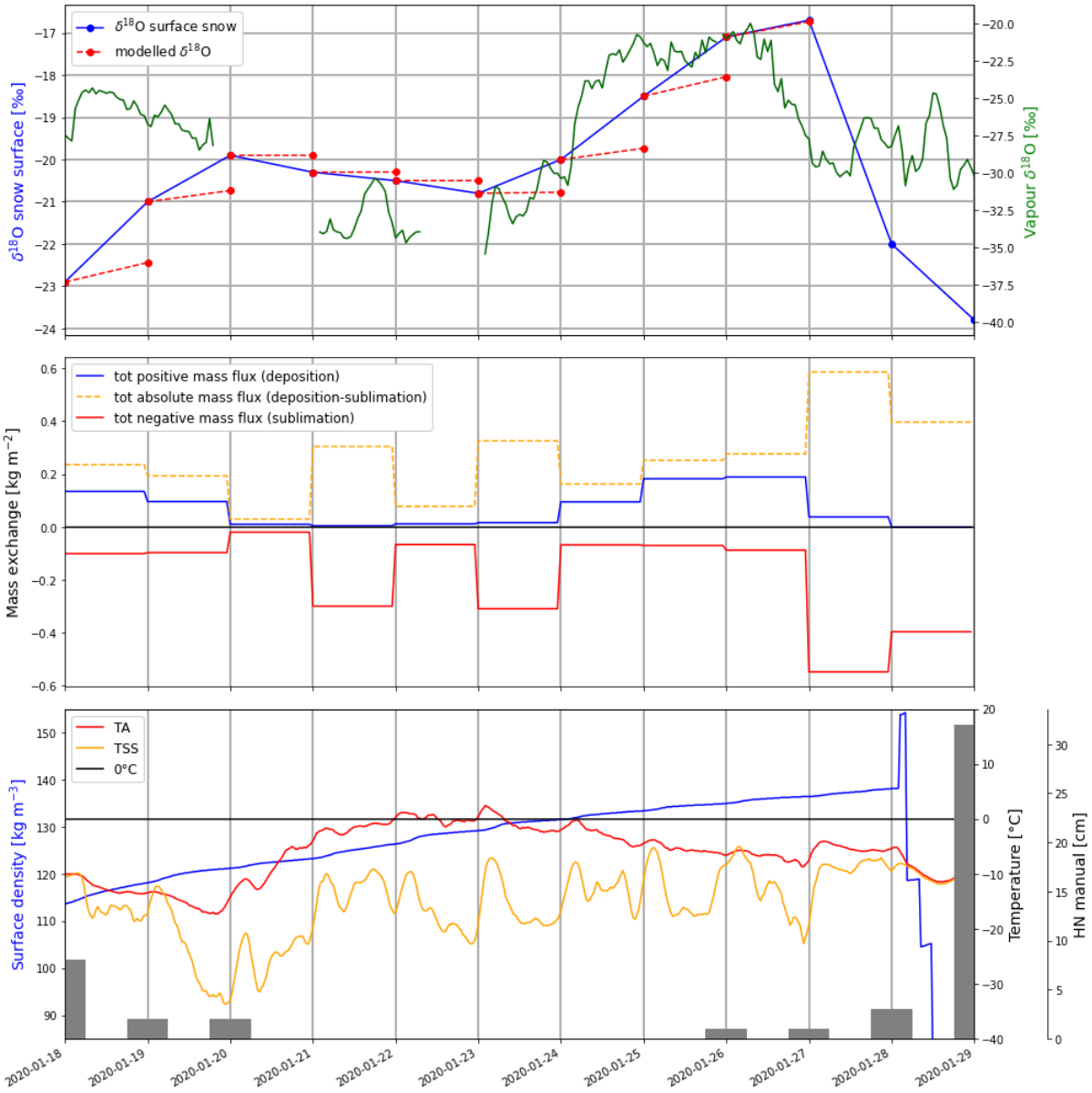

Figure 39: Simplified model accounting only for deposition during January 2020.

New snow as deposition

The model was run assuming that snowfalls are in isotopic equilibrium with the measured vapour and can be modelled as additional deposition. For that, the equilibrium fractionation factor is computed with the daily mean air temperature (not the snow surface temperature).

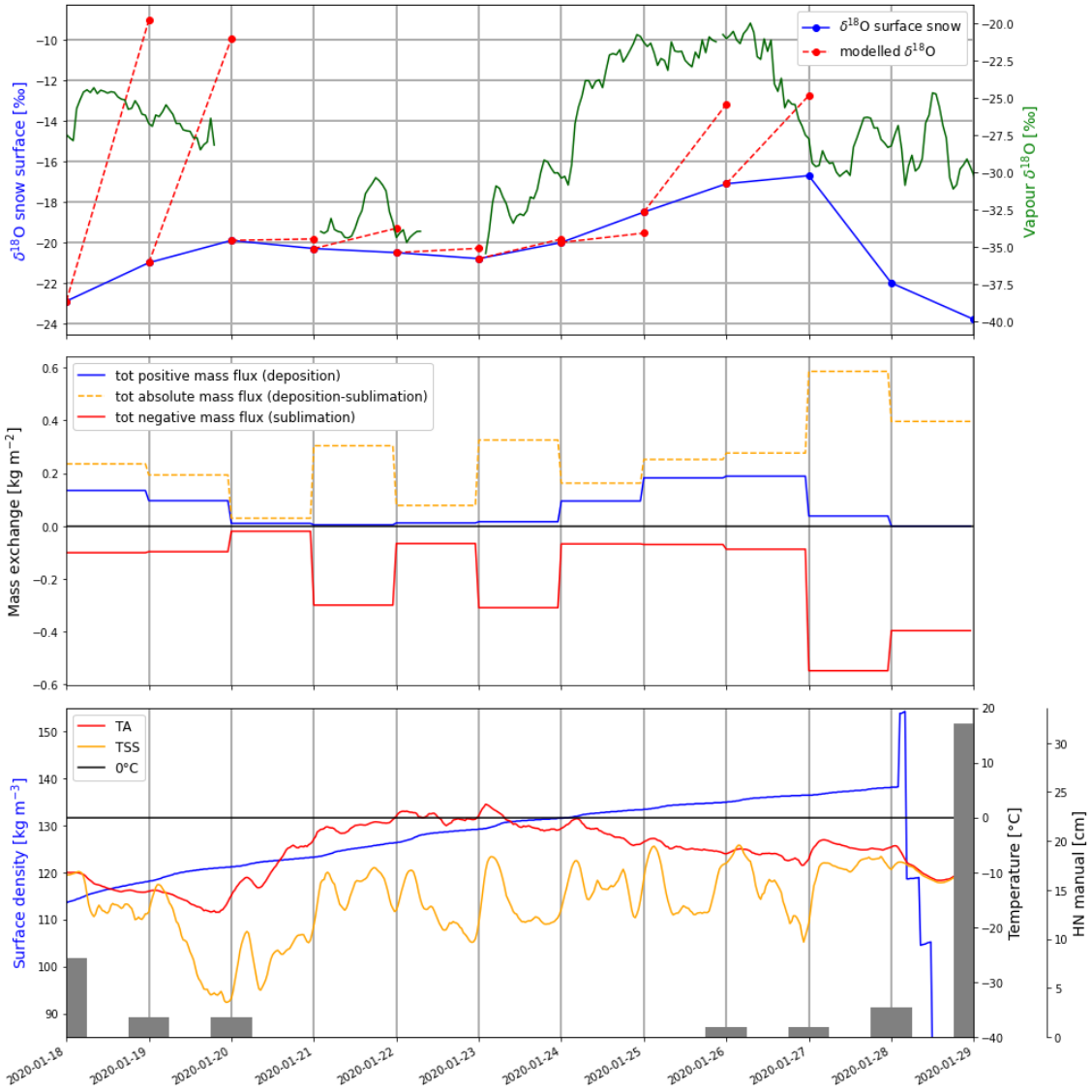

Figure 40: Model results for January 2020 assuming that new snow can be considered as deposition at equilibrium with the vapour isotopic composition

New snow considered at equilibrium with the measured vapour isotopic composition is modelled as an excessive enrichment of the surface. Several explanations are possible: (i) The altitude at which the precipitation is formed has a different vapour isotopic composition than the one measured (at two meters above ground) and the falling snow cannot reach equilibrium with the surrounding air. (ii) The fact that the Piccaro was not calibrated creates a shift in measured vapour isotopic values. (iii) The HN measurements are not precise enough and the estimated amount of new snow collected in the next profile is overestimated. (iv) The equilibrium fractionation constant from [Ellehoj et al., 2013] is not appropriate in this case.

(i) is probably the main explanation. This could be checked using back trajectories of air parcels at the altitude of precipitation (for example as in [Steen-Larsen et al., 2011]), but this goes beyond of the scope of this thesis. (ii) is a potential source of error and calibrations should be done in future studies. A correction by a constant value of the air isotopic composition was tried. This allows to reduce the overestimation of the enrichment, but the results are still unsatisfactory. (iv) was tested by modifying the relationship of [Ellehoj et al., 2013]. The formula was simply modified by a coefficient, as follows:

$$ln(\alpha) = Coef * (\frac{8312.5}{T^2} - \frac{49.192}{T} + 8.31 \times 10^{-2}) \quad (43)$$

The coefficient (Coef) was tested for various value and Coef=0.42 gives relatively good values (shown in Figure 41 below). To improve the equilibrium fractionation formula, multiple coefficients are probably needed. Using a single coefficient just show that another relationship might give a better fit. Improved results from a reduced equilibrium fractionation factor might partially be explained by kinetic effect. The reasons mentioned above (i-iii) are also potential explanations, but would not indicate that the formula from [Ellehoj et al., 2013] should be modified.

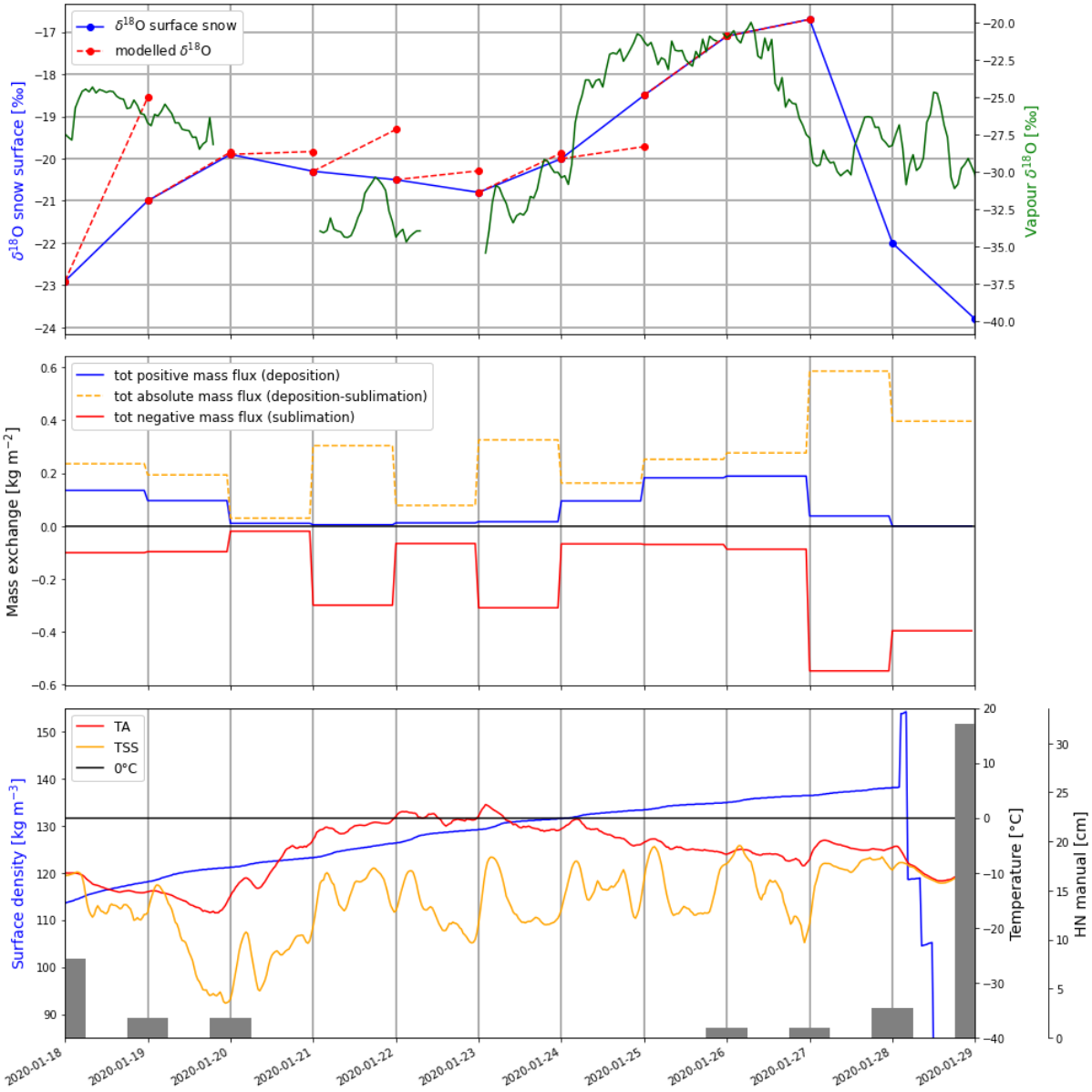

Figure 41: simplified model with modified equilibrium fractionation for deposition (and deposition from snowfall).

7.4.4. Modified model

The modified model was also run assuming non-fractionating sublimation. During the depletion period (20 to 23 of January), the modelled enrichment is reduced. This was expected as there is almost no deposition during those three days. The mass modelled as lost by non-fractionating sublimation is replaced by slightly more depleted snow from below. For those three days, these are the most coherent model results. However, the days with a measured enrichment are very poorly modelled.

Here, precipitation is not considered as deposition. The results would be very similar to the ones in Figure 40, since precipitation would become the main process influencing the snow surface.

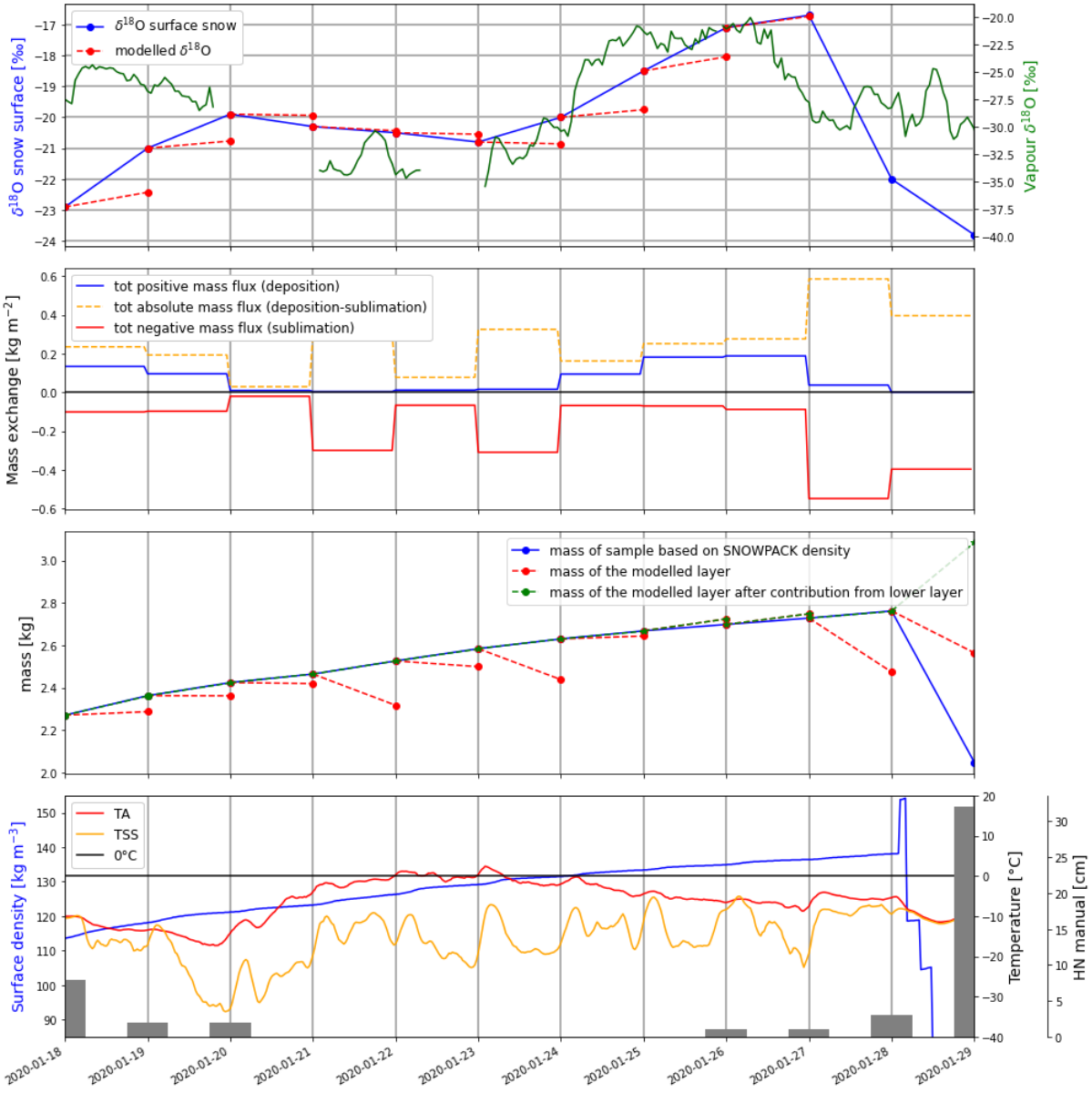

Figure 42: Modified model assuming non-fractionating sublimation.

7.5. December 2020 Dataset

The additional material for the December 2020 dataset is available in this section.

7.5.1. Measurement campaign

The two sites locations are shown on the map below. The wind sheltered site is protected by the small hill on the South-East. The wind exposed site is on the hill and has less wind protection from the topography.

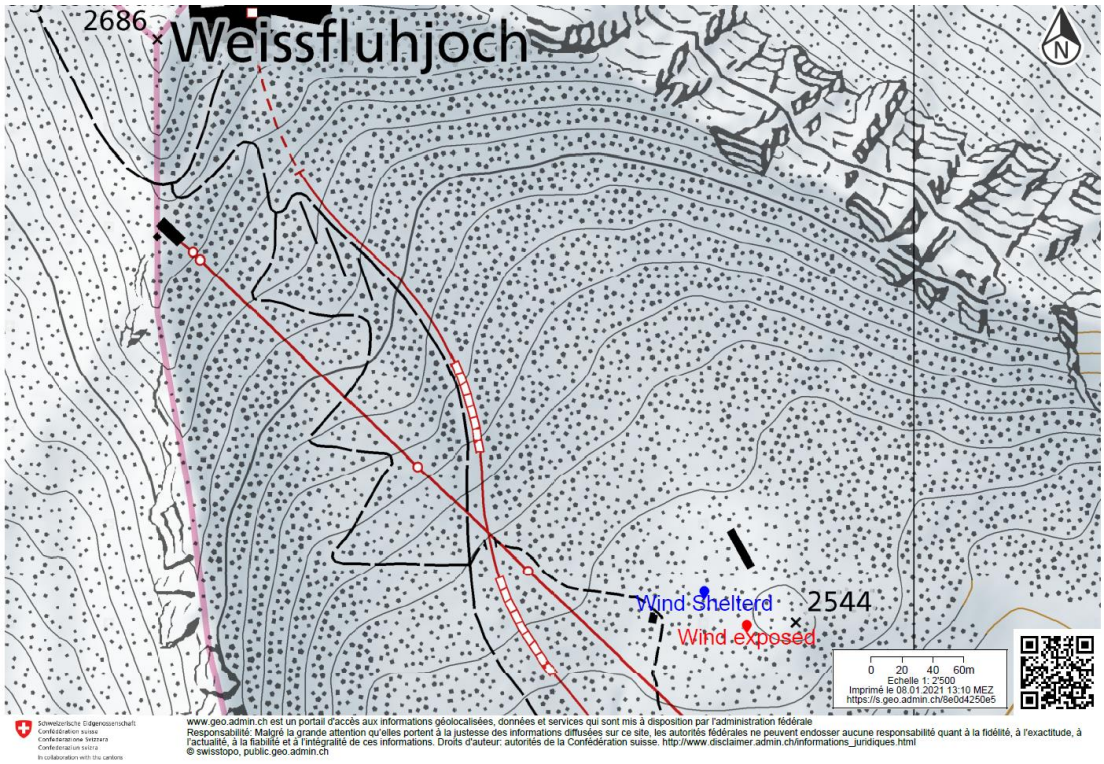

Figure 43: Map showing the WFJ test site with the wind sheltered and wind exposed area. In blue, the wind sheltered site and in red the wind exposed site. Map from: map.geo.admin.ch

The 50 ml plastic tubes are used to collect and store the 2 cm surface samples and mini profiles. They are also used to store the 1 cm surface samples after collection with the spatula. The drawn black line (on both sides of the tube) helps collecting samples of constant thickness.

Figure 44 Plastic tube (50 ml) for snow samples collection and storage.

The spatula with ledges is used to collect 1 cm snow samples. The snow is then stored in the 50 ml plastic tubes until analysis.

Figure 45: spatula with ledges. The width between the two ledges corresponds to the diameter of the 50 ml plastic tube.

Figure 46: 1 cm surface snow collection with the spatula with ledges.

7.5.2. Camera pictures

The Pictures shown below are illustrating the almost unchanged snow surface between the 15.12.2020 and the 16.12.2020. The measured 3 mm HN is not well visible. The samples collected on the 16.12.2020 in the morning might still include this new snow, but it was probably blown away or sublimated later.

Figure 47: Picture from the 15.12.2020 (top) and 16.12.2020(bottom). The date and time are printed on the lower right of each picture.

8. Bibliography

[Aemisegger et al., 2012] Aemisegger, F., Sturm, P., Graf, P., Sodemann, H., Pfahl, S., Knohl, A., and Wernli, H. (2012). Measuring variations of δ 18 o and δ 2 h in atmospheric water vapour using two commercial laser-based spectrometers: An instrument characterisation study. *Atmospheric Measurement Techniques*, 5(7):1491–1511.

[Ala-Aho et al., 2017] Ala-Aho, P., Tetzlaff, D., McNamara, J. P., Laudon, H., Kormos, P., and Soulsby, C. (2017). Modeling the isotopic evolution of snowpack and snowmelt: Testing a spatially distributed parsimonious approach. *Water resources research*, 53:5813–5830.

[Avak et al., 2019] Avak, S. E., Trachsel, J. C., Edebeli, J., Brütsch, S., Bartels-Rausch, T., Schneebeli, M., Schwikowski, M., and Eichler, A. (2019). Melt-induced fractionation of major ions and trace elements in an Alpine snowpack. *Journal of Geophysical Research: Earth Surface*, 124(7):1647–1657.

[Bartlett and Lehning, 2011] Bartlett, S. J. and Lehning, M. (2011). A theoretical assessment of heat transfer by ventilation in homogeneous snowpacks. *Water Resources Research*, 47(4).

[Berman et al., 2020] Berman, E. S., Fahrland, A., Gupta, M., Baer, D. S., and Leen, J. B. (2020). Spectral modeling for complex absorption spectrum interpretation. US Patent 10,557,792.

[Calonne et al., 2020] Calonne, N., Richter, B., Löwe, H., Cetti, C., ter Schure, J., Van Herwijnen, A., Fierz, C., Jaggi, M., and Schneebeli, M. (2020). The RHOSSA campaign: multi-resolution monitoring of the seasonal evolution of the structure and mechanical stability of an alpine snowpack. *The Cryosphere*, 14(6):1829–1848.

[Cappa et al., 2003] Cappa, C. D., Hendricks, M. B., DePaolo, D. J., and Cohen, R. C. (2003). Isotopic fractionation of water during evaporation. *Journal of Geophysical Research: Atmospheres*, 108(D16).

[Chaar, 2020] Chaar, R. (2020). Modelled evolution of isotopic composition in Antarctic snow and air. Master's thesis, EPFL and University of Edinburgh.

[Christner et al., 2017] Christner, E., Kohler, M., and Schneider, M. (2017). The influence of snow sublimation and meltwater evaporation on δD of water vapor in the atmospheric boundary layer of central Europe. *Atmospheric Chemistry and Physics*, 17(2):1207–1225.

[Clifton et al., 2008] Clifton, A., Manes, C., RÃ¼edi, J.-D., Guala, M., and Lehning, M. (2008). On shear-driven ventilation of snow. *Boundary-Layer Meteorology*, 126(2):249–261.

[Colbeck, 1982]Colbeck, S. C. (1982). An overview of seasonal snow metamorphism. *Reviews of Geophysics*, 20(1):45–61.

[Craig, 1961] Craig, H. (1961). Isotopic Variations in Meteoric Waters. *Science*, 133(3465):1702–1703.

[Craig and Gordon, 1965] Craig, H. and Gordon, L. (1965). *Deuterium and Oxygen 18 Variations in the Ocean and the Marine Atmosphere*. Laboratorio di geologia nucleare.

[Dansgaard, 1964] Dansgaard, W. (1964). Stable isotopes in precipitation. *Tellus*, 16(4):436–468.

[Ebner et al., 2017] Ebner, P. P., Steen-Larsen, H. C., Stenni, B., Schneebeli, M., and Steinfeld, A. (2017). Experimental observation of transient δ18O interaction between snow and advective airflow under various temperature gradient conditions. *The Cryosphere*, 11(4):1733 – 1743.

[Ellehoj et al., 2013] Ellehoj, M. D., Steen-Larsen, H. C., Johnsen, S. J., and Madsen, M. B. (2013). Ice-vapor equilibrium fractionation factor of hydrogen and oxygen isotopes: Experimental investigations and implications for stable water isotope studies. *Rapid Communications in Mass Spectrometry*, 27(19):2149–2158.

[Epstein et al., 1963] Epstein, S., Sharp, R. P., and Goddard, I. (1963). Oxygen-isotope ratios in Antarctic snow, firn, and ice. *The Journal of Geology*, 71(6):698–720.

[Fourteau et al., 2021] Fourteau, K., Domine, F., and Hagenmuller, P. (2021). Macroscopic water vapor diffusion is not enhanced in snow. *The Cryosphere*, 15(1):389–406.

[Friedman et al., 1991] Friedman, I., Benson, C., and Gleason, J. (1991). Isotopic changes during snow metamorphism. In *Stable isotope geochemistry: a tribute to Samuel Epstein*, pages 211–221.

[Gat, 1996] Gat, J. R. (1996). Oxygen and hydrogen isotopes in the hydrologic cycle. *Annual Review of Earth and Planetary Sciences*, 24(1):225–262.

[Gat and Gonfiantini, 1981] Gat, J. R. and Gonfiantini, R. (1981). *Stable isotope hydrology Deuterium and oxygen-18 in the water cycle*. IAEA, International Atomic Energy Agency (IAEA).

[Genereux and Hooper, 1998] Genereux, D. P. and Hooper, R. P. (1998). Oxygen and Hydrogen Isotopes in Rainfall-Runoff Studies. In KENDALL, C. and McDONNELL, J. J., editors, *Isotope Tracers in Catchment Hydrology*, pages 319 – 346. Elsevier, Amsterdam.

[Hachikubo and Akitaya, 1996] Hachikubo, A. and Akitaya, E. (1996). Surface hoar growing for several days.

[Hürkamp et al., 2019] Hürkamp, K., Zentner, N., Reckerth, A., Weishaupt, S., Wetzel, K.-F., Tschiersch, J., and Stumpp, C. (2019). Spatial and Temporal Variability of Snow Isotopic Composition on Mt. Zugspitze, Bavarian Alps, Germany. *Journal of Hydrology and Hydromechanics*, 67(1):49 – 58.

[IAEA, 2006] IAEA (2006). Reference sheet for international Measurements Standards. Technical report, IAEA (International Atomic Energy Agency).

[Jafari et al., 2020] Jafari, M., Gouttevin, I., Couttet, M., Wever, N., Michel, A., Sharma, V., Rossmann, L., Maass, N., Nicolaus, M., and Lehning, M. (2020). The impact of diffusive water vapor transport on snow profiles in deep and shallow snow covers and on sea ice. *Frontiers in Earth Science*, 8:249.

[Jamieson and Schweizer, 2000]Jamieson, J. B. and Schweizer, J. (2000). Texture and strength changes of buried surface-hoar layers with implications for dry snow-slab avalanche release. *Journal of Glaciology*, 46(152):151–160.

[Johnsen et al., 2000] Johnsen, S. J., Clausen, H. B., Cuffey, K. M., Hoffmann, G., Schwander, J., and Creyts, T. (2000). Diffusion of stable isotopes in polar firn and ice: the isotope effect in firn diffusion. In *Physics of ice core records*, pages 121–140. Hokkaido University Press.

[Lamb et al., 2017] Lamb, K. D., Clouser, B. W., Bolot, M., Sarkozy, L., Ebert, V., Saathoff, H., Möhler, O., and Moyer, E. J. (2017). Laboratory measurements of HDO/H2O isotopic fractionation during ice deposition in simulated cirrus clouds. *Proceedings of the National Academy of Sciences*, 114(22):5612–5617.

[Lehning et al., 2002a] Lehning, M., Bartelt, P., Brown, R. L., Fierz, C., and Satyawali, P. K. (2002a). A physical SNOWPACK model for the Swiss avalanche warning, Part II. Snow microstructure. *Cold Regions Science and Technology*, (35).

[Lehning et al., 2002b] Lehning, M., Bartelt, P., Brown, R. L., Fierz, C., and Satyawali, P. K. (2002b). A physical SNOWPACK model for the Swiss avalanche warning, Part III: meteorological forcing, thin layer formation and evaluation. *Cold Regions Science and Technology*, (35).

[Madsen et al., 2019] Madsen, M. V., Steen-Larsen, H. C., Hörhold, M., Box, J., Berben, S. M. P., Capron, E., Faber, A.-K., Hubbard, A., Jensen, M. F., Jones, T. R., Kipfstuhl, S., Koldtoft, I., Pillar, H. R., Vaughn, B. H., Vladimirova, D., and Dahl-Jensen, D. (2019). Evidence of Isotopic Fractionation During Vapor Exchange Between the Atmosphere and the Snow Surface in Greenland. *Journal of Geophysical Research: Atmospheres*, 124(6):2932–2945.

[Majoube, 1970] Majoube, M. (1970). Fractionation Factor of 18O between Water Vapour and Ice. *Nature*, 226(5252):1242–1242.

[Marty and Meister, 2012] Marty, C. and Meister, R. (2012). Long-term snow and weather observations at Weissfluhjoch and its relation to other high-altitude observatories in the alps. *Theoretical and Applied Climatology*, 110.

[Maruyama and Tada, 2014] Maruyama, S. and Tada, Y. (2014). Comparison of water isotope analysis between cavity ring-down spectroscopy and isotope ratio mass spectrometry. *Geochemical Journal*, 48(1):105–109.

[Masson-Delmotte et al., 2008] Masson-Delmotte, V., Hou, S., Ekaykin, A., Jouzel, J., Aristarain, A., Bernardo, R. T., Bromwich, D., Cattani, O., Delmotte, M., Falourd, S., Frezzotti, M., Gallée, H., Genoni, L., Isaksson, E., Landais, A., Helsen, M. M., Hoffmann, G., Lopez, J., Morgan, V., Motoyama, H., Noone, D., Oerter, H., Petit, J. R., Royer, A., Uemura, R., Schmidt, G. A., Schlosser, E., Simoes, J. C., Steig, E. J., Stenni, B., Stievenard, M., van den Broeke, M. R., van de Wal, R. S. W., van de Berg, W. J., Vimeux, F., and White, J. W. C. (2008). A Review of Antarctic Surface Snow Isotopic Composition: Observations, Atmospheric Circulation, and Isotopic Modeling. *Journal of Climate*, 21(13):3359–3387.

[Merlivat and Jouzel, 1979] Merlivat, L. and Jouzel, J. (1979). Global climatic interpretation of the deuterium-oxygen 18 relationship for precipitation. *Journal of Geophysical Research: Oceans*, 84(C8):5029–5033.

[Merlivat and Nief, 1967] Merlivat, L. and Nief, G. (1967). Fractionnement isotopique lors des changements d'état solide-vapeur et liquide-vapeur de l'eau a des températures inférieures a 0°C. *Tellus*, 19(1):122–127.

[Morin et al., 2020] Morin, S., Horton, S., Techel, F., Bavay, M., Coléou, C., Fierz, C., Gobiet, A., Hagenmuller, P., Lafaysse, M., Lizar, M., Mitterer, C., Monti, F., Müller, K., Olefs, M., Snook, J. S., van Herwijnen, A., and Vionnet, V. (2020). Application of physical snowpack models in support of operational avalanche hazard forecasting: A status report on current implementations and prospects for the future. *Cold Regions Science and Technology*, 170:102910.

[Moser and Stichler, 1974] Moser, H. and Stichler, W. (1974). Deuterium and oxygen-18 contents as an index of the properties of snow covers. *International association of hydrological sciences publication*, 114:122–135.

[Pielmeier and Schneebeli, 2003] Pielmeier, C. and Schneebeli, M. (2003). Stratigraphy and changes in hardness of snow measured by hand, ramsonde and snow micro penetrometer: A comparison with planar sections. *Cold Regions Science and Technology*, 37(3):393–405.

[Proksch et al., 2015] Proksch, M., Löwe, H., and Schneebeli, M. (2015). Density, specific surface area, and correlation length of snow measured by high-resolution penetrometry. *Journal of Geophysical Research: Earth Surface*, 120(2):346–362.

[Proksch et al., 2016] Proksch, M., Rutter, N., Fierz, C., and Schneebeli, M. (2016). Intercomparison of snow density measurements: bias, precision, and vertical resolution. *The Cryosphere*, 10(1):371–384.

[Schindler, 2020] Schindler, F. B. (2020). Influence of Post-Depositional Processes on the Stable Water Isotopic Composition in Snow and Air. Master's thesis, ETH Zurich.

[Schmucki et al., 2014] Schmucki, E., Marty, C., Fierz, C., and Lehning, M. (2014). Evaluation of modelled snow depth and snow water equivalent at three contrasting sites in switzerland using snowpack simulations driven by different meteorological data input. *Cold Regions Science and Technology*, 99:27 – 37.

[SLF, 2020] SLF (2020). Weissfluhjoch test site. https://www.slf.ch/en/about-the-slf/instrumented-field-sites-and-laboratories/flaechen-und-anlagen-fuer-schnee-und-eis/weissfluhjoch-test-site.html.

[Sodemann, 2006] Sodemann, H. (2006). *Tropospheric transport of water vapour: Lagrangian and Eulerian perspectives*. ETH Zurich, Logos Verlag, Berlin.

[Sokratov and Golubev, 2009] Sokratov, S. A. and Golubev, V. N. (2009). Snow isotopic content change by sublimation. *Journal of Glaciology*, 55(193):823–828.

[Steen-Larsen et al., 2011] Steen-Larsen, H. C., Masson-Delmotte, V., Sjolte, J., Johnsen, S. J., Vinther, B. M., Bréon, F.-M., Clausen, H. B., Dahl-Jensen, D., Falourd, S., Fettweis, X., Gallée, H., Jouzel, J., Kageyama, M., Lerche, H., Minster, B., Picard, G., Punge, H. J., Risi, C., Salas, D., Schwander, J., Steffen, K., Sveinbjörnsdóttir, A. E., Svensson, A., and White, J. (2011). Understanding the climatic signal in the water stable isotope records from the NEEM shallow firn/ice cores in northwest Greenland. *Journal of Geophysical Research: Atmospheres*, 116(D6).

[Stössel et al., 2010] Stössel, F., Guala, M., Fierz, C., Manes, C., and Lehning, M. (2010). Micrometeorological and morphological observations of surface hoar dynamics on a mountain snow cover. *Water Resources Research*, 46(4).

[Stössel et al., 2008] Stössel, F., Lehning, M., Manes, C., Guala, M., and Fierz, C. (2008). Formation of Surface Hoar in Alpine Terrain. In *AGU Fall Meeting Abstracts*, volume 2008, pages H11A–0728.

[Sturm and Benson, 1997] Sturm, M. and Benson, C. S. (1997). Vapor transport, grain growth and depth-hoar development in the subarctic snow. *Journal of Glaciology*, 43(143):42–59.

[Thurnherr et al., 2020] Thurnherr, I., Kozachek, A., Graf, P., Weng, Y., Bolshiyanov, D., Landwehr, S., Pfahl, S., Schmale, J., Sodemann, H., Steen-Larsen, H. C., Toffoli, A., Wernli, H., and Aemisegger, F. (2020). Meridional and vertical variations of the water vapour isotopic composition in the marine boundary layer over the Atlantic and Southern Ocean. *Atmospheric Chemistry and Physics*, 20(9):5811–5835.

[Trachsel, 2019] Trachsel, J. (2019). *Microscale Distribution of Environmental Proxies in Snow*. PhD thesis, ETH Zurich.

[Vionnet, 2012] Vionnet, V. (2012). *Études du transport de la neige par le vent en conditions alpines : observations et simulations à l'aide d'un modèle couplé atmosphère/manteau neigeux*. Theses, Université Paris-Est.

[Weber, 2017] Weber, N. (2017). WFJ_MOD: Meteorological and snowpack measurements from Weissfluhjoch, Davos, Switzerland.

[West et al., 2006] West, J. B., Bowen, G. J., Cerling, T. E., and Ehleringer, J. R. (2006). Stable isotopes as one of nature's ecological recorders. *Trends in Ecology & Evolution*, 21(7):408 – 414. Twenty years of TREE - part 2.

[Yau and Rogers, 1996] Yau, M. and Rogers, R. (1996). *A Short Course in Cloud Physics*. Elsevier Science.